

**Phenotypic and chemotypic characterization
of GABA-shunt mutants in *Arabidopsis thaliana***

Dissertation

Submitted for:

The Fulfillment of the Degree of Doctor of Philosophy
(PhD) in the Faculty of Mathematics and Natural
Sciences of the University of Cologne

Submitted by:

Dereje Worku Mekonnen

Cologne, 2012

**Phenotypic and chemotypic characterization
of GABA-shunt mutants in *Arabidopsis thaliana***

Inaugural-Dissertation

Zur

Erlangung des Doktorgrades
der Mathematisch-Naturwissenschaftlichen Fakultät
der Universität zu Köln

vorgelegt von

Dereje Worku Mekonnen

Aus Wonji, Ethiopia

Köln, 2012

Die dieser Dissertation zugrundeliegenden experimentellen Arbeiten wurden in der Zeit Juni 2009 bis Dezember 2012 am Botanischen Institut der Universität zu Köln angefertigt

Berichterstatter: Prof. Dr. Ulf-Ingo Flügge

PD Dr. habil. Veronica Maurino

Tag der mündlichen Prüfung: 04.12.12

Contents

List of Figures	v
List of Tables.....	vii
Acknowledgement.....	viii
Abstract	ix
Zusammenfassung	x
General Introduction	1
I. Microbes	2
II. Yeast	3
III. Mammals	4
IV. Plants	4
References	6
Chapter one: Characterization of Arabidopsis <i>gad</i> mutants	9
1. Introduction	9
2. Methodology	12
2.1. Generation of single and double mutants	12
2.2. Phenotypic analysis	12
2.3. Analysis of water content	14
2.4. Analysis of stomata conductance, number and gas exchange.....	14
2.5. Expression analysis of target genes.....	15
2.6. GC-MS and HPLC analysis of metabolites.....	16
2.7. Na ⁺ and K ⁺ measurement	18
3. Results	19
3.1. Analysis of <i>GAD</i> transcripts.....	19
3.2. Generation of <i>gad1/2</i> double mutant plants	20
3.3. Analysis of GABA content and compensatory effect of <i>GADs</i>	21
3.4. Phenotypic analysis	23
3.5. Transcript analysis of potassium transporters	34
3.6. Analysis of Potassium uptake	36
3.7. Metabolic profiling.....	37
3.8. Expression analysis of <i>GAD3</i> and <i>GAD4</i> after salt treatment.....	40
4. Discussion	42
4.1. The truncated <i>GAD2</i> transcript lacks decarboxylase activity	42
4.2. <i>GAD1</i> and <i>GAD2</i> proteins synthesize most of the GABA in shoots and roots.....	43
4.3. GABA plays a role in the normal development of Arabidopsis	43
4.4. The <i>gad1/2</i> mutant metabolite was differentially regulated under salt and drought stress.	44

4.5. GABA accumulation during salt and drought stress is important to prevent dehydration.....	45
4.6. <i>GAD</i> mutations enhance the transpiration rate by affecting the stomata density.....	47
4.7. Stomata closure was partially impaired in <i>gad1/2</i> mutant	48
4.8. GABA shunt plays a role in potassium homeostasis.....	49
5. Conclusions	50
References	51
Chapter Two: Investigation on GHB/SSA toxicity.....	55
1. Introduction	55
2. Materials and Methods	57
2.1. Generation of mutant lines	57
2.2. Phenotypic analysis	58
2.3. Chemotypic analysis	58
2.4. Enzyme activity assay	59
2.5. Yeast strains and growth medium	60
2.6. H ₂ O ₂ analysis.....	60
2.7. Metabolite extraction and measurment	60
3. Results:	62
3.1. <i>Arabidopsis thaliana</i>	62
3.1.1. Generation of <i>ghbdh1/2</i> double mutant.....	62
3.1.2. Phenotypic and chemotypic analysis.....	63
3.1.3. Searching of the third putative GHB dehydrogenase.....	66
3.1. 4. Generation of the <i>ghbdh1/2</i> x <i>at4g20930</i> triple mutant	67
3.1.5. Phenotypic characterization and gel staining assay	68
3.2. <i>Saccharomyces cerevisiae</i>	70
3.2.1. The GABA shunt in yeast	70
3.2.2. Identification of the putative yeast GHB dehydrogenase.....	71
3.2.3. Phenotypic analysis of <i>gnd1</i> and <i>gnd2</i> mutants	71
3.2.5. Assessment of SSA/GHB as alternative carbon source	73
3.2.6. Analysis of H ₂ O ₂ induction	75
4. Discussions.....	77
5. Conclusion.....	79
References	80
Chapter Three: Investigation of the fate of GHB	82
1. Introduction	82
2. Materials and Methods	83
2.1. Feeding of GHB	83
2.2. GHB extrusion and time course experiment	83

3. Results	84
3.1. Analysis of GHB metabolism	84
3.2. Analysis of GHB metabolism <i>via</i> peroxisomal fatty acid beta oxidation pathway ..	85
3.3. Analysis of GHB metabolism back to the GABA shunt.....	86
4. Discussion	90
5. Conclusion.....	92
References	93
Chapter Four: Investigation on <i>ssadh</i> suppressor lines	94
1. Introduction	94
2. Materials and Methods	97
2.1. GADs Knock-out/down.....	97
2.1.1. Generation of the <i>gad1/2-amigad3/4</i> lines.....	97
2.1.2. Amplification of the amiGAD3/4 insert.....	97
2.1.3. Preparation of the Entry Clone.....	97
2.1.4. Preparation of the expression clone	98
2.1.5. Plant transformation	98
2.1.6. Generation of a <i>gad1/2-amigad3/4-ssadh</i> line	99
2.1.7. Phenotypic analysis	99
2.1.8. Metabolite and hydrogen peroxide (H ₂ O ₂) measurement	100
2.2. EMS induced mutation.....	101
2.2.1. Generation and screening of EMS mutants.....	101
2.2.2. Phenotypic characterization of EMS lines	101
2.2.3. Isolation of mapping populations	101
2.2.4. Mapping of EMS-induced mutations	102
2.2.5. Genomic DNA extraction for whole genome sequencing	102
3. Results	103
3.1. GAD Knock out/down	103
3.1.1. Isolation of the triple <i>gad1/2-ssadh</i> mutants	103
3.1.2. Phenotypic analysis	103
3.1.3. Metabolic Analysis and H ₂ O ₂ measurement	105
3.1.4. Generation of the <i>gad1/2-amigad3/4-ssadh</i> line.....	106
3.2. Suppression of the <i>ssadh</i> phenotype by EMS mutation.....	108
3.2.1. Preliminary selection of the EMS suppressor lines.....	108
3.2.2. Phenotypic characterization of selected EMS suppressor lines	108
3.2.3. Metabolic analysis of the EMS suppressor lines.....	111
3.2.4. Generation of mapping populations	113
3.2.5. PCR-based mapping of the EMS mutations.....	114

3.2.6. Full genome sequencing of 7D, 13J, 17J and 21H EMS lines	115
4. Discussion	122
4.1. GAD Knock out/down	122
4.1.1. Simultaneous mutation of <i>gad1/2</i> genes partially rescued the <i>ssadh</i> phenotype .	122
4.1.2. The <i>ssadh</i> phenotype is not correlated to the GHB levels	123
4.2. Suppression of the <i>ssadh</i> phenotype by EMS mutation.....	124
4.2.1. EMS mutation improved the growth of <i>ssadh</i> plants.....	124
4.2.2. The <i>ssadh</i> phenotype is unrelated to the GHB level	124
4.2.3. Full genome sequencing identified seven candidate genes	125
Conclusion.....	129
References	130
Appendix 1: Abbreviations	132
Appendix 2: List of primers	136

List of Figures

Figure 1. Schematic representation of the GABA shunt in <i>Arabidopsis</i>	1
Figure 2. Expression analysis of <i>GAD</i> transcripts.....	19
Figure 3. qRT-PCR analysis of the <i>GADs</i> transcript levels.....	19
Figure 4. Schematic representation of <i>GAD1</i> and <i>GAD2</i> genes and transcript analysis.....	21
Figure 5. Analysis of GABA content in leaves and roots of wild type and <i>gad1/2</i> plants.	22
Figure 6. Relative expression of <i>GAD3</i> and <i>GAD4</i> in leaves and roots.....	22
Figure 7. Phenotype of a three-week-old wild type and <i>gad1/2</i> plants.....	24
Figure 8. Analysis of cell numbers in Wt and <i>gad1/2</i> plants.	24
Figure 9. Phenotypic and water content analysis of wild type and <i>gad1/2</i> plants	25
Figure 10. Leaf stomata conductance of wild-type and <i>gad1/2</i> plants.....	26
Figure 11. GABA content in the leaves of Wt, <i>gad1</i> , <i>gad2</i> and <i>gad1/2</i> plants treated without and with drought.....	28
Figure 13. Leaf stomata conductance of plants grown on 5 mM GABA.....	30
Figure 12. Phenotype of Wt, <i>gad1</i> , <i>gad2</i> and <i>gad1/2</i> plants treated with drought stress.....	29
Figure 14. Stomata conductance in light to dark transition.....	30
Figure 15. Transpiration rate measurement using the gas exchange method.....	31
Figure 16. Comparison of the shoot phenotype of soil grown wild-type and <i>gad1/2</i> plants treated without or with 150 mM NaCl	32
Figure 17. Root growth phenotype of Wt and <i>gad1/2</i> plants in response to salt stress	33
Figure 18. Phenotype of Wt and <i>gad1/2</i> plants on ½ MS plate containing mannitol.	33
Figure 19. Comparison of Na ⁺ and K ⁺ in the shoots of Wt and <i>gad1/2</i> plants.	34
Figure 20. Relative expression analysis of potassium transporters.....	35
Figure 21. Root growth analysis of wild type, <i>gad1/2</i> and <i>pop2</i> plants under low K ⁺	36
Figure 22. GC-MS analysis of major TCA cycle metabolites	39
Figure 23. Transcript analysis of <i>GAD3</i> and <i>GAD4</i> in leaves after salt stress.....	41
Figure 24. Schematic representation of <i>GAD2</i> protein with predicted catalytic residues	42
Figure 25. Schematic representation of T-DNA insertion in the <i>GHBDH1</i> and <i>GHBDH2</i>). .	62
Figure 26. GC/MS analysis of major GABA shunt related and TCA cycle metabolites	63
Figure 27. Phenotypic analysis of wild type and <i>ghbdh1/2</i> double mutant.	64
Figure 28. GC/MS analysis of GHB content in wild type and <i>ghbdh1/2</i> double plants	65
Figure 29. Enzyme activity assay on native gels with total protein extract	66
Figure 30. Phylogenetic tree indicating the degree of divergence	67

Figure 31. Enzyme activity assay for total protein extract.....	68
Figure 32. Enzyme activity assay for wild type, <i>at4g20930</i> , <i>ghbdh1/2</i> and <i>ghbdh1/2</i> x <i>at4g20930</i> lines on native gel.....	69
Figure 33. Phenotype of wild type and <i>ghbdh1/2</i> x <i>at4g20930</i> lines on ½ MS plates.....	69
Figure 34. Schematic representation of the GABA shunt in yeast.....	70
Figure 35. Phenotypic analysis of Wt, <i>gnd1</i> and <i>gnd2</i> yeast strains	72
Figure 36. Phenotypic analysis of Wt, <i>gnd1</i> and <i>gnd2</i> strains on 0.5 mM GHB.	72
Figure 37. Phenotypic analysis of Wt and <i>uga2</i> strains on SSA and GHB plates.	73
Figure 38. Analysis of SSA and GHB as alternative carbon source	74
Figure 40. GC/MS analysis of GABA shunt metabolites in Wt and <i>uga2</i> strains	75
Figure 39. Analysis of SSA as sole carbon source on YNB plates.....	75
Figure 41. Analysis of the generation of H ₂ O ₂ in wild type and <i>uga2</i> strains	76
Figure 42. Analysis of GHB dynamics in wild type and <i>ghbdh1/2</i> mutant plants.....	84
Figure 43. Analysis of GHB extrusion back to the medium	85
Figure 44. Analysis of the fate of GHB in <i>kat2</i> and <i>pxa1</i> mutants	85
Figure 45. Schematic representation of the <i>ssadh</i> and <i>pop2</i> alleles	86
Figure 46. Analysis of GHB dynamics in the Wt and <i>gs</i> lines.....	87
Figure 47. Analysis of time dependent change in levels of GABA-shunt metabolites.....	88
Figure 48. Analysis of GABA shunt-related metabolites in Wt and <i>gs</i> lines.....	89
Figure 49. Analysis of <i>GABA-T</i> and <i>SSADH</i> transcript.	89
Figure 50. Screening of triple <i>gad1/2</i> x <i>ssadh</i> plants	103
Figure 51. Phenotype of four-weeks-old wild type, <i>gad1/2-ssadh</i> and <i>ssadh</i> plants.....	104
Figure 52. Metabolic analysis in Wt, <i>gs</i> and <i>gad1/2Xssadh</i> triple mutants..	105
Figure 53. Measurement of hydrogen peroxide in the plant extracts of wild type, <i>gad1/2</i> x <i>ssadh</i> triple mutants (L1, L5 and L6) and <i>ssadh</i> lines.	106
Figure 54. HPLC analysis of GABA and Alanine from Wt and six <i>gad1/2-amigad3/4</i> lines.....	107
Figure 55. Phenotypic analysis of EMS suppressor lines grown on ½ MS plate.....	108
Figure 56. Phenotypic analysis of <i>gs</i> and EMS lines on SSA plates.....	109
Figure 57. Phenotype of Wt, <i>gs</i> , 7D, 13J, 17J, 21H and <i>ssadh</i> plants grown on soil.....	110
Figure 58. GCMS analysis of major GABA shunt and TCA cycle intermediates in the shoot extract of wild type, <i>gs</i> , 7D, 13J, 17J, 21H and <i>ssadh</i> lines.....	111
Figure 59. Preliminary screening of the 21H x <i>Ler</i> and 17J x <i>Ler</i> F2 population on plate.	112
Figure 60. Schematic representation of the positions of markers designed to map the position of the EMS mutation on each chromosome	113

List of Tables

Table 1. Abundance of amino acids ($\mu\text{mol/g}$ FW) in the flower of wild-type and <i>gad1/2</i> plants	23
Table 2. Analysis of conductance per stomate in the abaxial and adaxial side of leaves from wild type and <i>gad1/2</i> plants	27
Table 3. Abundance of amino acids ($\mu\text{mol/g}$ FW) in the leaves and roots of wild type and <i>gad1/2</i> plants under control and 150 mM NaCl treatment conditions	37
Table 4. Abundance of amino acids ($\mu\text{mol/g}$ FW) in leaves of wild-type, <i>gad1</i> and <i>gad2</i> plants grown under normal growth conditions.....	40
Table 5. Rough mapping of EMS-induced mutation in lines 17J (A) and 21H (B) after.....	114
Table 6. Mapping of EMS-induced mutations in lines 17J (A) and 21H (B) with chromosome 2 and 5-specific primers	115
Table 7. Mutations obtained in chromosome 5 of line 17J	117
Table 8. Mutations obtained in chromosome 5 of line 21H.....	118
Table 9. Analysis of SNP's that resulted in amino acid substitutions.....	119
Table 10. Mutations obtained in chromosome 2 of line 17J and 21H.....	121

Acknowledgement

First of all, I would like to thank the Almighty God and his mother Saint Virgin Marry for helping me throughout my life. Next, I would like to thank the graduate school IGSDHD program for financial support during my stay in Germany. I am grateful for Prof. Ulf-Ingo Fluegge who allowed me work in his lab, supervised my work and commented on my dissertation. My unreserved gratitude also extended to Dr. Frank Ludewig who supervised my work on daily basis, and evaluated my dissertation critically. I cannot go without mentioning the support of the graduate school office, Dr. Isabell Witt and Kathy Joergen, who both helped me tremendously in private issues. My sincere appreciation also goes to Dr. Nina Zellerhoff and Dr Stephan Kruegger for their technical support and Dr. Benni Franka of Bonn for his provision of the leaf porometer without whom the project would not have been successfully completed. I would like to thank all members of the group of Prof. Fluegge who gave me constructive ideas during the progress seminar and private discussions. The moral contribution of my wife Lydia Getachew is worthy of anything, without her I would not have finished my study with great satisfaction. Her assistance during my difficult days was immense. I have to say that I would not be here without the valuable advice of my father Worku Mekonnen. Simply, he is an outstanding father who advised me almost day and night from my early elementary school days. He guided me through my successful educational career. May God bless my father!!! The last, but not the least, I would like to thank my mother, sisters and friends back in Ethiopia and also friends here in Germany for giving me a morale throughout my study periods..

Abstract

γ -Aminobutyric acid (GABA) is a four carbon non protein amino acid, and the pathway that involves its production and degradation is called the GABA shunt. The GABA shunt is a short enzymatic pathway that involves three enzymes: glutamate decarboxylase (GAD), GABA transaminase (GABA-T) and succinic semi aldehyde dehydrogenase (SSADH). GABA shunt is conserved almost in all organisms studied so far. The pathway starts in the cytosol and finishes in mitochondria in higher organisms like plants and mammals, whereas, in yeast it is exclusively cytosolic. The presence of GABA in plants has been known since over half a century ago. The induction of its accumulation under biotic and abiotic stresses has been well documented. However, the specificity of the response and the role of GABA and the GABA shunt under stress conditions have been elusive. Several Arabidopsis GABA shunt mutants have been studied and were shown to have defects in vegetative growth, reproductive growth and response to stress. To describe some, *gad1* mutant was shown to have a reduced root growth. The *pop2-1* mutant, defective in the activity of GABA-T, accumulated a very high level of GABA in the flower and that led to a pollen tube elongation defect. Arabidopsis *ssadh* mutants exhibited a severe growth phenotype, accumulated high γ -hydroxybutyric acid (GHB) and H₂O₂, and were sensitive to high-light conditions.

In this work, several mutant lines have been generated and investigated to answer a range of questions; these include study on the specificity of the GABA response during abiotic stress, identifying the reasons for severe *ssadh* growth phenotype and suppression of the *ssadh* phenotype. Arabidopsis *gad1/2* mutant is depleted in GABA and is unable to induce GABA synthesis under drought, salt and osmotic stress. Hence, the mutant plants were oversensitive to these stresses, indicating that GABA accumulation during abiotic stresses was a specific response. In an attempt to identify the cause of *ssadh* phenotype, exogenous GHB was fed to wild type and *ghbdh1/2* mutants. The GHB application, however, did not elicit the severe *ssadh*-like phenotype. But, treatment of wild type and *ghbdh1/2* mutant with SSA re-produced the *ssadh* phenotype, suggesting that SSA, but not GHB, was the cause of the severe *ssadh* phenotype. To suppress the *ssadh* phenotype, the potential accumulation of SSA was blocked by simultaneous mutation of *Gad1/2*. This, indeed, partially suppressed the *ssadh* phenotype. Suppression of *ssadh* phenotype mediated by ethyl methanesulfonate (EMS) induced mutation was also successful. Based on the range of phenotypes obtained in GABA shunt mutants, further studies on the role of the GABA shunt in plants is important.

Zusammenfassung

γ -Aminobuttersäure (GABA) ist eine aus vier C-Atomen bestehende Aminosäure, die nicht in Proteinen vorkommt. Der Stoffwechsel zur Herstellung und zum Abbau von GABA wird als ‚GABA shunt‘ bezeichnet. Dieser kurze Stoffwechselweg besteht aus drei enzymatischen Schritten, die die Glutamat Decarboxylase (GAD), die GABA Transaminase (GABA-T) und die Succinsemialdehyd Dehydrogenase katalysieren. Der Stoffwechselweg ist in fast allen bisher untersuchten Organismen konserviert und beginnt in höheren Organismen wie Pflanzen und Säugetieren im Cytosol und endet in den Mitochondrien, in Hefe ist er rein cytosolisch. Das Vorhandensein von GABA in Pflanzen ist seit über einem halben Jahrhundert bekannt. Ebenso ist gut dokumentiert, dass GABA in Pflanzen bei biotischem und abiotischem Stress akkumuliert. Die Spezifität dieser Stressantwort und die Rolle von GABA bzw. des ‚GABA shunt‘ dabei sind allerdings bisher unklar. Einige ‚GABA shunt‘ Mutanten wurden bereits untersucht. Es konnte gezeigt werden, dass bei diesen Defekte in der vegetativen und reproduktiven Wachstumsphase sowie in der Stressantwort auftraten. Um nur ein paar zu nennen; von der *gad1* Mutante konnte ein verringertes Wurzelwachstum gezeigt werden. Die *pop2-1* Mutante ohne GABA-T Aktivität akkumuliert sehr viel GABA in Blüten, was zu einem Defekt im Pollenschlauchwachstum führt. Arabidopsis *ssadh* Mutanten zeigen einen starken Wachstumsphänotyp, akkumulieren GABA und H₂O₂ und sind besonders sensitiv gegenüber Starklicht.

Im Verlauf dieser Arbeit wurden einige Mutanten hergestellt und untersucht, um eine Reihe von Fragen zu klären, u.a. ob die GABA-Antwort auf abiotischen Stress spezifisch ist, und was der Grund für den starken *ssadh* Phänotyp ist, und wie er unterdrückt werden kann. Die Arabidopsis *gad1/2* Mutante enthält weniger GABA und kann die GABA-Synthese auch bei Trocken-, Salz- und osmotischem Stress nicht induzieren. Die Mutanten sind überempfindlich gegenüber diesen Stressarten, was darauf hindeutet, dass die Akkumulation von GABA bei Stress eine spezifische Antwort ist. Beim Versuch, den Grund für den *ssadh* Phänotyp herauszufinden, wurden Wildtyp-Pflanzen und *ghbdh1/2*-Mutanten mit exogenem GHB versorgt, was nicht zu einem *ssadh*-ähnlichen Phänotyp führte. Allerdings konnte der *ssadh* Phänotyp durch Versorgung der Pflanzen mit SSA reproduziert werden, was nahelegt, dass die Akkumulation von SSA und nicht die von GHB den starken *ssadh* Phänotyp hervorruft. Um den *ssadh* Phänotyp zu unterdrücken, sollte die Akkumulation von SSA mittels Mutation von *GAD1* und *GAD2* verhindert werden. Dieser Ansatz führte in der Tat zu einer partiellen Rettung des Phänotyps. Ein anderer Ansatz, den *ssadh* Phänotyp zu reprimieren, war ebenfalls erfolgreich, die Mutagenese mit Ethylmethansulfonat (EMS). Basierend auf einer Reihe von Phänotypen der ‚GABA shunt‘ Mutanten wird es auch in Zukunft wichtig sein, dessen Rolle in weiteren Experimenten zu untersuchen.

General Introduction

γ -amino butyric acid (GABA) is a four carbon non-protein amino acid which is naturally produced in many organisms. GABA differs from other amino acids which are incorporated into a protein by the fact that it has its amino group on the γ -carbon whereas the others have the amino group on the α -carbon. GABA in plants was discovered for the first time more than half a century ago (Steward et al. 1949). Later, in 1950 the compound was discovered as a component of the mammalian central nervous system (Roth et al., 2003). The metabolism of GABA involves the activity of three enzymes and the pathway is known as the GABA shunt. The GABA shunt generally involves the generation of GABA from the decarboxylation of glutamate by glutamate decarboxylase (GAD) in the cytosol, the transamination of GABA by GABA transaminase (GABA-T) to form succinic semialdehyde (SSA) and the oxidation of SSA to succinic acid (SA) by SSA dehydrogenase (SSADH) which then enters the TCA cycle (Fig. 1). GABA has a diverse function which varies from species to species. The components of the GABA shunt and the cellular compartment in which it is active differs from species to species. Here, the functions of GABA and the components of the GABA shunt in microbes, yeast, plants and mammals are briefly described.

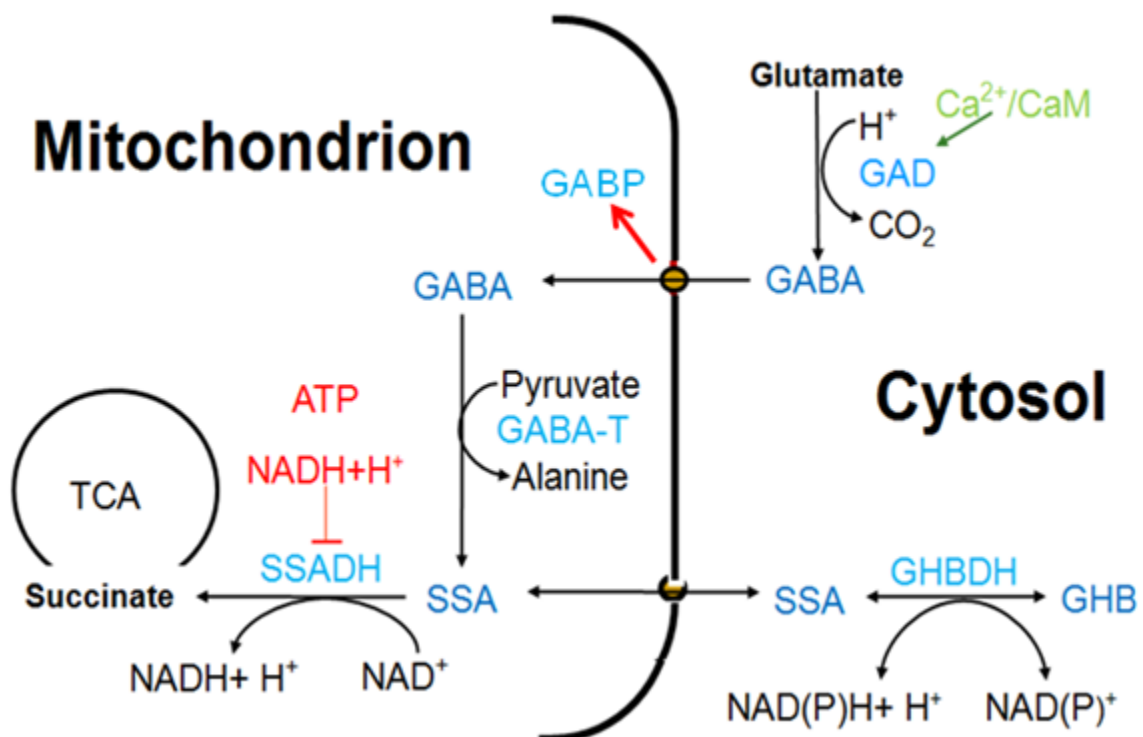


Figure 1. Schematic representation of the GABA shunt in *Arabidopsis*

I. Microbes

Most bacteria contain all GABA shunt genes. These are glutamate decarboxylase (GAD), GABA transporter, GABA transaminase and succinic semialdehyde dehydrogenase (SSADH). The number of copies of each gene existing in the genome is variable among the species. For example, the *E.coli* genome possesses two copies of *GAD* genes, *gadA* and *gadB* (Le Vo et al., 2011), whereas some strains of *Streptococcus thermophilus* has one gene copy (Somkuti et al., 2012). In contrast, *Pseudomonas syringae* pv. DC3000 and some strains of *Streptococcus thermophilus* do not have *GAD* genes at all (Somkuti et al., 2012; Park et al., 2010). Similarly, the GABA-T (*gabT*) and SSADH (*gabD*) are found in variable copy numbers among the bacterial species. *E. coli* possesses one copy of the *gabT* gene (Le Vo et al., 2011) which contrasts to *P. syringae* DC3000 with three copies of *gabT* genes (Park et al., 2010). *P. syringae* pv. tomato DC3000 is also known to contain three *gabD* gene copies. Since bacteria are organisms without membrane-bound compartments (organelles), all GABA shunt-related genes, except GABA transporter, are localized in the cytosol.

Mutants deficient in one of the GABA shunt genes has been characterized and exhibited sensitivity to various conditions. The synthesis of GABA has been demonstrated to consume protons and thereby confer tolerance to extreme acidity. The bacterial food-borne pathogen *L. monocytogenes* mutated in *gadDID2* (glutamate decarboxylase) genes accumulated a reduced amount of GABA and this is associated with a 3.2 log unit reduction in growth at pH 3.0 compared to the wild type (Karatzas et al., 2012). *Pseudomonas syringae* DC3000 strain lacking all three *gabT* genes was unable to utilize GABA from the host and is therefore unable to elicit hypersensitive response on tobacco leaves (Park et al., 2010). *E. coli* K12 strain defective in its NAD-dependent succinic semialdehyde dehydrogenase activity was shown to be sensitive to externally applied SSA, and also unable to utilize 4-hydroxyphenylacetate as a sole nitrogen source (Skinner and Cooper 1982).

GABA in bacteria is used as a source of nitrogen and carbon and as signaling molecule. *P. syringae* pv. tomato DC3000 strain was able to grow on GABA as a sole carbon and nitrogen source which is derived from the tomato apoplast (Rico and Preston, 2008; Park et al., 2010). *E. coli* K12 mutant strains, which have a several-fold higher activity of GABA-T, were able to grow on GABA as a sole carbon and nitrogen source (Dover and Halpern, 1972). Similarly, *Rhizobium leguminosarum* bv. *viciae* inoculated in liquid Vincent minimal medium (VMM)

supplemented with GABA as a sole nitrogen source were able to grow (Prell et al., 2002). In case of pathogenic bacteria, the utilization of GABA as carbon source from the host cell promotes virulence. The virulence of DC3000 *Pseudomonas* strain mutated in GABA-T (*gabT*) genes was reduced because of its inability to utilize the host GABA (Park et al., 2010).

Another important role of GABA is the modulation of quorum sensing. GABA was shown to mediate the interaction of plants and pathogens. The role of GABA in modulating quorum sensing is best described in *Agrobacterium*. Here GABA, like SSA and GHB, is also metabolized *via* a pathway encoded by the *attKLM* operon (Chevrot et al., 2006). The activation of this operon by GABA basically represses the production of *N*-(3-oxooctanoyl)-homoserine lactone (OC8-HSL), which is a quorum-sensing signal in this bacterium (Chevrot et al., 2006).

II. Yeast

The GABA shunt in *Saccharomyces cerevisiae* comprises three enzymes (GAD, GABAT and SSADH). Unlike higher plants and animals, the GABA shunt in yeast is exclusively localized in the cytosol. The *S. cerevisiae* genome possesses one copy of the glutamate decarboxylase (*Gad1*), GABA transaminase (*UGA1*) and succinic semialdehyde (*UGA2*) genes. The genome also contained a vacuolar membrane GABA transporter, *UGA4*, (Andre et al., 1993; Andre and Jauniaux., 1990; Coleman et al., 2001). The expression of the GABA shunt genes (*UGA1* and *UGA2*) is regulated by Uga3p, Dal81p and Gln3p (Ramos et al., 1985; Vissers et al., 1989). The expression of *UGA1* and *UGA4* is enhanced by the presence of GABA (Ramos et al., 1985).

S. cerevisiae strains defective in GABA shunt gene have been characterized and exhibited sensitivity to various stresses. Yeast *ugal* strains showed a three-fold reduced growth on media containing glutamate and GABA as a nitrogen source compared to wild type, and this was associated with an increased accumulation of SSA (Ramos et al., 1985). On the other hand, overexpression of glutamate decarboxylase increased the tolerance to oxidants, H₂O₂ and diamide (Coleman et al., 2001).

III. Mammals

Since its discovery in mammalian brain in 1950, GABA is known to serve as an inhibitory neurotransmitter (Roberts, 1986; DeFelipe 1993; Ribak and Yan 2000). GABA acts at inhibitory synapses by binding to a transmembrane receptor in the plasma membrane. In mammals, three GABA receptors, GABA_A, GABA_B and GABA_C, have been identified. GABA_A and GABA_C receptors are both ligand-gated chloride channels (Owen and Kriegstein 2002). GABA_B, on the other hand, is chloride-independent G-protein-coupled receptor (Bowery et al., 1980).

Human cell and rat are the two most widely used model systems to study the metabolism of GABA in mammals. The GABA shunt in mammals comprises a cytosolic GAD and a mitochondrial GABA- and SSADH (Petroff, 2002). In addition, the existence of a GABA transporter (GAT1) in glutamatergic neurons has been reported (Roettger and Amara 1999; Martin and Tobin 2000). The human and rat genome contain two copies of GAD genes (GAD65 and GAD67) and one copy of GABA-T and SSADH (Petroff, 2002; Niranjala et al., 1995). The expression of GAD67 is dominant in both organisms and was shown to be responsible for the majority of GABA (~70%) produced in the brain (Martin and Tobin 2000). Mice completely lacking GAD67 activity died immediately after birth indicating the major role of GAD67 (Asada et al., 1997; Ji et al., 1999). The activation of GAD by inorganic phosphate and its inhibition by ATP, GABA and aspartate has been reviewed previously (Petroff et al., 2002).

In humans, the most known disorder associated with a GABA shunt deficiency is GHB aciduria. This disorder is caused by the deficiency in SSADH function, and manifested by an increased accumulation of gamma hydroxybutyric acid (GHB) in physiological fluids, such as plasma, urine etc. (Jacobs et al., 1981, Hogma et al., 2001). A deficiency in GABA-T function in human is rare, and causes an abnormal phenotype which includes psychomotor retardation, hypotonia, hyperreflexia, lethargy etc. (Medina Kauwe et al., 1999).

IV. Plants

GABA in plants has been discovered for the first time more than half a century ago in potato tuber (Steward et al., 1949). However, little attention has been given to its role in plants until recent years. GABA has been associated with biotic and abiotic stress responses. Mazzucotelli

et al. (2006) has reported a rapid accumulation of GABA in barley and wheat seedlings in response to cold treatment. GABA accumulation also increased in the shoot and root of *Arabidopsis* plants after salt treatment (Renault et al., 2010). Apart from stress response, GABA has also been implicated in plant development. Akhiro et al. (2008) reported an accumulation of GABA in tomato fruit immediately before the breaker stage. Recently, GABA was associated with a signaling function in plants although the receptors have not been identified yet (Palinevelu et al., 2003).

In plants, the GABA shunt comprises a cytosolic GAD, and mitochondrial GABA-T and SSADH. In addition, cytosolic (GAT1) and mitochondrial (GABP) GABA transporters were shown to be involved in GABA metabolism (Meyer et al., 2006; Michaeli et al., 2011). Unlike mammalian GADs, most plant GADs characterized so far are regulated by calcium / calmoduline (Zik et al., 1996). The number of *GAD* genes varies between species; however, GABA-T and SSADH are encoded by a single gene in most plants. The *Arabidopsis* genome contain five copies of *GAD* genes (*GAD1*, At5g17330; *GAD2*, At1g65960; *GAD3*, At2g02000; *GAD4*, At2g02010; *GAD5*, At3g17760). However, only two nuclear encoded GAD genes have been reported in rice (Akama and Takaiwa, 2007).

Mutants of the GABA shunt in *Arabidopsis* have been characterized and displayed variable growth phenotypes. Plants deficient in GABA-T function exhibited a defect in reproductive organs (Palinevelu et al., 2003). *Arabidopsis gaba-t (pop2)* plants accumulated high amounts of GABA in flowers leading to a failure in pollen tube elongation and also a misguidance of the pollen tube (Palanivelu et al., 2003). The *pop2* mutant also displayed an oversensitive phenotype against salt stress (Renault et al., 2010). *Arabidopsis* plants which are deficient in SSADH activity displayed a stunted growth, necrotic leaf lesions (Fait et al., 2004) and an elongated life cycle. These *ssadh* plants are further sensitive to high light intensity. These *ssadh* plants accumulated higher levels of hydrogen peroxide and GHB. Interestingly, the mutant phenotype of *ssadh* plants was completely suppressed by a simultaneous mutation of the *GABA-T* gene (Ludewig et al., 2008).

References

- Akama K, Takaiwa F (2007)** C-terminal extension of rice glutamate decarboxylase (OsGAD2) functions as an autoinhibitory domain and overexpression of a truncated mutant results in the accumulation of extremely high levels of GABA in plant cells. *J. Exp. Bot.* 58: 2699–2707.
- Akihiro T, Koike S, Tani R, et al. (2008)** Biochemical mechanism on GABA accumulation during fruit development in tomato. *Plant and Cell Physiology* 49:1378–1389.
- Andre B, Hein C, Grenson M, and Jauniaux JC (1993)** Cloning and expression of the UGA4 gene coding for the inducible GABA-specific transport protein of *Saccharomyces cerevisiae*. *Mol. Gen. Genet.* 237:17–25.
- Andre B, Jauniaux JC (1990)** Nucleotide sequence of the yeast *UGA1* gene encoding GABA transaminase. *Nucleic Acids Res. USA* 18:3049.
- Asada H, Kawamura Y, Maruyama K, et al. (1997)** Cleft palate and decreased brain gammaaminobutyric acid in mice lacking the 67-kDa isoform of glutamic acid decarboxylase. *Proc. Natl. Acad. Sci.* 94:6496–9.
- Bowery NG, Hill DR, Hudson AL, et al. (1980)** Baclofen decreases neurotransmitter release in the mammalian CNS by an action at a novel GABA receptor. *Nature* 283: 92–94.
- Chevrot R, Rosen R, Haudecoeur E, et al. (2006)** GABA controls the level of quorum-sensing signal in *Agrobacterium tumefaciens*. *Proc. Natl. Acad. Sci. USA* 103:7460–7464.
- Coleman ST, Fang TK, Rovinsky SA, et al., (2001)** Expression of a glutamate decarboxylase homologue is required for normal oxidative stress tolerance in *Saccharomyces cerevisiae*. *J. Biol. Chem.* 276:244–250.
- Cooper JR, Bloom FE, Roth RH (2003)** *The Biochemical Basis of Neuropharmacology*. Oxford University Press. p106.
- DeFelipe J (1993)** Neocortical neuronal diversity: chemical heterogeneity revealed by colocalization studies of classical neurotransmitters, neuropeptides, calcium-binding proteins, and cell surface molecules. *Cereb Cortex* 3:273–89.
- Dover S, Halpern YS (1972)** Utilization of γ -Aminobutyric Acid as the Sole Carbon and Nitrogen Source by *Escherichia coli* K-12 Mutants. *Journal of Bacteriology*: 835-843.
- Fait A, Yellin A, Fromm H (2004)** GABA shunt deficiencies and accumulation of reactive oxygen intermediates: insight from *Arabidopsis* mutants. *FEBS Letters* 579: 415–420.
- Hogema BM, Gupta M, Senephansiri H, et al. (2001)** Pharmacologic rescue of lethal seizures in mice deficient in succinate semialdehyde dehydrogenase. *Nat Genet* 29:212-216.
- Jakobs C, Bojasch M, Monch E, et al. (1981)** Urinary excretion of gamma-hydroxybutyric acid in a patient with neurological abnormalities. The probability of a new inborn error of metabolism. *Clinica Chimica Acta* 111: 169-178.

Ji F, Kanbara N, Obata K (1999) GABA and histogenesis in fetal and neonatal mouse brain lacking both isoforms of glutamic acid decarboxylase. *Neurosci Res* 33:187–94.

Karatzas KAG, Suur L, O’Byrne CP (2012) Characterization of the Intracellular Glutamate Decarboxylase System: Analysis of Its Function, Transcription, and Role in the Acid Resistance of Various Strains of *Listeria monocytogenes*. *Appl. Environ. Microbiol.* 2012, 78(10):3571.

Le Vo TD, Kim TW, Hong SH (2011) Effects of glutamate decarboxylase and gamma-aminobutyric acid (GABA) transporter on the bioconversion of GABA in engineered *Escherichia coli*. *Bioprocess Biosyst Eng* (2012) 35:645–650.

Ludewig F, Hueser A, Fromm H, Beauclair L, Bouche N (2008) Mutants of GABA transaminase (POP2) suppress the severe phenotype of succinic semialdehyde dehydrogenase (*ssadh*) mutants in *Arabidopsis*. *PLoS ONE* 3(10): e3383. doi:10.

Martin DL, Tobin AJ (2000) Mechanisms controlling GABA synthesis and degradation in the brain. *GABA in the nervous system: the view at fifty years*. Philadelphia: Lippincott Williams and Wilkins. 25–41.

Mazzucotelli E, Tartari A, Cattivelli L, Forlani G (2006) Metabolism of γ -aminobutyric acid during cold acclimation and freezing and its relationship to frost tolerance in barley and wheat. *Journal of Experimental Botany* 57: 3755–3766.

Medina-Kauwe LK, De Meirleir LT, et al. (1999) 4-aminobutyrate aminotransferase (GABA-transaminase) deficiency. *J. Inherit. Metab. Dis.* 22: 414-427.

Meyer A, Eskandari S, Grallath S, Rentsch D (2006) AtGAT1, a High Affinity Transporter for γ -Aminobutyric Acid in *Arabidopsis thaliana*. *The Journal of Biological Chemistry* 281 (11): 7197–7204.

Michaeli S, Fait A, Lagor K, et al. (2011) A mitochondrial GABA permease connects the GABAshunt and the TCA cycle, and is essential for normal carbon metabolism. *The Plant Journal* 67(3):485-98.

Niranjala JKT, Lali MK, Gibson KM (1995) Gamma-aminobutyric acid (GABA) metabolism in mammalian neural and non-neural tissues. *Camp. Biochem. Physiol.* 112A (2): 247-263.

Owens DF, Kriegstein AR (2002) Is There More To GABA Than Synaptic Inhibition? *Neuroscience* 3:717.

Petroff OAC (2002) GABA and Glutamate in the Human Brain. *The Neuroscientist* 2002 8: 562.

Palanivelu R, Brass L, Edlund AF, Preuss D (2003) Pollen tube growth and guidance is regulated by POP2, an *Arabidopsis* gene that controls GABA levels. *Cell* 114:47.

Park DH, Mirabella R, Bronstein PA, et al. (2010) Mutations in γ -aminobutyric acid (GABA) transaminase genes in plants or *Pseudomonas syringae* reduce bacterial virulence. *Plant J.* 64: 318–330.

Prell J, Boesten B, Poole P, Prierer UB (2002) The *Rhizobium leguminosarum* bv. *viciae* VF39 gamma aminobutyrate (GABA) aminotransferase gene (*gabT*) is induced by GABA and highly expressed in bacteroids. *Microbiology* 148:615–623.

Ramos F, Guezzar M, Grenson M, Wiame JM (1985) Mutations affecting the enzymes involved in the utilization of 4-aminobutyric acid as nitrogen source by the yeast *Saccharomyces cerevisiae*. *Eur. J. Biochem.* 149:401–404.

Renault H, Roussel V, Amrani AEl, et al. (2010) The *Arabidopsis pop2-1* mutant reveals the involvement of GABA transaminase in salt stress tolerance. *BMC Plant Biol*, 10:1–16.

Renault H, Roussel V, Amrani A El, et al. (2010) The *Arabidopsis pop2-1* mutant reveals the involvement of GABA transaminase in salt stress tolerance. *BMC Plant Biol.* 10:20.

Ribak CE, Yan XX (2000) GABA neurons in the neocortex. In: Martin DL, Olsen RW, editors. *GABA in the nervous system: the view at fifty years*. Philadelphia: Lippincott Williams and Wilkins. P. 357–368.

Rico A, Preston GM (2008) *Pseudomonas syringae* pv. *tomato* DC3000 uses constitutive and apoplast-induced nutrient assimilation pathways to catabolize nutrients that are abundant in the tomato apoplast. *Molecular Plant-Microbe Interactions* 21(2): 269–282.

Roberts E (1986) Failure of GABAergic inhibition: a key to local and global seizures. *Adv Neurol* 44:319–341.

Roettger VR, Amara SG (1999) GABA and glutamate transporters: therapeutic and etiological implications for epilepsy. *Adv Neurol.* 79:551–560.

Somkuti GA, Renye Jr. JA, Steinberg DH (2012) Molecular analysis of the glutamate decarboxylase locus in *Streptococcus thermophilus* ST110. *J. Ind Microbiol Biotechnol.* 39(7):957-963.

Skinner MA, Cooper RA (1982) An *Escherichia coli* Mutant Defective in the NAD-Dependent Succinate Semialdehyde Dehydrogenase. *Arch Microbiol* 132:270-275.

Steward FC, Thompson JF, Dent CE (1949) γ -Aminobutyric acid: a constituent of the potato tuber? *Science* 110:439-440.

Vissers S, Andre B, Muyldermans F, Grenson M (1989) Positive and negative regulatory elements control the expression of the *UGA4* gene coding for the inducible 4-aminobutyric-acid-specific permease in *Saccharomyces cerevisiae*. *Eur. J. Biochem.* 181:357–361.

Zik M, Arazi T, Snedden WA, Fromm H (1998) Two isoforms of glutamate decarboxylase in *Arabidopsis* are regulated by calcium/calmodulin and differ in organ distribution. *Plant Mol. Biol.* 37:967–975.

Chapter one: Characterization of *Arabidopsis gad* mutants

1. Introduction

The GABA shunt is the major route for GABA metabolism in plants although there are indications that GABA can also be synthesized from polyamines like spermidine and putrescine (Bouchereau et al., 1998). Glutamate decarboxylase (GAD) catalyzes the decarboxylation of glutamate to GABA. The enzyme is localized in the cytosol in all organism studied so far. GADs have been discovered in many species; however, only plant GADs are known to bind calmoduline (CaM) (Baum et al., 1993; Baum et al., 1996). The *Arabidopsis* genome contains of five *GAD* genes which are dispersed over four chromosomes.

The five *GAD* genes share significant sequence similarities and show organ-specific expression patterns. *GAD1* is mainly expressed in roots, and *GAD2* transcripts are detectable in almost all organs (Zik et al., 1998, Turano and Fang, 1998). *GAD5* is specifically expressed in floral organs. *GAD3* and *GAD4* are only weakly expressed. However, *GAD3* transcripts have been detected in siliques under normal growth conditions and in shoots under stress conditions; *GAD4* is also detected in shoots under such conditions (Renault et al., 2010). The activity GAD is enhanced by an acidic pH (Shelp et al., 1999, Shelp et al., 2006). The C-terminus of GAD protein contains a calmoduline (CaM) binding domain, and a protein lacking this domain is inactive (Zik et al., 1998). The C-terminus of the wheat OsGAD has been shown to function as an auto-inhibitor, as the truncated form promoted the over-accumulation of GABA (Akama and Takaiwa, 2007). Furthermore, Baum et al. (1996) reported the importance of CaM binding domain for the regulation of GABA metabolism in petunia plants.

GABA has been shown to accumulate in response to biotic and abiotic stresses (Bown and Shelp, 1997; Kinnersley and Turano, 2000). The possible role of GABA in maintaining e.g., C/N balance, regulating cytosolic pH, scavenging of reactive oxygen species and many more has been discussed previously (Bouche and Fromm, 2004). In recent years, the role of GABA in reproduction has become clear. The *Arabidopsis pop2* mutants (*gaba-t*), which over-accumulated GABA in flowers, exhibited a pollen tube elongation defect after pollination as shown by *in vitro* and *in vivo* experiments (Palanivelu et al., 2003; Renault et al., 2011). Furthermore, GABA has been demonstrated to mediate plant pathogen interactions. Park and co-workers (2010) reported a reduced growth of a *Pseudomonas* strain on *pop2-1* leaves

accumulating higher GABA contents which in turn has been correlated to a reduced expression of virulence genes encoded by the pathogen. An increase in GABA accumulation from 0.8mM to 2-3mM in tomato apoplast after infection by *Cladosporium fulvum* has also been reported (Solomon and Oliver, 2002). The preferential accumulation of GABA compared to proline in tobacco leaves in response to water stress showed its role as in antioxidant activity (Liu et al., 2011). The effect on vegetative growth by modifying gene expression patterns (Renault et al., 2011) has demonstrated the range of roles GABA could play in normal plant growth and development.

Recently, GABA could be linked to a signaling function in plants. In the mammalian central nervous system the signaling function of GABA together with the receptor molecules, GABA_A, GABA_B and GABA_C, has already been established (Takeuchi and Onodera, 1972; Shimada et al., 1992). To date no GABA receptor is known in plants. However, a group of 20 genes (AtGLRs) encode proteins which share structural homologies with mammalian glutamate receptors (iGLuRs) (Lam et al., 1998; Lacombe et al., 2001). This class of proteins also contains ligand binding domains which share homology with the GABA_B receptors of vertebrates. AtGLRs are assumed to be involved in glutamate signaling despite there is a report that shows binding of glycine as well (Dubos et al., 2003). The potential interaction of GABA with this AtGLR domain thereby modulating the response to external stimuli has been discussed (Bouche et al., 2003). Although there are reports indicating the coupling of glutamate and calcium signaling through AtGLR (Kim et al., 2001; Dubos et al., 2003), GABA failed to trigger the transient elevation of calcium in Arabidopsis plants expressing aequorin (Lancien and Roberts, 2006).

To date, many reports indicate an accumulation of GABA in response to various biotic and abiotic stresses. However, the specificity of the response and the primary role or importance of GABA, i.e. as metabolite or in signaling, under such stress conditions remained vague. Studies regarding the role of GABA on plant growth and development or on plant stress response were carried out either by feeding non-physiological concentrations of GABA or by using mutant lines accumulating high GABA amounts. The external application of GABA could potentially have a pleiotropic effect. The use of high GABA-accumulating lines indeed provides a basis for understanding the role of GABA. Further studies with the opposite scenario, i.e. less GABA-containing lines, would further allow the insights into the role GABA could have in normal growth and in plant stress responses.

In this study, a direct evidence for the specificity of the response and the involvement of GABA under salt and drought stress conditions was provided by investigating the GABA-less *gad1/2* mutants. The findings indicate that under salt and drought stress conditions the GABA shunt is a major route for the metabolism of glutamate. The Arabidopsis *gad1/2* knockout plants have been found to be sensitive to salt and drought stress. The sensitivity to salt stress was related to the osmotic component of the salt treatment. Exposure to drought stress also revealed an early wilting of the *gad1/2* leaves compared to the wild type. The wilting phenotype was correlated to an increase in transpiration rate in the abaxial and adaxial sides of the leaf. Further study on the leaf anatomy revealed a 15% increase in stomata density on both sides of *gad1/2* leaves. Calculation of the conductance per stoma indicated an increment of stomata aperture. The findings provided here also support the involvement of the GABA shunt in leaf development. Taking all data together we conclude that the rapid response of GABA plays a signaling role at the early stages of the stress and further accumulation serves as an osmo-protectant.

2. Methodology

2.1. Generation of single and double mutants

The respective F1 single mutants, *gad1* (SALK_017810) and *gad2* (GK_474E05) seeds were purchased from the respective stock centers. F2 plants were screened for homozygosity by genotyping. For that, genomic DNA extraction from the individual plants was carried out as described; Leaf samples were collected in 1.5 ml eppendorf tubes containing 2-3 mm size glass beads and snap-frozen in liquid nitrogen. The samples were crushed to powder using a tissue lyzer (Qiagen, Cat.No.85220) for three minutes at a frequency of 20 s⁻¹. Then, 200 µl of extraction buffer (0.2 M Tris HCl, pH 7.5, 25 mM EDTA, 0.5% SDS and 250 mM NaCl) was added and homogenized for another 90 sec. The mixture was centrifuged for one min at 14,000 rpm and 150 µl of the supernatant was transferred to a new tube. Next, an equal volume of 100% isopropanol was added, mixed and incubated at room temperature for five minutes. Finally, the mixture was centrifuged at maximum speed for five minutes and the pellet was dissolved in 100 µl ddH₂O. PCR was performed using 2 µl of the DNA extract. For the generation of the double mutant, the respective single mutants were crossed by emasculating the mother plant, followed by pollination with the pollen from the male parent. To find the homozygous double mutant, a similar procedure was applied as for the single mutants. The generated double mutant was termed *gad1/2*.

2.2. Phenotypic analysis

2.2.1. Rosette area, cell number, shoot weight and root weight

Seeds of the wild type and *gad1/2* genotypes were germinated and grown on soil under green house condition. Approximately, one week after germination, the individual seedlings were transplanted to small pots filled with soil. The plants were maintained under green house conditions for another two weeks and pictures were taken from 14 plants of each genotype. The total rosette area was calculated using Flaechenbestimmung Blatt software (V.1.0.4.6 Dating GmbH, Tuebingen, Germany). For cell number determination, the third or fourth leaves of at least ten plants were collected and de-pigmented by immersing the leaves in 100% ethanol, and then incubating at 60 °C for 20 minutes. The procedure was repeated two times and the de-pigmented leaves were rinsed with distilled water. The picture of the leaf lower epidermis was taken under a fluorescent microscope in a bright field using the 40x objective. The dimensions of the microscopic field were determined using a scale bar. For each leaf, the cell

count was performed at least four positions (microscopic fields) on the leaf. For shoot and root fresh weight analysis, 20 four-week-old wild type and *gad1/2* plants were harvested and immediately weighed.

2.2.2. Plant growth and stress treatment conditions

A) On soil

Long day: Seeds of Wt and *gad1/2* mutant Arabidopsis plants were germinated and grown on soil in a greenhouse. At two-leaf stage (~ten days after sowing), the individual seedlings were transferred to small pots of six cm in diameter filled with soil and maintained in the greenhouse (16 h/8 h light / dark cycle). Two weeks after transplanting, the salt stress treatment without or with 150 mM NaCl was commenced, and the treatment was repeated every three days. For drought stress treatment, the watering was withheld from drought-treated plants, and the control plants were supplied with water every third day. For the osmotic stress treatment four-week-old plants were treated without (control) or with 300 mM mannitol. For GABA feeding experiment, both wild type and *gad1/2* plants were irrigated every three days from two- leaf stage on.

Short day: Seeds of Wt and *gad1/2* were sown and germinated in the green house. Approximately ten days after sowing, the seedlings were transferred to pots as described above. The trays were then transferred to short day conditions into a growth chamber (16 h dark, ~23°C and 60-70% RH). Two weeks after transplanting, the salt stress treatment without or with 150 mM NaCl was started and continued every fourth day. For drought treatment plants of the same age were continued to get water (control) or prevented from getting water (drought stress).

B) On plates

Seeds of Wt, *pop2-1* and *gad1/2* were germinated and grown on ½ MS agar plates for ten days. Then, seedlings of the three genotypes were transferred to a fresh sucrose-free ½ MS plate without or with 50 mM and 100 mM NaCl. For the osmotic stress treatment, the plantlets were transferred to ½ MS plates containing 100 mM, 200 mM and 300 mM mannitol. The tip of the roots was marked to monitor growth. The plates were then incubated in a growth chamber under long day (16 h/8 h day / night) condition. Pictures were taken five

days after transfer. The ability to grow on low potassium was monitored by transferring 10-day-old seedlings to modified ½ MS plates containing 5 µM, 50 µM, 100 µM, 200 µM, 300 µM, 400 µM and 500 µM KCl. To get better information about the role of GABA in potassium uptake, high GABA accumulating *pop2* line was included in the experiment. The preparation of low potassium containing plates was carried out essentially as described by Renault et al. (2010).

2.3. Analysis of water content

To quantify the drought and osmotic stress phenotype, water content analysis was performed as follows. The whole above-ground tissue was harvested from the control and drought-stressed wild type and *gad1/2* plants. The fresh weight of the plants was immediately measured and the samples were oven dried at 80°C for two days. The sampling was continued every other day for plants growing in the growth chamber, and every day for plants grown under green house conditions for six rounds. Each day, five plants per treatment / genotype were collected and recorded. The weight of the dried samples was measured and the percent water content was calculated as shown below. The percent water content was plotted against the treatment duration.

$$\%WC = (FW - DW) / FW * 100$$

where, WC is water content; FW is fresh weight and DW is dry weight.

2.4. Analysis of stomata conductance, number and gas exchange

Seeds of Wt, *gad1*, *gad2* and *gad1/2* were germinated and grown on soil under green house conditions. For stomata counting, the third and fourth leaves were marked. After three weeks of growth, watering was stopped and stomata conductance was measured on both the abaxial and adaxial sides of a leaf using a leaf porometer (Model SC-1, Decagon Devices, Inc). The measurement was performed every day at noon for 6 days. Five plants per genotype and three leaves per plant were measured every day. For stomata counting, the marked third and fourth leaves were collected from wild type and *gad1/2* plants, and the chlorophyll was removed by ethanol treatment and incubation at 65°C for 20 min. The non-green leaves were placed on a slide and stomata were counted under the microscope. For each leaf three counts were performed on three different microscopic fields. A total of 26 leaves were analyzed from each genotype.

For gas exchange measurement, two plants each from wild type and *gad1/2* were taken and incubated overnight in the dark. The next day, each plant/pot was placed into a cuvette to which 345 ppm CO₂ source was attached to. The detector was connected to the three cuvettes via a plastic tube. The two tubes were connected to two cuvettes containing the plants and the third tube connected to the reference water vapor source. The detector measures the relative H₂O content compared to the reference, depending on the stomata opening and closure regulated by light, CO₂ and ABA treatment. The experimental set up was established as follows. First, the whole system was run with empty cuvettes for 20 minutes under dark condition to equilibrate the system. Next, the plants were placed in the cuvettes in dark condition and the moisture content was measured for 45 minutes. Following this, red light was turned on both plants and the moisture content from both plant cuvettes was measured for 45 minutes. Blue light was added to the previous red light and the measurement was continued for another 45 minutes. After 45 minutes, only the blue light was turned off and the moisture content was measured for another 45 minutes. Next, the red light was turned off to leave the plants in dark, and the moisture content was measured for 45 minutes. Finally, calibration of the measurements was performed by diluting the CO₂ source with gaseous N₂ flowing at 20 ml/min for 20 minutes. For the ABA response measurement, four leaves with the longest petiole were taken from overnight dark incubated wild type and *gad1/2* plants. The petioles of the leaves were immediately immersed into water, and the tip of the petioles (~2-3mm) was immediately removed with a sharp razor. The leaves were allowed to suck in water through the petioles for four to five minutes. Care was taken to avoid any contact of water and the leaf blade. Next, the leaves were transferred to a modified 50 ml falcon tube containing 15ml water in which the petioles of the leaves were inserted into the water via the opening provided at the center of the cap. The injection of ABA (10 µM) was carried out by syringe and needle into the falcon tube through the cap opening. The measurement of the stomata response was carried out as described above. The detector measures the water content every second.

2.5. Expression analysis of target genes

A) RNA extraction

Leaf samples (~100-200 mg) were collected from control and 150 mM NaCl treated wild type and *gad1/2* plants, and snap-frozen in liquid nitrogen. RNA extraction was carried out as described before with minor modifications (Logemann et al., 1987). Briefly, frozen tissue was

crushed to powder using a pre-cooled electrical drill machine. Immediately, 1 ml of Z6 buffer (8 M Guanidium hydrochloride, 20 mM MES, 20 mM EDTA, pH 7.0) containing 0.7% (v/v) beta-mercaptoethanol was added and homogenized by vortexing. Then, 500 µl PCI (Phenol: Chloroform: Isoamylalcohol 25:24:1) was added and mixed by inverting the tube ten to 15 times. After incubation for three minutes at room temperature, samples were spun down for ten minutes at 4°C with 14,000 rpm. The aqueous phase (700 µl) was transferred to a new tube and 1/20V of acetic acid (1 M) and 0.7V ethanol (100%) was added, mixed and incubated at room temperature for ten minutes. The mix was spun down with 14,000 rpm for ten minutes at 4°C. The pellet was then washed first with 500 µl of sodium acetate, pH 5.0, followed by a second wash with 500 µl of 70% ethanol. Finally, the pellet was air-dried and dissolved with 100 µl of RNAase-free distilled water.

B) cDNA synthesis and RT-PCRs

Prior to cDNA synthesis, the total RNA was treated with DNAase (Promega) for one hour at 37°C. The concentration of RNA was determined using NanoDrop (NanoDrop 1000 V.3.8), and the integrity of the RNA was verified on a 1% agarose gel. cDNA was synthesized from 1.5 µg of total RNA in 20 µl of total reaction volume according to the manufacturers protocol (Bioscript). The cDNA synthesized was diluted three-fold and tested for its quality by running an actin PCR (cDNA 2 µl, Taq buffer 2 µl, dNTP mix 0.6 µl, primer F+R 1 µl, Taq Polymerase 0.05 µl and ddH₂O to 20 µl) for 28 cycles. Equal volume of the PCR product was loaded on 1% agarose gel and the band intensity was compared visually. Finally, the expression of the target genes was analyzed by qRT-PCR using CYBR green as a reporter dye and primers specific to each gene (see appendix). Actin was used as an internal standard. The relative expression of each gene was calculated using qgene96 software.

2.6. GC-MS and HPLC analysis of metabolites

A) GC-MS:

Leaf material (100-200 mg) was collected from 4-week-old wild type and *gad1/2* plants treated without or with 150 mM NaCl and snap-frozen in liquid nitrogen. Metabolite extraction was carried out essentially as described before (Renault et al., 2010). In brief, the tissue was pulverized and 300 µl of methanol and 30 µl of ribitol (dissolved 0.3 mg/ml in methanol) as internal standard was added. The mixture was incubated at 70°C for 15 minutes

and then 200 µl of chloroform was added and incubated at 37°C for five minutes while agitating. Then, 400 µl of ultra-pure HPLC grade water was added, mixed and centrifuged for five minutes. Three aliquots of 160 µl of the upper phase were taken in three glass vials and vacuum dried. For derivatization 40 µl methoxyamine hydrochloride (dissolved 20 mg/ml pyridine) was added and incubated at 30°C for 90 minutes. Next, 70 µl MSTFA (*N*-methyl-*N*-trimethylsilyl trifluoroacetamid) was added and incubated at 37°C for 30 minutes. Finally, 100 µl of the derivatized extract was transferred to a glass tube. The samples were analyzed using a GC-MS system from Agilent technologies (6890N GC system fitted to 5973 model selective mass detector MS) with the following parameters. Helium gas, as a carrier, was injected at a flow rate of 1ml/min with 1 µl of the derivatized sample in split-less mode into the column (Model No. Agilent 19091S-433, capillary 30 m x 250 µm x 25µm). Initially, the oven was maintained at 70°C for five minutes and then increased to 280°C with a ramp of 5°C per minute. Before the next sample was injected, the oven was cooled down to 70°C. During the measurement of all samples, the inlet and the mass spectrometer temperature was maintained at 250°C and 280°C, respectively.

B) HPLC:

Shoot and root materials (100-200 mg) were collected from 4-week-old wild type, *gad1*, *gad2* and *gad1/2* plants treated without or with 150 mM NaCl, and snap-frozen in liquid nitrogen. The samples were crushed to powder with a pre-cooled electrical drill machine. Immediately, 1 ml of extraction buffer1 (25% methanol and 75% methyl-tert-butyl-ether), pre-cooled at -20°C, was added and briefly vortexed. The samples were incubated at RT for one hour while shaking. Then, the samples were sonicated for 15 minutes in an ultra-sonication bath cooled with ice. Following this, 650 µl of extraction buffer2 (H₂O: Methanol, 3:1) was added, briefly vortexed and spun down for five minutes at 14000 rpm. Next, 500 µl of the middle phase consisting of the amino acids dissolved in buffer2 was transferred to a new Eppendorf tube. Finally, the extract was diluted five times in ultra pure HPLC grade water and measured using the HPLC machine (Thermo Scientific Dionex Ultimate 3000 fitted to RF2000 fluorescent detector). For determination of the amino acid concentrations in the samples, standard curves were established by running standard amino acid combinations of known concentration. The machine automatically performed the derivatization procedure by mixing 25 µl of *o*-phthalaldehyde (OPA, 0.2 ml / 1.8 ml water dissolved), 25 µl of the sample and 7.5 µl of

borate buffer (1 M pH 7.5). After 30 seconds, the machine injected 5 μ l of the derivatized sample to a column (Phenomenex S.N. 597237-4, hyperclone 3 μ ODS, 150 x 4.60 mm 3micron size). For quantification of the chromatograms chromeleon software was used (Chromeleon version 6.8; S.N 22551, Dionex).

2.7. Na⁺ and K⁺ measurement

At least 500 mg of fresh shoot material was harvested from five-week-old wild type and *gad1/2* Arabidopsis plants, and freeze dried in liquid nitrogen. The tissue was ground to powder using mortar and pestle. The powder was transferred to falcon tubes and incubated at 80°C for five days with the lid open. Next, 10-20 mg of dry material was measured and transferred to a new 15 ml falcon tube. Then, 1 ml of 65% (v/v) HNO₃ was added and incubated at 95°C for one hour in a water bath for complete digestion. The sample was then cooled down to room temperature and diluted with double de-ionized water to a final volume of 10 ml. The concentration of the respective elements was measured using inductively coupled plasma mass spectrophotometer (ICP-MS). Argon was used as a carrier gas.

3. Results

3.1. Analysis of *GAD* transcripts

The Arabidopsis genome contains five putative *GAD* genes. The organ-specific expressions of the respective genes have previously been reported (Zik et al., 1998, Bouche et al., 2004). However, the contribution of each homologue to the total GABA pool in shoots and roots has not been determined. Here, the relative expression of each of the five homologues in leaves and roots was compared. Like in previous reports (Bouché et al., 2004), *GAD1* is mainly expressed in the root and contributes approximately 80% for the total *GAD* transcript in the root (Fig. 2).

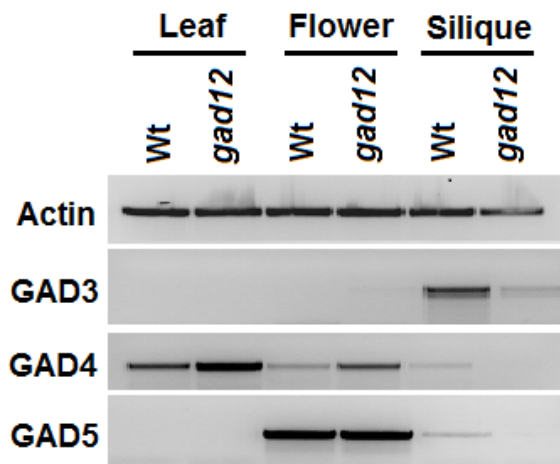


Figure 2. Expression analysis of *GAD* transcripts in young siliques, flowers and leaves of wild type and *gad1/2* plants. Primers specifically amplifying the transcript of the respective genes were used.

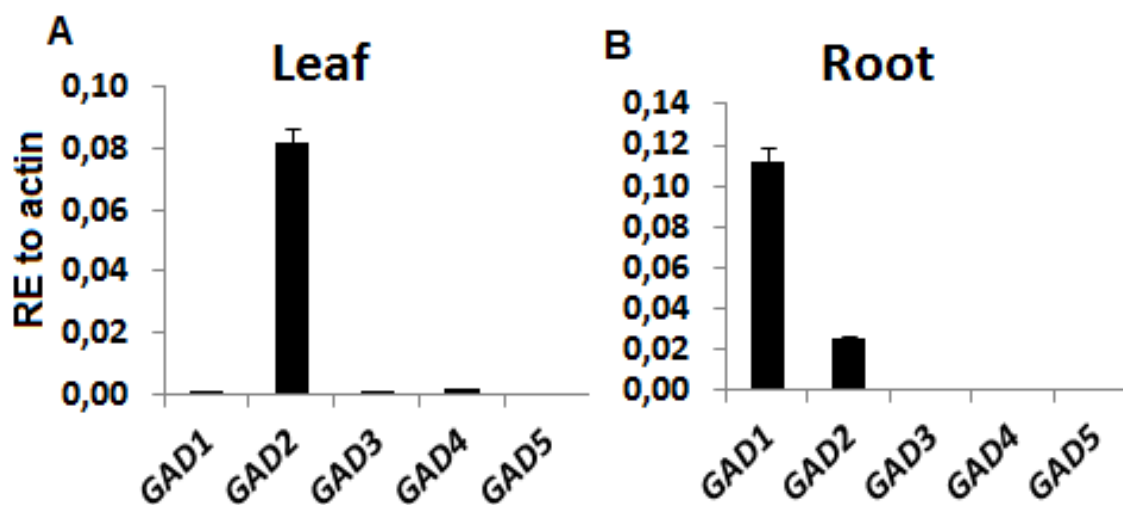


Figure 3. qRT-PCR analysis of the transcript levels of *GAD1*, *GAD2*, *GAD3*, *GAD4* and *GAD5* in the leaf (A) and root (B) of wild-type plants relative to actin; three biological replicates and two technical replicates were used. Error bar represent the standard error of means.

GAD2, which is known to be expressed in all tissues (Turano and Fang, 1998), showed a higher expression in leaves and contributes more than 90% to the total *GAD* transcript in leaves (Fig. 3). *GAD3* and *GAD5* showed a very weak expression in both leaves and roots (Fig. 3A&B). However, a considerable amount of *GAD3* transcripts have been detected in siliques (Fig. 2) perhaps indicating the specificity to this organ. *GAD5* transcript was exclusively detected in the floral organ (Fig. 2). *GAD4* seems to be expressed in all organs despite its expression is very weak. In general, *GAD1* and *GAD2* account for almost all *GAD* transcripts in leaves and roots under normal growth conditions.

The next question was whether mutations in *GAD1* and *GAD2* would lead to a major change in the GABA pool in leaves and roots. To test this, a *gad1/2* double mutant line was generated and the absence of full-length transcripts was confirmed by RT-PCR (Fig. 4C). Subsequently, the level of GABA in shoots and roots of *gad1/2* plants was compared to wild type.

3.2. Generation of *gad1/2* double mutant plants

The *gad1/2* double mutant was generated by crossing the respective single mutants (SALK_017810 and GABI_474 E05) as shown below (Fig. 4A). SALK_017810 has a T-DNA insertion in the 5th exon of the open reading frame (ORF). GABI_474 E05 has the T-DNA insertion in the 6th exon of the ORF. *GAD2* is characterized by possessing a very long (>3 Kb) intronic region.

PCR analysis of *GAD1* and *GAD2* using gene-specific primers flanking the T-DNA insertion did not yield a product (Fig. 4B). However, the primer combination of LB (T-DNA specific) and gene-specific primer yielded a product indicating that the T-DNA insertion was homozygous (Fig. 4B). To confirm the knockout of the *gad1* and *gad2* at transcript level, PCR was performed on the cDNA of *gad1/2*. Indeed, *GAD1* transcript was not detected after 36 cycles of amplifications. However, a truncated *GAD2* fragment could be amplified and consistently showed a stronger band intensity and stability (Fig. 4C). Sequence analysis of the truncated fragment revealed an unexpected result: The amplicon consisted of exon1, exon2, and part of exon6 sequences (Fig. 4C), whereas exon3, exon4 and exon5 and part of exon 6 were all absent. Strikingly, nine bases of unknown origin, most likely from the vector, were inserted between the junction of exon2 and exon6. *In silico* translational analysis of the truncated transcript revealed the presence of a frame shift in exon6 which induced a premature stop codon. If translated, the protein will have a length of 108 amino acid residues.

The predicted catalytic and co-factor binding residues, which are encoded by bases situated in the missing exons were all absent in the truncated version. Therefore, it is unlikely that this protein has a decarboxylase activity and is involved in in GABA synthesis.

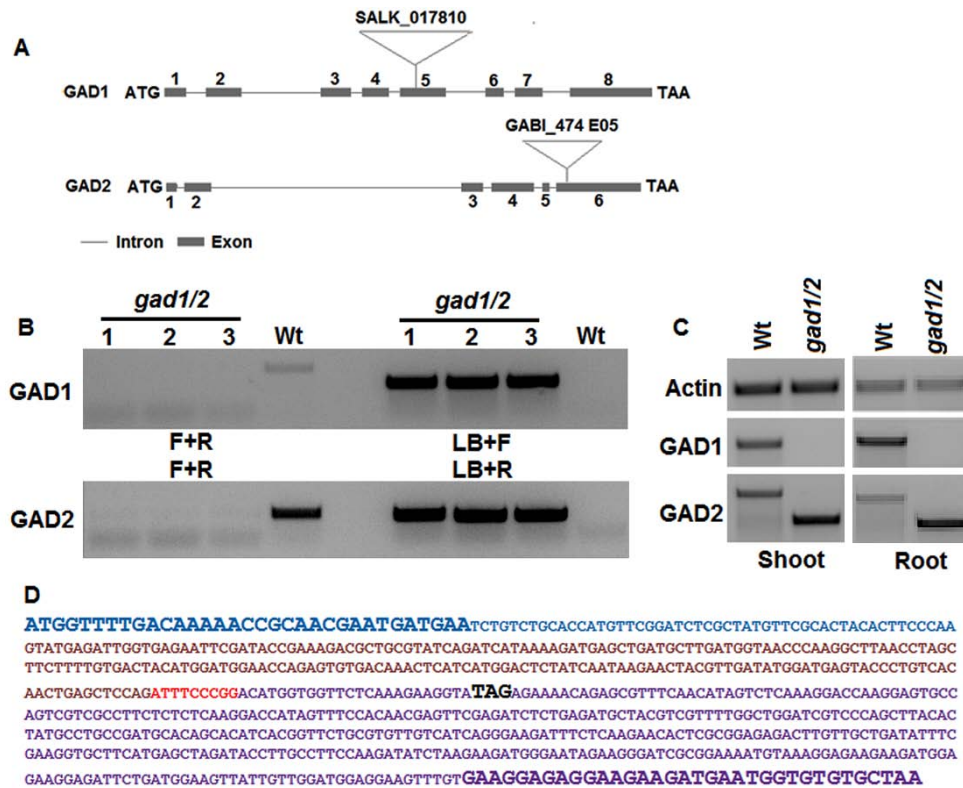


Figure 4. (A) Schematic representation of *GAD1* and *GAD2* genes showing the position of respective T-DNA insertions; (B) Screening of *GAD1* and *GAD2* mutants with gene and T-DNA specific primer combinations; (C) Transcript analysis of *GAD1* and *GAD2* genes from Wt and *gad1/2* plants in leaves and roots; (D) Truncated version of the *GAD2* transcript; sequences in light blue represent exon1; sequences in light blue and bold have not been sequenced and are added for reconstruction; brown sequences represent the full exon2 sequence; sequences with red color are of unknown origin; sequences in purple color represent exon6 downstream of the T-DNA insertion; bold purple sequences have not been sequenced but added for reconstruction; black bold sequences represent the premature stop codon inserted due to a frame shift. F, R and LB represent gene-specific forward, reverse and T-DNA specific primers respectively.

3.3. Analysis of GABA content and compensatory effect of *GADs*

Generally, GABA accumulation in both genotypes was significantly higher in roots than in leaves, an observation that is in line with the previous report of Renault et al. (2010). However, the GABA level in leaves and roots of the *gad1/2* mutant was 10-fold and 45-fold decreased, respectively, compared to the wild type (Fig. 5B&C).

To determine the compensatory effect of other *GAD* homologues in response to *gad1/2* mutations, the transcript levels of *GAD3*, *GAD4* and *GAD5* was analyzed in leaves and roots of wild type and *gad1/2* plants. As expected, the expression of *GAD3* is very low in leaves as

well as in roots (Fig. 3), and *GAD5* was undetectable. Unlike *GAD3* and *GAD5*, *GAD4* transcript was six-fold up-regulated in leaves and by 60% in roots of *gad1/2* plants, indicating a compensatory effect for the mutation in *GAD1* and *GAD2* (Fig. 6).

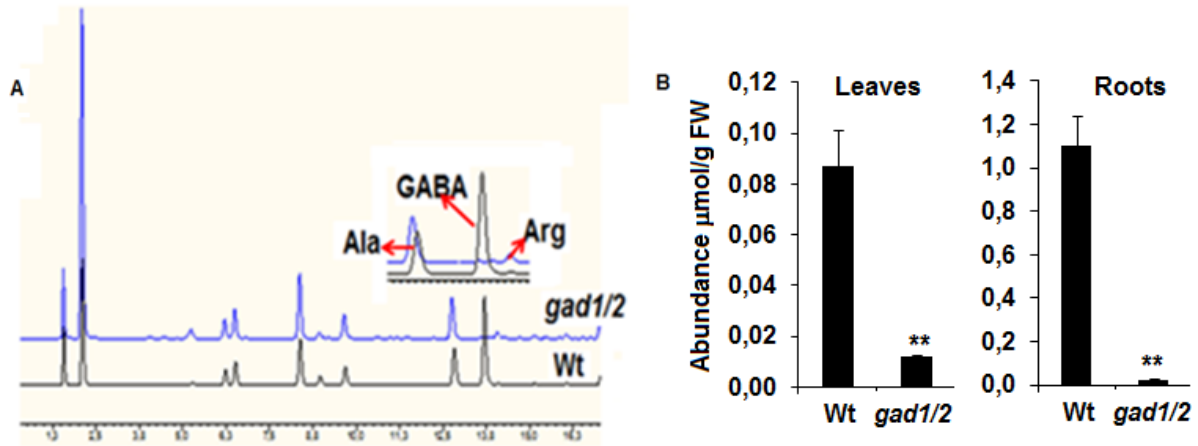


Figure 5. The chromatogram (A) showing the peak of GABA and adjacent amino acids from HPLC measurement; Comparison of GABA accumulation in leaves (B) and roots (C) of wild type and *gad1/2* plants. GABA content in the leaves is the average of three independent measurements; Error bars represent the standard error of means, $n=5$; the chromatogram from the Wt and *gad1/2* double mutant was overlaid in one window. Chromatograms are representatives of multiple measurements of root samples; asterisks represent statistical significance after student t-test, $**\sim P<0.01$.

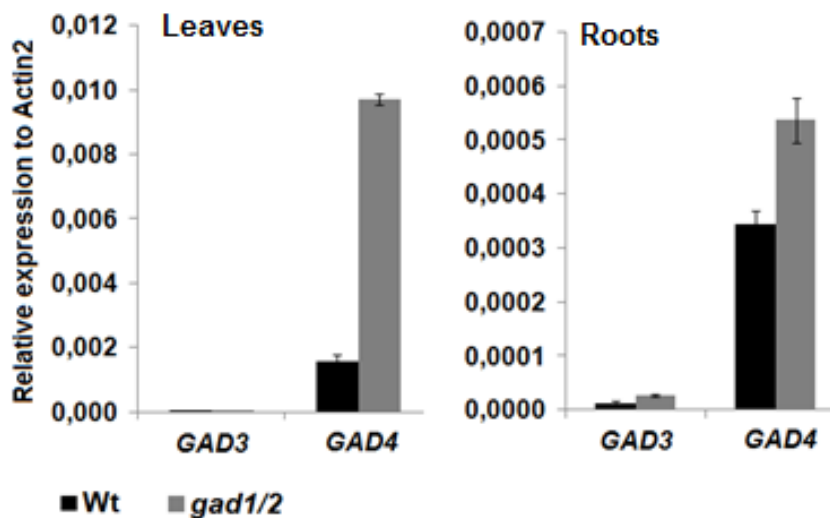


Figure 6. Relative expression of *GAD3* and *GAD4* in leaves and roots of wild-type and *gad1/2* plants; Leaf and root samples were collected from four-week-old plants; Values are the mean of three biological replicates and each with duplicate measurement; error bars represent the standard error.

Next, the effect of *gad1/2* mutation on the content of GABA in flowers was compared, as GABA plays a role in proper fertilization of gametes (Palanivelu et al., 2003). A comparable

level of GABA in the flower extracts of the two genotypes was observed, indicating that *GAD5* is exclusively important for production of GABA in flowers (Table 1).

Table 1. Abundance of amino acids ($\mu\text{mol/g}$ FW) in the flower of wild-type and *gad1/2* plants

	Asp	Glu	Asn	Ser	Gln	Gly	Thr	Ala	Arg	GABA	Val
Wt	14,70	20,01	9,46	6,03	29,62	0,31	2,64	3,31	0,23	0,33	0,94
<i>gad1/2</i>	14,95	24,70	8,06	8,99	30,39	1,26	3,95	4,89	0,07	0,28	1,14
t-test	ns	**	ns	**	ns	**	**	**	**	ns	*

Numbers in the table represent the average value of five independent plants. Means were compared after student t-test, * $P < 0.05$, ** $P < 0.01$, and ns-non significant ($P > 0.05$); Abbreviations: Glu-glutamate, Asn-asparagine, Ser-serine, Gln-glutamine, Gly-glycine, Thr-threonine, Ala-alanine, Arg-arginine, Val-valine.

3.4. Phenotypic analysis

3.4.1. Growth performance

GABA is considered as an essential intermediate in metabolism, transport and storage of nitrogen and carbon (Bouché and Fromm, 2004). The degradation of GABA *via* the GABA shunt contributes to the energy demand of the plant for normal growth and development. Here, the effect of blocking of the GABA shunt on the growth performance of *gad1/2* plants was analyzed. For that, the total green area of the rosette was measured in three-week-old plants. Indeed, after three weeks of growth, the total rosette area of *gad1/2* plants was significantly lower compared to the wild type under normal growth conditions (Fig. 7B). The reduced rosette area led to a significant reduction in shoot fresh weight (Fig. 7C). Furthermore, the root fresh biomass was marginally reduced although it was not statistically significant (Fig. 7D). However, the primary root length consistently looked shorter than the wild type. Taken together, the result indicates a defect in the development of *gad1/2* plants.

The next question was whether the reduced rosette area of the *gad1/2* plants was due to reduced cell number or a reduced cell growth. To answer this question, the cell density was analyzed from 3rd and 4th leaves of a four-week-old wild type and *gad1/2* plants. Surprisingly, the cell density was similar between the two genotypes (Fig. 8A&B), suggesting that the

average cell size was the same. However, the overall cell number on the entire leaf is significantly reduced which is manifested by reduced rosette area.

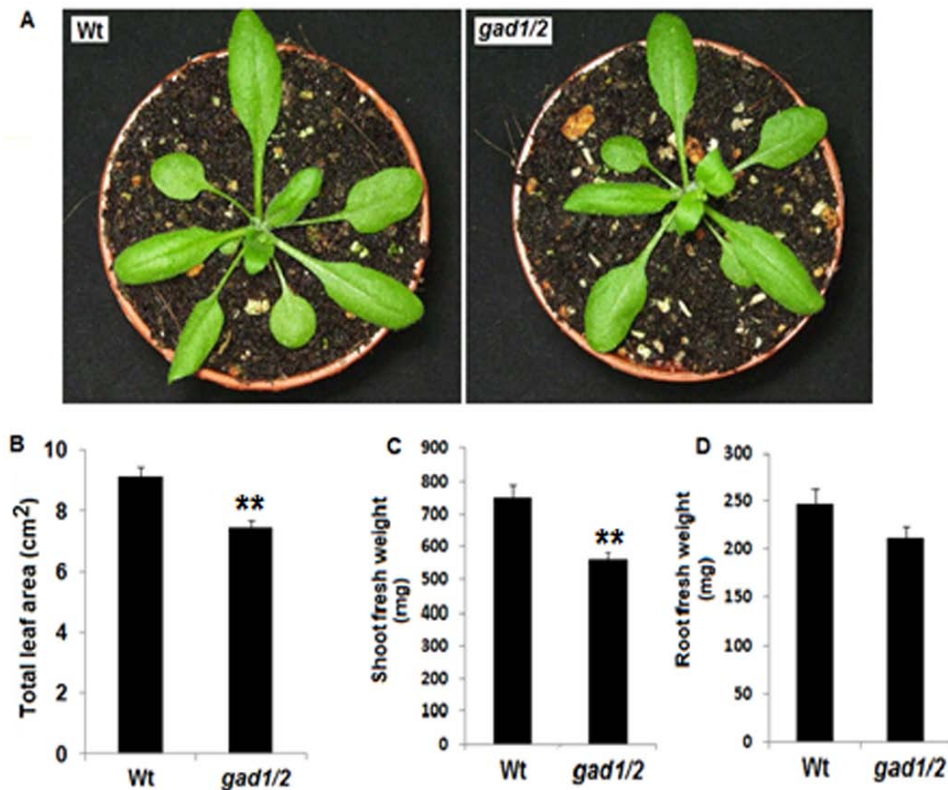


Figure 7. Phenotype of a three-week-old wild type and *gad1/2* plants grown under long-day conditions in the green house (A), quantification of the total rosette area (B), shoot fresh weight (C) and root fresh weight (D) of four-week-old wild type and *gad1/2* plants. Pictures are representative of 14 independent plants. For cell number counting, 10 leaves were analyzed. For fresh weight analysis shoots and roots from at least 18 plants were weighed. Error bars in the bar chart represent the standard error of means; asterisks represent statistical significance after student t-test $**\sim P < 0.01$.

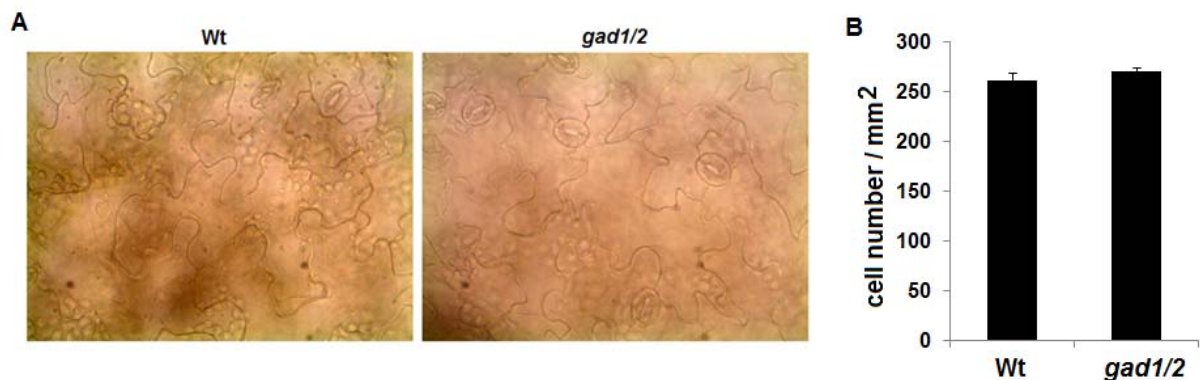


Figure 8. The abaxial side of leaf epidermis was photographed under a fluorescent microscope in the bright field (A); at least three positions on leaf blade were pictured and counted (B). A total of ten leaves were counted per genotype. Error bars represent the standard error of means.

3.4.2. Analysis of drought tolerance

Next, the response of the GABA-less *gad1/2* plants to stress conditions (salt, drought and osmotic stress) was analyzed; as GABA has been implicated in biotic and abiotic stress tolerance (Bown and Shelp, 1997; Kinnersley and Turano, 2000).

A) Water content measurement

The oversensitivity of *gad1/2* plants under drought condition was examined, as GABA has been reported to accumulate during drought stress (Bown and Shelp, 1997). Six days after the onset of drought treatment, the leaves of *gad1/2* plants were completely wilted under green house conditions, whereas wild-type leaves still maintained the turgidity (Fig. 9A). To quantify the observed phenotype, the shoot water content of wild-type and *gad1/2* plants was measured after the onset of drought stress treatment. In a growth chamber, the water content in the shoot of *gad1/2* plants was significantly reduced compared to wild type six days after the onset of drought treatment (Fig. 9B). However, the visual phenotype was not as severe as it was in the green house.

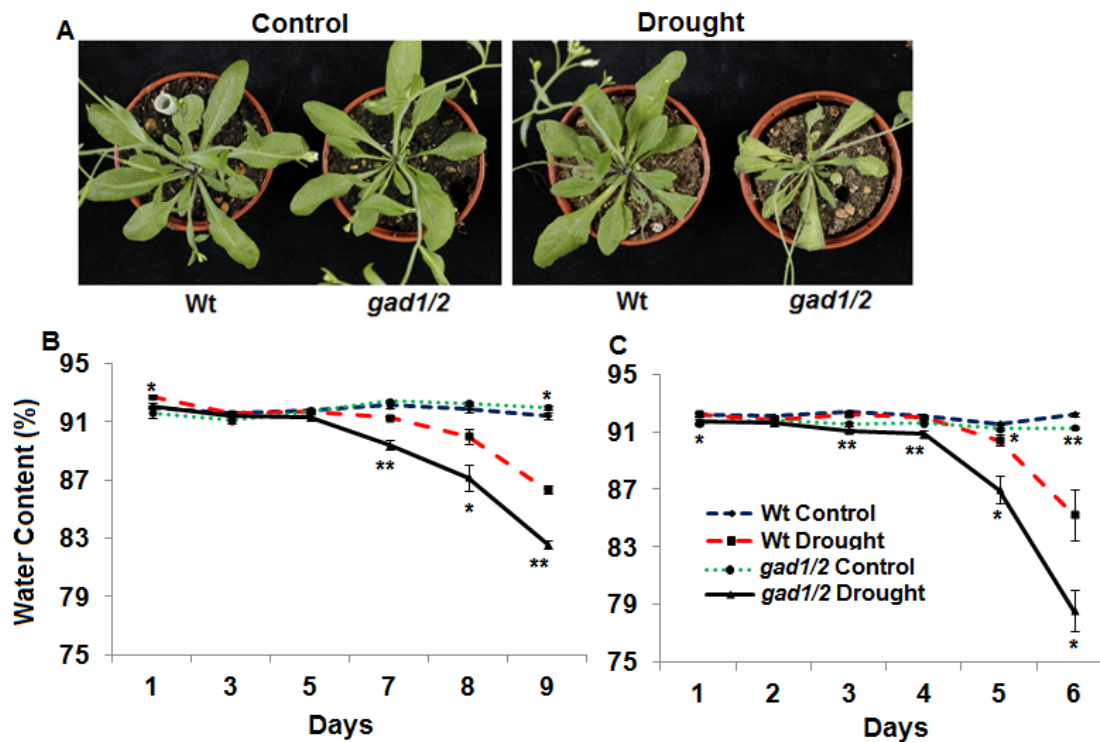


Figure 9. Phenotypic and water content analysis of wild type and *gad1/2* plants treated with drought and osmotic stress. (A) Phenotype of Wt and *gad1/2* plants treated with drought; picture was taken six days after the onset of drought treatment. (B) Water content of Wt and *gad1/2* plants after 300 mM mannitol treatment; day one represents the third day after the last mannitol treatment. Analysis of water content in wild-type and *gad1/2* plants treated for drought under growth chamber conditions (B) and greenhouse conditions (C); similarly, day one represents the third day after the last watering; asterisks represent statistical significance after student t-test, *~ $P < 0.05$ and **~ $P < 0.01$.

Under green house conditions, the water content was reduced significantly in *gad1/2* plants already after four days (Fig. 9C). The question remained why *gad1/2* plants contained less water than the wild type. Generally, plants could lose water through evaporation from the leaf surface, transpiration through stomata and through the root if they are osmotically stressed. However, the loss of water through roots is less likely as the plants were grown under normal conditions.

B) Stomata conductance and stomata density measurement

To reveal the contribution of transpiration for drought over-sensitivity of *gad1/2* plants, the leaf stomata conductance was compared to the wild type. Most plant species contain stomata mainly in the abaxial side (side facing against the sun light) of the leaf. However, Arabidopsis contain stomata on both sides of the leaf, and hence the stomata conductance was measured in both the abaxial and adaxial sides of leaves.

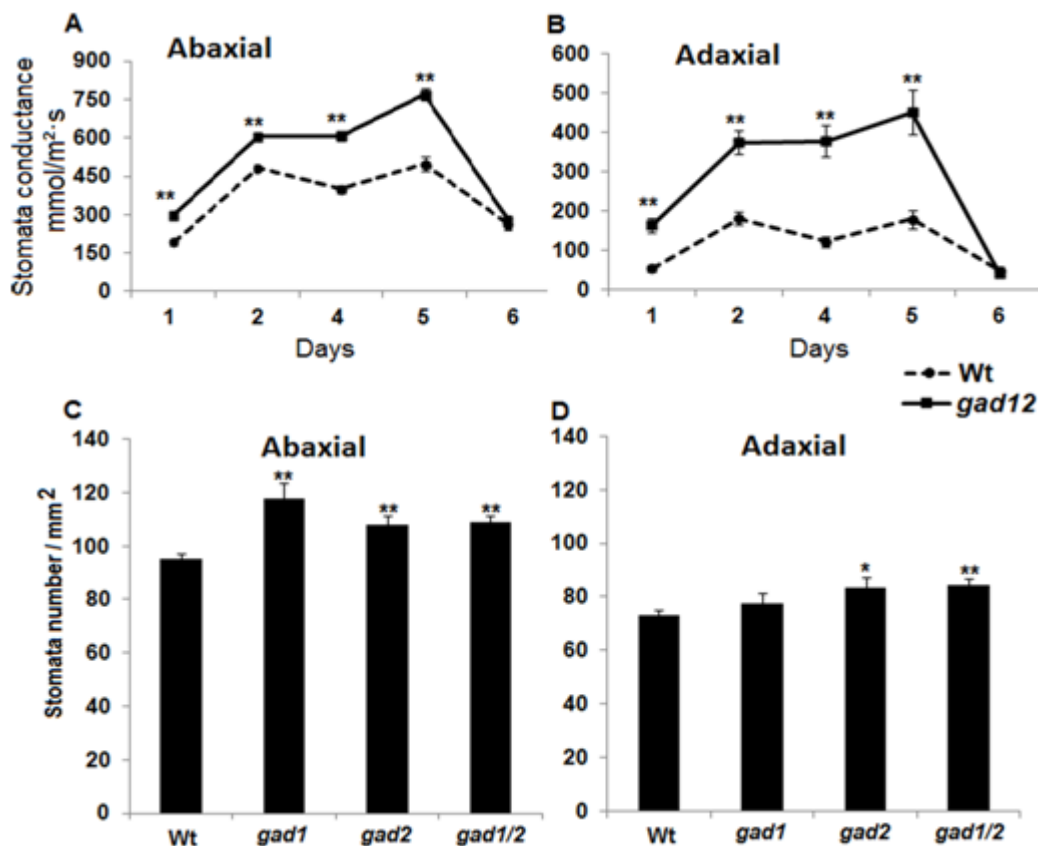


Figure 10. Stomata conductance of wild-type and *gad1/2* plants in abaxial (A) and adaxial (B) sides of the leaves; stomata conductance measurement was commenced on the last watering day and continued for six days. Stomata number was counted on the abaxial (C) and adaxial (D) sides of leaves from four-week-old wild-type, *gad1*, *gad2*, and *gad1/2* plants; error bars represents the standard error of means of five independent plants for stomata conductance, and seven independent plants for stomata number count; asterisks represent statistical significance after student t-test, *~ $P < 0.05$ and **~ $P < 0.01$.

Interestingly, the stomata conductance of *gad1/2* plants was significantly higher on both sides of the leaf over five days of measurement (Fig 10A&B). On day six, the stomata conductance of the two genotypes was the same on both sides of the leaf (Fig 10A&B). However, on day six *gad1/2* plants were already wilted but wild-type plants maintained leaf turgidity (Fig. 9A).

The next question addresses was the increased stomata conductance in *gad1/2* leaves. Stomata conductivity is known to be a function of stomata density, stomata size and stomata aperture. To determine the contribution of stomata density for an increase in leaf stomata conductance, the numbers of stomata on both sides of leaf number three and four was counted. Indeed, stomata density was increased by about 15% in both the abaxial and adaxial sides of *gad1/2* leaves ($P < 0.001$) compared to the wild type (Fig. 10).

To get an insight about the contribution of the stomata aperture for an increase in leaf conductivity, the average conductance per stoma was calculated. For that, the average conductance of the leaf over the first five days was divided by the average stomata number. Interestingly, the conductance per stomate was 26% higher in the abaxial side of *gad1/2* leaves. In the adaxial side, the conductance per stomata was increased by 120% in *gad1/2* leaves (Table 2).

Table 2. Analysis of conductance per stomate in the abaxial and adaxial side of leaves from wild type and *gad1/2* plants

	Wt		<i>gad1/2</i>	
	Abaxial	Adaxial	Abaxial	Adaxial
Stomata number (stomata/ m ²)	95116131 (±1949475)	72860818 (±2357349)	108915055 (±2654370)	84357695 (±2572622)
Average conductance mmol/(m ² ·s)	392,5 (±16.6)	135,1 (±15.0)	569,7 (±17.3)	342,5 (±36.4)
Conductance (nmol/stomata. sec.)	4,03	1,73	5,07	3,80
Conductance (% of Wt)	100	100	126	220

Values of stomata numbers represent the average of 26 leaves.

C) Correlation between GABA content and drought sensitivity

To correlate the drought oversensitivity of *gad1/2* plants to the GABA level, the phenotype of the single mutants was analyzed. It could be assumed that the presence of one of the two most

abundantly expressing GAD genes would suppress the drought oversensitive phenotype. Metabolic analysis revealed both single mutants accumulated a significantly reduced level of GABA under normal growth conditions compared to the wild type, but only marginally higher compared to the double mutant (Fig. 11). Unexpectedly, also the single mutants exhibited oversensitivity to drought stress compared to the wild type plants (Fig. 12).

This oversensitivity of the single mutants raised the question whether the drought stress oversensitivity was a GABA-specific response; since, in the single mutants the compensatory role of the other homologues *GAD* genes was expected under drought condition. The GABA content in the leaves of the single mutants along with the wild type was therefore analyzed after drought treatment. As expected, the wild type showed an increase in GABA content (Fig. 11). However, in the *gad2* single mutant and the double mutant there is a non-significant increase in GABA content which contrasts to *gad1* mutant that showed a significantly reduced ($P < 0.05$) GABA level in the leaves after drought stress (Fig. 11). This observation strongly suggests that *GAD1* and *GAD2* are non-redundant genes. Measurement of leaf stomata conductance revealed a significantly higher transpiration rate on both sides of the leaf in the *gad1* and *gad2* single mutants compared to wild type (Fig. 12), as also observed in the *gad1/2* double mutant.

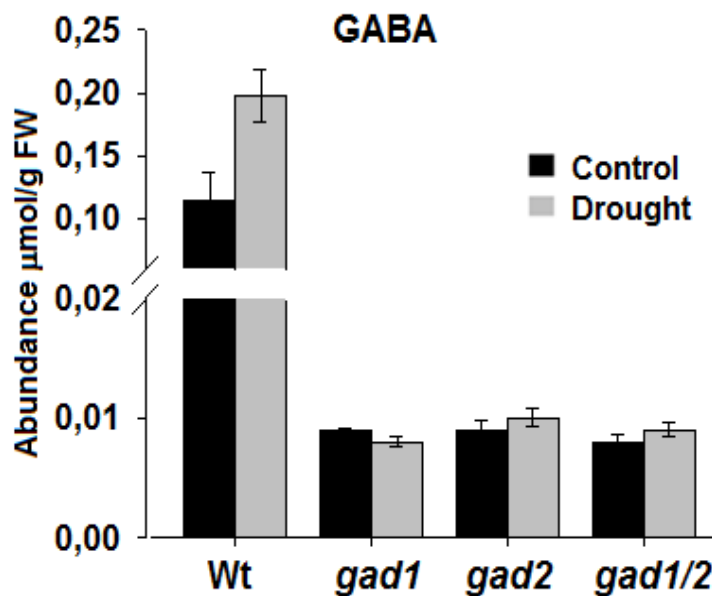


Figure 11. GABA content in the leaves of Wt, *gad1*, *gad2* and *gad1/2* plants treated without and with drought. Values are means of at least eight replications; error bars represent standard error of means; asterisks represent statistical significance after student t-test, *~ $P < 0.05$.

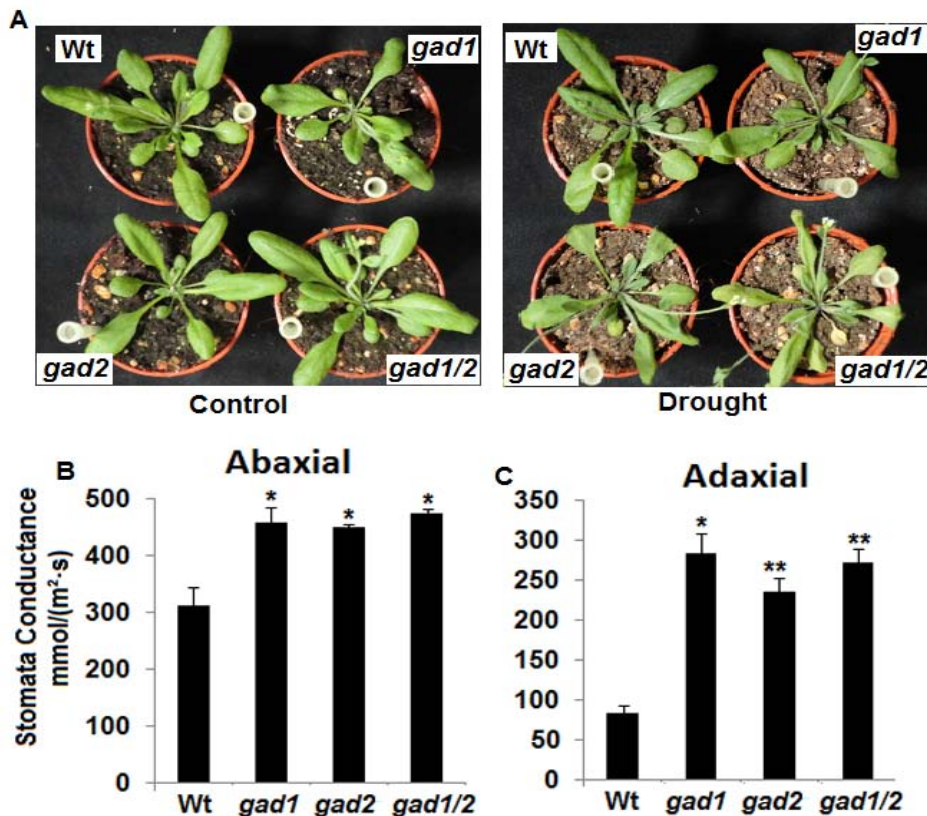


Figure 12. Phenotype of four-weeks-old Wt, *gad1*, *gad2* and *gad1/2* plants treated without and with drought stress (A); pictures were taken six days after the onset of the treatment; stomata conductance of Wt, *gad1*, *gad2* and *gad1/2* plants in abaxial (B) and adaxial (C) sides of the leaves; stomata conductance measurement was commenced on the last watering day and continued for three days. Values are the average of three days measurements; each day five independent plants and three leaves per plant were measured; asterisks represent statistical significance after student t-test, *~ $P < 0.05$ and **~ $P < 0.01$.

The attempt to correlate the GABA level to drought stress tolerance using *gad1* and *gad2* mutants was not successful as the two genes did not complement each other. Therefore, drought stress response analysis was repeated by feeding external GABA. For that, wild type and *gad1/2* plants were irrigated with 5 mM GABA starting from two-leaf stage of the plants. After four weeks, the stomata conductivity was measured and showed higher transpiration rate in *gad1/2* leaves on both the abaxial and adaxial sides of the leaf (Fig. 13). Furthermore, the *gad1/2* plants wilted earlier than the wild type. To confirm that GABA was taken up by the plants, the GABA content was analyzed in leaves. Indeed, GABA was taken up which can be clearly observed in the wild-type (Fig. 13C). In *gad1/2* leaves, the GABA content was significantly increased but by far lower compared to wild type leaves under normal growth conditions (Fig. 13C).

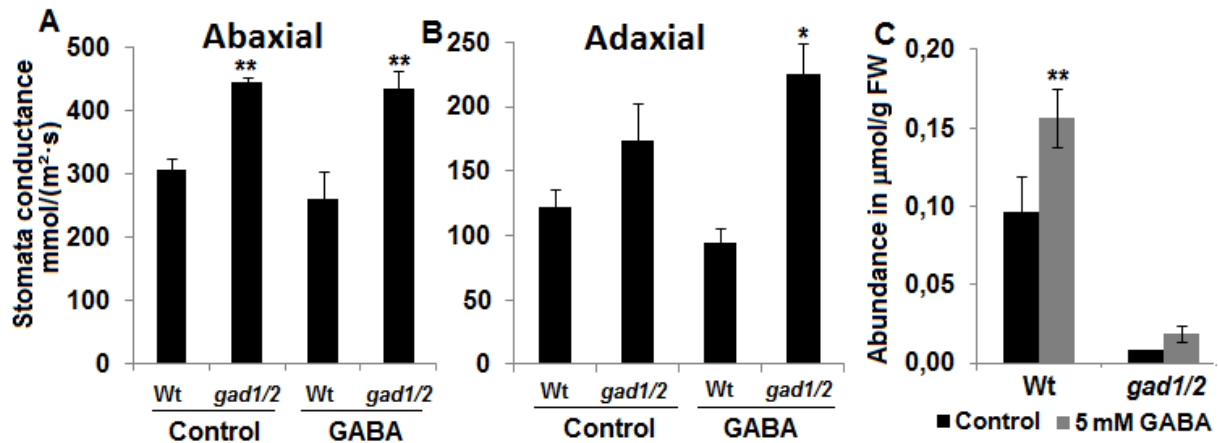


Figure 13. Leaf stomata conductance of the abaxial (A) and adaxial (B) sides of a wild-type and *gad1/2* plants grown without and with 5 mM GABA treatment; measurement of GABA in leaves of wild-type and *gad1/2* plants irrigated with 5 mM GABA (C). For the stomata conductance measurement four plants from each genotype and three leaves per plant were measured. n=6, for GABA measurements; error bars represent the standard error of means; asterisks represent statistical significance after student t-test, *~P<0.05 and **~P<0.01.

D) Stomata response to stimuli

It was then analyzed whether these GABA-less mutants are defective in sensing and closing the stomata upon drought stress. The ability of the mutants to close stomata was analyzed by placing the plants under condition that trigger stomata opening and closing. Light is known to modulate the opening and closing of stomata (Cousson et al., 1995).

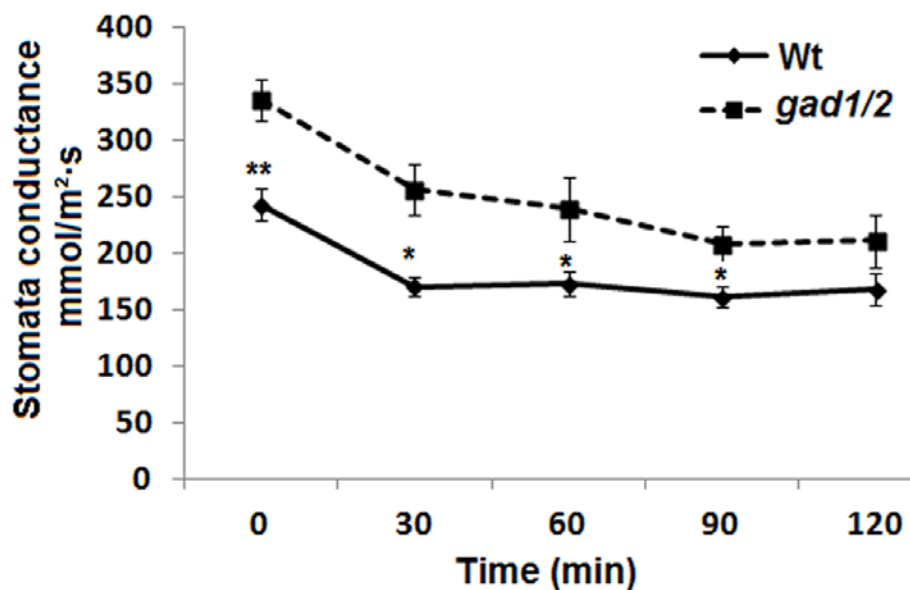


Figure 14. Stomata conductance of the abaxial side of five-weeks-old wild-type and *gad1/2* leaves incubated in the dark; values are means of three measurements from three independent plants; three leaves were measured from each plant; asterisks represent statistical significance after student t-test, *~P<0.05 and **~P<0.01.

To test that, wild type and *gad1/2* plants were germinated and grown under long-day conditions for five weeks and transferred to dark. Then, the stomata conductance was measured at different time points. Interestingly, the wild-type plants attained the lowest stomata conductance value already after 30 minutes, perhaps indicating its closure (Fig. 14). On the other hand, *gad1/2* plants responded very slowly and attained the lowest transpiration rate, similar to wild type, only after two hours in the dark (Fig. 14).

To corroborate the porometer data, the transpiration rate measurement was repeated in a different experimental set up and laboratory. For that, the wild type and *gad1/2* mutant plants were subjected to stimuli (light and ABA) to trigger turgor change in the guard cells, and then the transpiration rate was measured using the GAS exchange analyzer. Generally, the transpiration rate of the intact *gad1/2* plant was always higher than the wild type under dark, light or ABA treatment conditions (Fig. 15A&B), supporting the result obtained from the leaf porometer measurement.

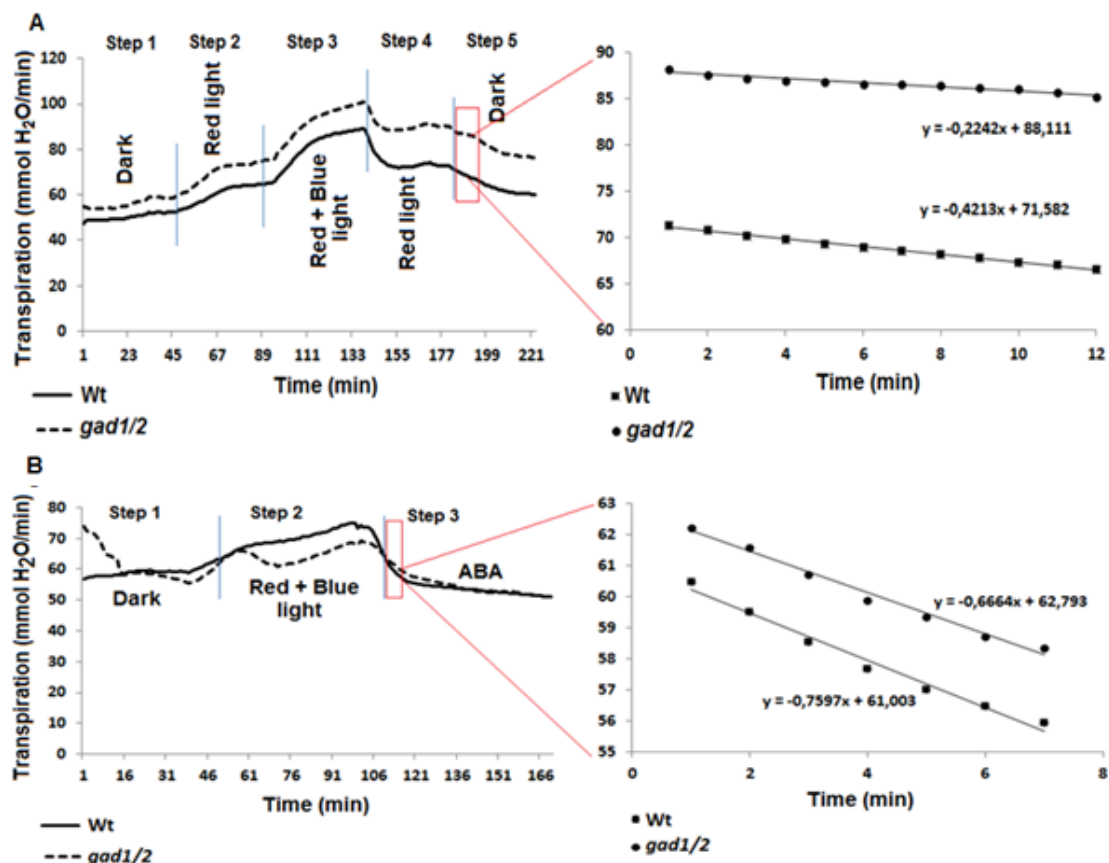


Figure 15. Transpiration rate measurement of wild type and *gad1/2* mutant using the gas exchange method under different light regime (A) and ABA treatment (B); the machine recorded the relative water content every second; the values were the average of 60 seconds measurement. The linear graphs on the right represent the zoomed in form of the left graph selected with the red box.

However, in the experiment using leaves detached from the plant, the transpiration rate of the *gad1/2* leaves consistently decreased while in the wild type the transpiration was gradually increased in the dark period. The transpiration rate then remained lower than the wild type for the next light periods until the ABA treatment. Stomata opening response seems to be unaffected in the *gad1/2* mutant, as the transpiration rate increased at a similar rate after red and blue light treatment (Fig. 15A&B). Interestingly, the stomata closure of *gad1/2* seemed to be more affected as the transpiration rate decreased at lower rate after transition to dark and 10 μ M ABA treatments. Overall, the oversensitivity of the *gad1/2* plants to drought stress is partly due to the inability of the leaves to close the stomata during the night.

3.4.3. Analysis of salt tolerance

For salt stress treatment, three-week-old wild-type and *gad1/2* plants were treated without or with 150 mM NaCl under long-day conditions. One week after the onset of the treatment, the leaves of *gad1/2* plants started to show a wilting phenotype and one more week further, most of the *gad1/2* leaves had lost turgidity (Fig. 16). However, the ionic stress-specific symptoms of salt stress like chlorosis and necrosis were not observed. To get further insight on the salt stress response, the root elongation of wild type and *gad1/2* plants was monitored on $\frac{1}{2}$ MS plates containing 50 mM and 100 mM NaCl. Unexpectedly, *gad1/2* plants did not show a root growth defect compared to Wt on 50 mM and 100 mM NaCl containing plates (Fig. 17A&B).

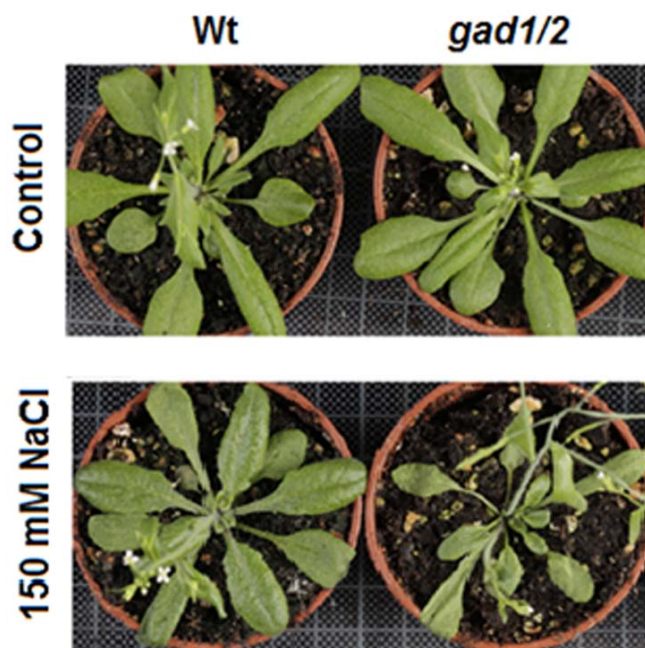


Figure 16. Comparison of the shoot phenotype of soil grown wild-type and *gad1/2* plants treated without or with 150 mM NaCl; picture was taken from a representative of plants showing a similar phenotype

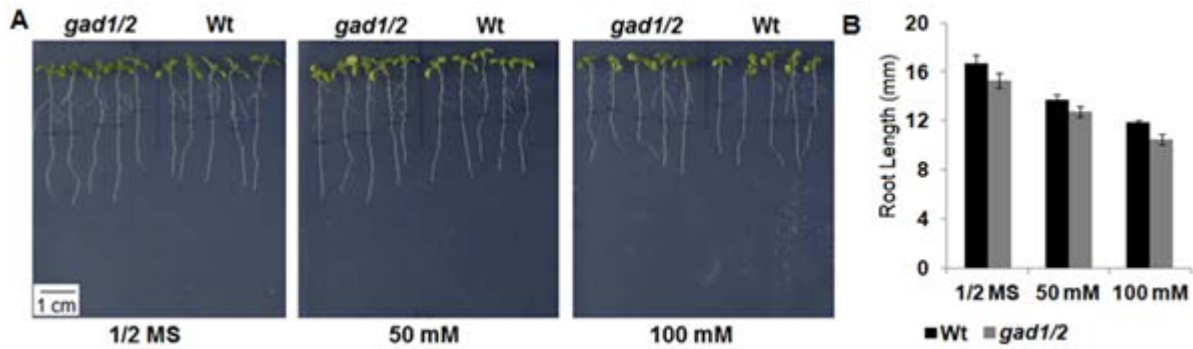


Figure 17. Analysis of root growth phenotype of Wt and *gad1/2* plants in response to salt stress (A); seeds of wild type and *gad1/2* were germinated and grown on $\frac{1}{2}$ MS plate for approximately five days. Then plantlets were transferred to $\frac{1}{2}$ MS plate without and with 50 and 100 mM NaCl. Pictures were taken after three days of incubation; root length (B) was measure using ImajeJ.

Salt-induced stress is known to have two components, i.e. ionic and osmotic components. To determine the contribution of the osmotic component, four-week-old soil grown wild-type and *gad1/2* plants were treated with 300 mM mannitol, and the water content was measured in shoot samples for three consecutive days. As expected, the *gad1/2* mutants contained a significantly reduced amount of water three and four days after the last mannitol treatment (Fig. 18B). To determine the effect of osmotic stress on the plant growth, the root elongation of wild-type and *gad1/2* plants was monitored on $\frac{1}{2}$ MS plates containing 100, 200 and 300 mM mannitol. However, there was no difference in root growth between the wild-type and *gad1/2* plants after the osmotic treatment (Fig. 18A).

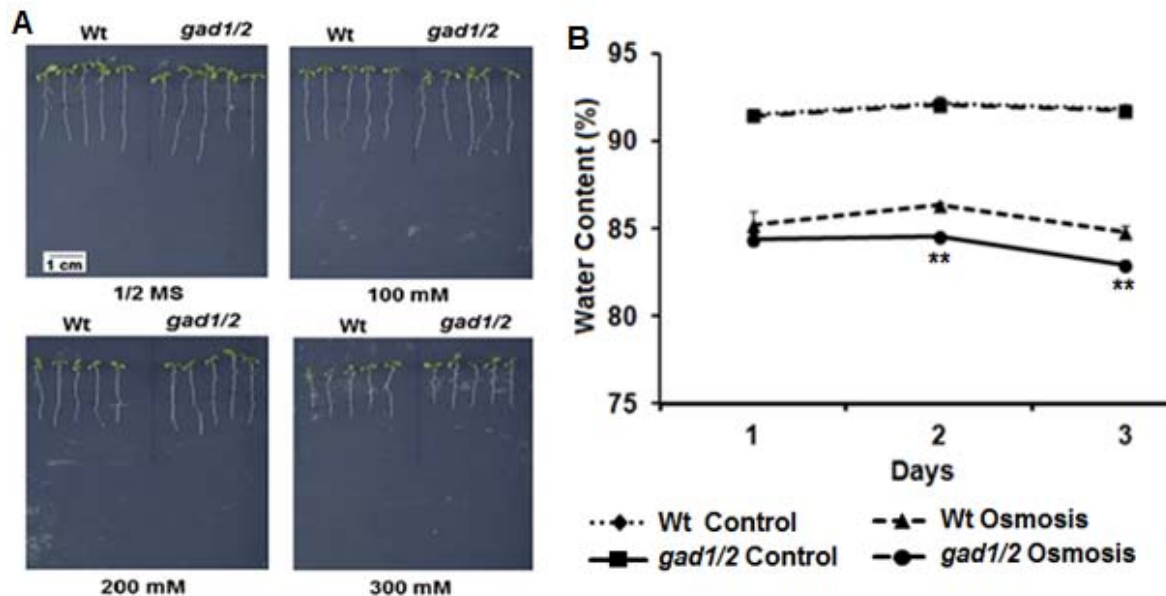


Figure 18. Phenotype of Wt and *gad1/2* plants grown on $\frac{1}{2}$ MS plate without and with 100, 200 and 300 mM mannitol (A); water content analysis of wild-type and *gad1/2* plants grown on soil supplemented without and with 300 mM mannitol; Five plants were harvested on each day for water content measurements; asterisks represent the statistical significance after student t-test, **~P<0.01.

To test whether the salt oversensitive phenotype was due to the accumulation of toxic elements, the level of sodium in the shoot of wild-type and *gad1/2* plants treated without or with 150 mM NaCl was compared. Under control conditions, the level of sodium was similar between the two genotypes. However, after 150 mM NaCl treatment *gad1/2* plants accumulated a significantly higher level of sodium in shoots compared to wild type (Fig. 19A).

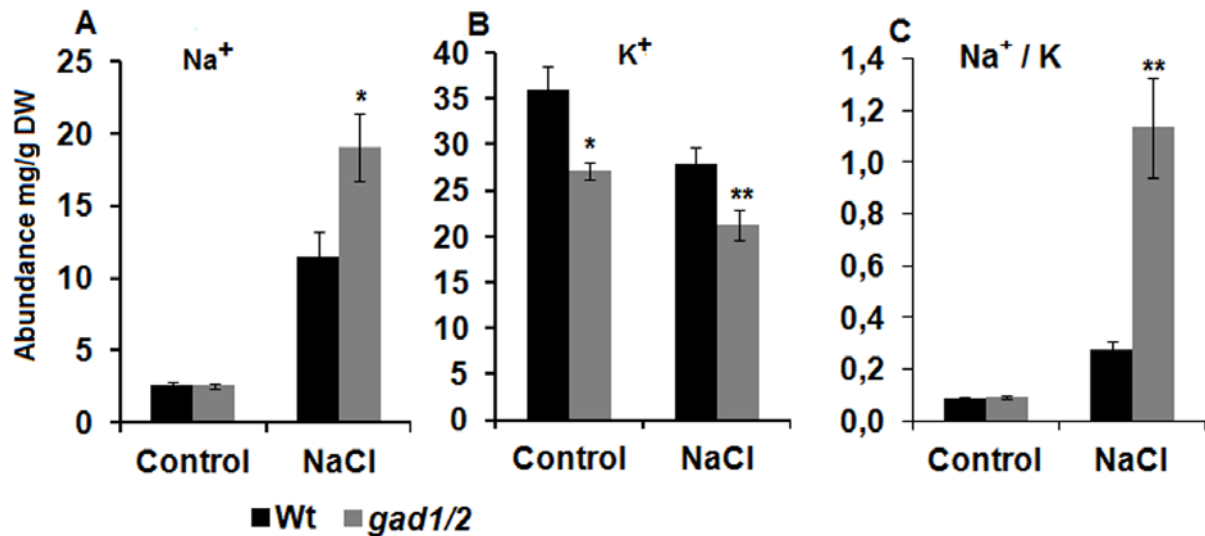


Figure 19. Comparison of Na⁺ (A) and K⁺ (B) in the shoots of Wt and *gad1/2* plants treated with or without 150 mM NaCl; the ratio of sodium to potassium (C) was calculated; error bars represent the standard errors of means of at least ten biological replicates; asterisks represent statistical significance after student t-test, *~P<0.05 and **~P<0.01.

In contrast, the level of potassium was significantly reduced under control conditions (Fig. 19B), and treatment with 150 mM NaCl further reduced the K⁺ content in both genotypes (Fig. 19B). To get an insight about the sodium and potassium homeostasis, the ratio of Na⁺ to K⁺ was calculated (Fig. 19C). Indeed, the Na⁺/K⁺ ratio was significantly higher in the *gad1/2* plants compared to wild type after 150 mM NaCl treatment. To determine the ionic stress-specific response of the mutant, wild-type and *gad1/2* plants were treated with 10 mM LiCl. One week after the onset of treatment, both genotypes displayed the sign of chlorosis and burning on the edges of the leaves.

3.5. Transcript analysis of potassium transporters

Element analysis showed a significant reduction of potassium content in the shoot of GABA-less *gad1/2* plants (Fig. 19B). Previously, the accumulation of a significantly higher level of potassium in high GABA accumulating *pop2* plants under normal growth condition has been

reported (Renault et al., 2010). Based on these observations, it is tempting to speculate on a correlation between the GABA status and potassium homeostasis. To test that, the transcript level of some of the potassium channels (*AKT1*, *HAK5*, *KAT1* and *GORK*) was analyzed in leaves and roots of wild-type and *gad1/2* plants. *AKT1* transcripts, which seems to be expressed abundantly, showed a significant reduction (>50%) in the leaf of *gad1/2* plants (Fig. 20). In contrast, the other three potassium channels (*HAK5*, *KAT1* and *GORK*) showed an increase in expression (Fig. 20). In roots, all genes tested showed an increase in the level of transcripts in the *gad1/2* mutant (Fig. 20). Treatment with 150 mM NaCl generally induced the expression of all analyzed genes, except *AKT1*, in the leaf and root of *gad1/2* plants compared to wild-type (Fig. 20). The transcript level of *AKT1* reduced in the leaf and remained unchanged in the root of *gad1/2* plants compared to wild type after 150 mM NaCl treatment (Fig. 20).

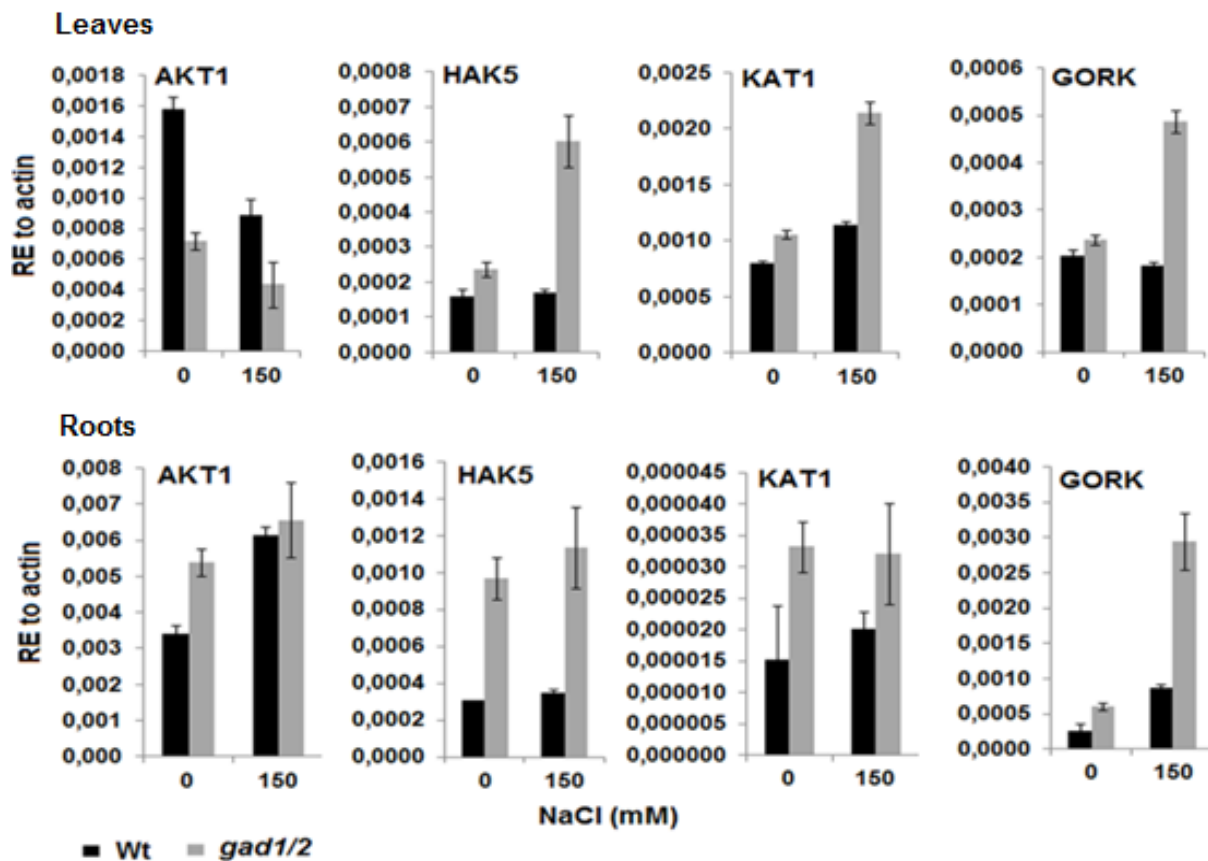


Figure 20. Relative expression (RE) analysis of potassium transporters (*AKT1*, *HAK5*, *KAT1* and *GORK*) in the leaf and root of wild-type and *gad1/2* plants treated without and with 150 mM NaCl ; Values are means of three biological replicates; each sample measured in duplicates; error bars represent the standard error of means.

3.6. Analysis of Potassium uptake

The expression of some of the potassium transporters seemed to be de-regulated by the knock-out of *gad1* and *gad2*. The next obvious question was whether this de-regulation has any effect on the uptake of potassium from the growth medium. For this, the root elongation of *gad1/2* plants was compared to wild-type grown on agar plates containing increasing concentrations of potassium (5 μ M to 500 μ M KCl). For a better correlation of potassium uptake with the GABA content, the *pop2* line which accumulates high GABA was included in the experiment.

Root growth of *gad1/2* mutant plants was significantly reduced compared to wild type on plates with a potassium concentration of 300 μ M and 400 μ M (Fig. 21). However, there was no significant difference to the wild type on potassium concentration less than 300 μ M but generally, the growth was reduced (Fig. 21). A surprising phenotype was observed in *pop2* plants which continued to grow despite very low potassium concentrations (Fig. 21).

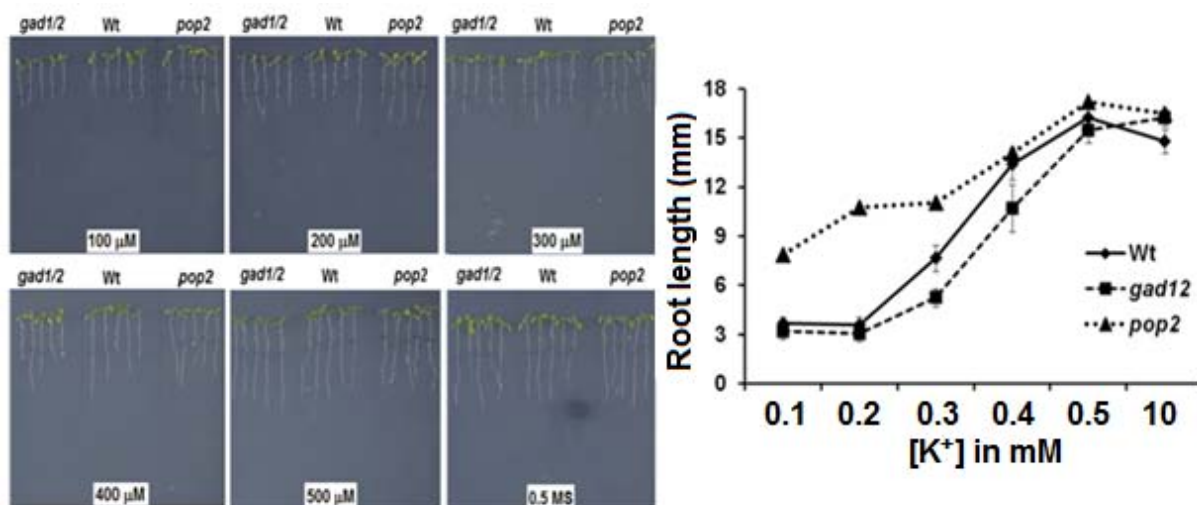


Figure 21. Root growth analysis of wild type, *gad1/2* and *pop2* plants under potassium deficient conditions; seeds of the three genotypes were germinated and grown on $\frac{1}{2}$ MS plates. Five-days-old plantlets were transferred to modified $\frac{1}{2}$ MS plates containing 100 μ M, 200 μ M, 300 μ M, 400 μ M and 500 μ M KCl as potassium source and also to full $\frac{1}{2}$ MS as a control. Pictures were taken after three days of incubation. Bar = 1cm. Root length was measured using ImageJ software.

3.7. Metabolic profiling

A) 150 mM NaCl treatment

The possible metabolic disorder that might be caused by the salt stress treatment was investigated in leaves and roots of wild-type and *gad1/2* plants. Generally, the total amino acid content was found to be higher in shoots than roots of both genotypes (Table 3). Glutamate, in particular, was significantly low in roots of both wild-type and *gad1/2* plants compared to the accumulation in the shoot. Comparison of the glutamate content between the two genotypes resolved a 29% and 142% increase in the shoot and root of *gad1/2* mutant, respectively (Table 3), indicating that a significant portion of the glutamate pool is mobilized *via* the GABA shunt. Other most abundant amino acids (Asn, Gln, Thr, and Ala) and GABA showed a higher accumulation in leaves of wild type compared to *gad1/2* mutants under control condition (Table 3), although this is significant only for glutamate and GABA.

Table 3. Abundance of amino acids ($\mu\text{mol/g}$ FW) in the leaves and roots of wild type and *gad1/2* plants under control and 150 mM NaCl treatment conditions

	Control						150 mM NaCl					
	Leaves			Roots			Leaves			Roots		
	Wt	<i>gad1/2</i>	t-test	Wt	<i>gad1/2</i>	t-test	Wt	<i>gad1/2</i>	t-test	Wt	<i>gad1/2</i>	t-test
Asp	5,50	6,24	ns	0,58	0,60	ns	7,14	6,45	ns	1,29	1,12	ns
Glu	8,96	11,56	**	1,46	3,53	**	12,33	13,13	ns	4,12	5,48	*
Ser	0,57	0,56	ns	0,29	0,39	ns	0,67	0,68	ns	0,85	0,91	ns
Asn	3,95	3,27	ns	0,42	0,56	ns	8,09	9,99	**	2,16	2,38	ns
Gln	2,83	2,09	*	0,91	1,08	ns	3,43	3,05	ns	3,01	2,77	ns
Gly	0,11	0,08	ns	0,12	0,09	ns	0,13	0,10	ns	0,20	0,18	ns
Thr	1,35	1,30	ns	0,32	0,42	ns	1,18	1,21	ns	0,98	0,85	ns
Ala	1,25	1,15	ns	0,61	0,81	ns	1,35	1,07	ns	1,28	1,06	ns
GABA	0,07	0,00	**	1,10	0,02	**	0,11	0,01	**	2,77	0,05	**
Arg	0,08	0,07	ns	0,01	0,08	ns	0,10	0,13	*	0,02	0,03	**
Tyr	0,04	0,08	**	0,03	0,03	ns	0,08	0,16	**	0,06	0,05	ns
val	0,25	0,30	**	0,09	0,15	*	0,29	0,47	**	0,29	0,24	ns
Trp	0,03	0,03	ns	0,14	0,02	**	0,04	0,15	*	0,25	0,10	**
Phe	0,08	0,10	*	0,03	0,03	ns	0,10	0,25	**	0,08	0,07	ns
Ileu	0,13	0,14	ns	0,05	0,07	ns	0,15	0,29	**	0,11	0,09	ns
Leu	0,12	0,17	**	0,06	0,10	**	0,17	0,37	**	0,16	0,15	ns
Lys	0,10	0,12	*	0,03	0,02	ns	0,12	0,23	**	0,05	0,06	ns

Values are the mean of eight biological replicates for shoot and five biological replicates for root; student t-test comparing abundance in wild-type and *gad1/2* plants; asterisks represent significant ($P < 0.05$, *), highly significant ($P < 0.01$, **)

The same amino acids, however, showed lower accumulation in the root of the wild type compared to the level in *gad1/2* roots under control conditions (Table 3). The less abundant amino acids (Trp, Phe, Ileu), on the other hand, showed a higher accumulation in leaves of *gad1/2* plants compared to wild type, and the increment was significant for most of them (Table 3).

Treatment with 150 mM NaCl almost doubled the accumulation of GABA in the leaf and root of wild-type plants. In roots of wild-type plants, 138 $\mu\text{mol/g}$ FW of GABA was recorded after 150 mM NaCl treatment, an observation that is in line with the previous report of Renault et al. (2010) (Table 3). The *gad1/2* mutant also contained 0.3 and 2.7 μmol GABA per gram FW in leaves and roots, respectively, after salt treatment. The GABA precursor glutamate, showed a 37% and 174% higher accumulation in leaves and roots of wild-type plants, respectively, after 150 mM NaCl treatment. All less abundant amino acids showed a significantly higher accumulation in leaves of *gad1/2* plants. However, in roots, all except tryptophan showed a similar level of accumulation (Table 3).

Furthermore, the effect of *gad1/2* mutations on the accumulation of some TCA cycle metabolites was analyzed. The knockout of *gad1/2* genes significantly decreased the accumulation of fumarate, oxaloacetate, malate and citrate but not succinate (Fig. 22A&B). However, 150 mM NaCl treatment significantly increased the accumulation of malate, oxaloacetate and citrate but not succinate and fumarate in *gad1/2* shoots (Fig. 22B). In the wild-type this treatment led to a lower accumulation of all analyzed TCA cycle metabolites (Fig. 22A). Taking together, it can be assumed that TCA cycle and GABA shunt are strongly linked to each other. Proline is one of the products of glutamate metabolism and is known to be induced during abiotic stresses. Hence, its accumulation in wild-type and *gad1/2* plants was compared before and after 150 mM NaCl treatment. Proline accumulation could not be detected under controlled conditions in both genotypes (Fig. 22C&D). However, treatment with 150 mM NaCl increased proline accumulation in both genotypes. The accumulation of proline in *gad1/2* leaves was 63-fold higher compared to its accumulation in wild-type leaves. This observation suggests that glutamate metabolism favors the production of GABA over proline

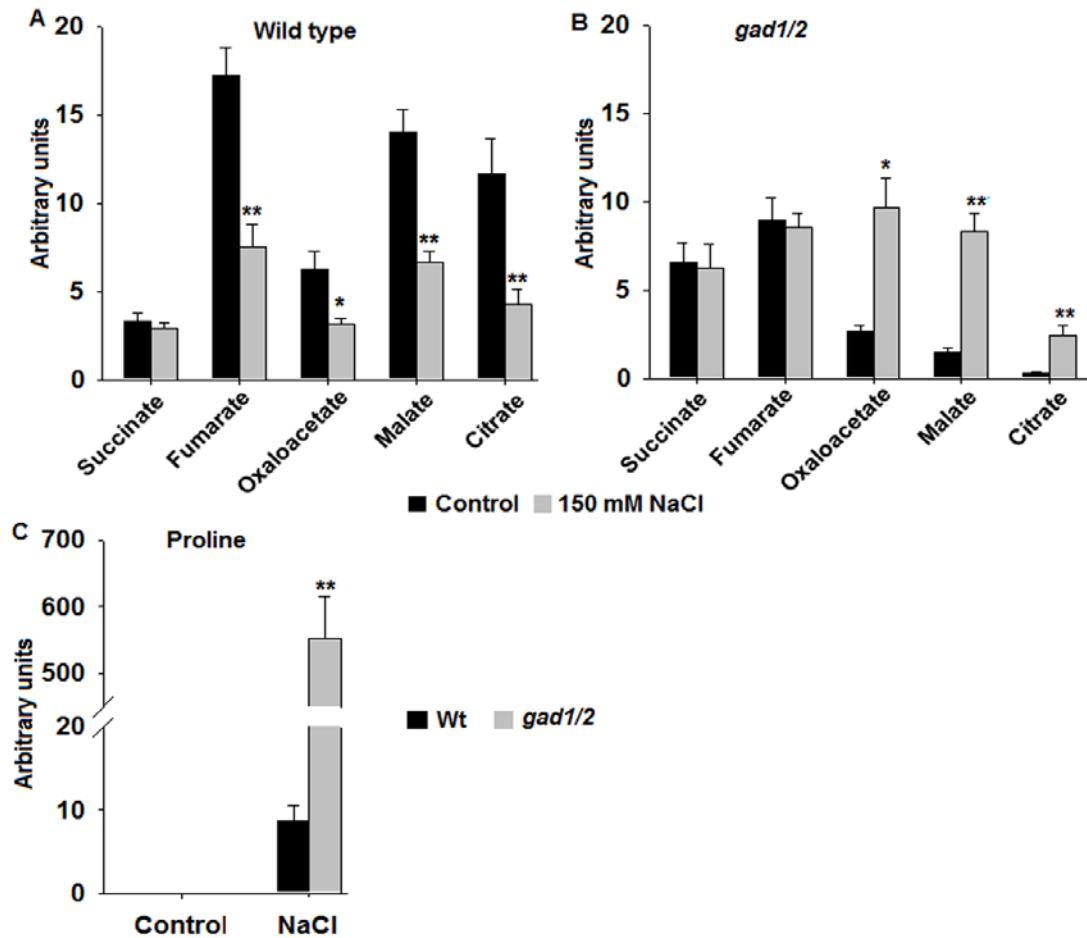


Figure 22. GC-MS analysis of major TCA cycle metabolites; leaf material from four-week-old wild-type (A) and *gad1/2* (B) plants treated without and with 150 mM NaCl were used; proline was also measured in leaf extracts of wild-type (C) and *gad1/2* (D) plants; the values are the mean of at least three biological replicates, each of which was measured in triplicates; error bars represent the standard error of means; asterisks represent statistical significance after student t-test, *~ $P < 0.05$ and **~ $P < 0.01$.

B) Drought treatment

Drought-induced metabolic disorder was investigated in leaves of wild-type, *gad1*, *gad2* and *gad1/2* plants. Under normal growth conditions, the content of most amino acids did not differ between the wild-type and the mutants. As expected, the level of GABA was dramatically reduced in single and double mutants under normal growth conditions. The GABA content in the double mutant was also significantly different from the level in the *gad1* mutant. On the other hand, the GABA precursor, glutamate, was significantly increased in single and double mutants. However, there was no difference in the level of glutamate between single and the double mutants.

Table 4. Abundance of amino acids ($\mu\text{mol/g}$ FW) in leaves of wild type, *gad1 gad2* and *gad1/2* plants grown under normal and drought stress conditions.

	Control				Drought			
	Wt	<i>gad1</i>	<i>gad2</i>	<i>gad1/2</i>	Wt	<i>gad1</i>	<i>gad2</i>	<i>gad1/2</i>
Asp	5.722	5.698	4.858	5.006	5.766	5.350	7.067*	6.535
Glu	8.874	8.310	7.018	9,719	7.603	7.617	8.946	8.553*
Ser	0.657	0.461**	0.407*	0.474**	0.830	0.710	0.726	0.708
Asn	3.662	3.635	3.004	3.421	3.137	4.030*	4.392**	5.494**
Gln	3.542	2.721	2.010*	2.440*	5.890	5.110	5.027	4.682*
Gly	0.253	0.197	0.149*	0.148*	0.237	0.220	0.300	0.228
Thr	0.757	0.665	0.542*	0.604*	1.210	1.040	1.127	1.047
Ala	2.167	1.628*	1.214**	1.258**	2.564	2.101**	2.488	2.143
GABA	0.115	0.009*	0.009*	0.008*	0.198	0.008**	0.010**	0.009**

The drought treatment led generally to an increase in the accumulation of most amino acids. In *gad1* plants, the accumulation of asparagine was significantly increased whereas the level of alanine was significantly reduced compared to the wild type (Table 4). In *gad2* leaves, the accumulation of both aspartate and asparagine were significantly increased compared to the wild type in response to drought stress. Most notably, the glutamate level did not increase further in *gad2* and the double mutant but was even reduced as is the case for *gad1* (Table 4). In the *gad1/2* mutant, the glutamate level remained significantly higher after drought stress whereas that of the glutamate precursor, glutamine, was significantly reduced compared to the wild type.

3.8. Expression analysis of *GAD3* and *GAD4* after salt treatment

GABA is known to accumulate under salt stress condition, and this is associated with an increase in GAD transcript levels (Renault et al., 2010). In this study, GABA accumulation was enhanced in *gad1/2* shoot and root following salt stress. Therefore, the expressions of *GAD3* and *GAD4* were analyzed in leaves and roots of wild-type and *gad1/2* plants after 150 mM NaCl treatment. *GAD3* expression was generally unchanged in leaves and roots before and after the treatment (Fig. 23A). *GAD4* expression was approximately four-fold induced in the root of *gad1/2* plants, an observation that is in line with the previous finding of Renault et al. (2010) (Fig. 23D). Unexpectedly, the expression of *GAD4* in the leaves was reduced almost by half following 150 mM NaCl treatment (Fig. 23B).

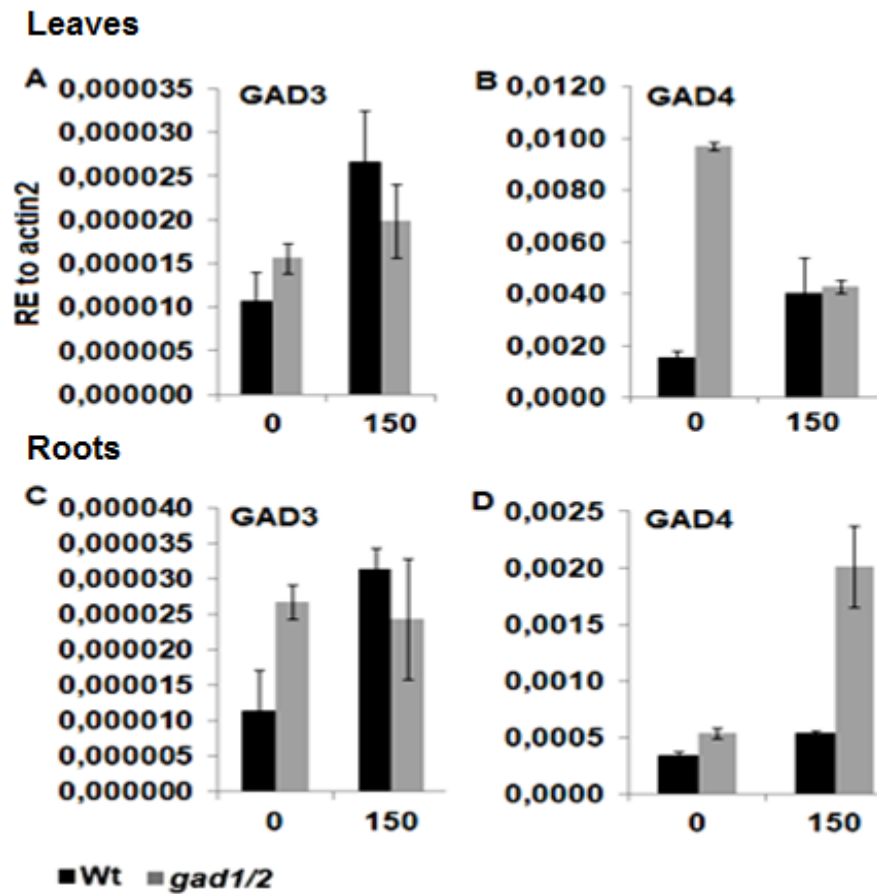


Figure 23. Transcript analysis of *GAD3* and *GAD4* in leaves (A&B) and roots (C&D) of wild-type and *gad1/2* plants treated without or with 150 mM NaCl; leaf and root samples were collected from four-weeks-old plants; values are the mean of three biological replicates and each with duplicate measurement; error bars represent the standard error.

4. Discussion

4.1. The truncated *GAD2* transcript lacks decarboxylase activity

Sequencing of the truncated *GAD2* fragment revealed that the transcript completely lacks the 3rd, 4th and 5th exon in addition to the first 34 bases of the 6th exon. Glutamate decarboxylases belong to the pyridoxal phosphate-dependent aspartate aminotransferase superfamily proteins (Marchler-Bauer et al., 2011). The residues which are important for pyridoxal phosphate binding, a cofactor in the catalytic activity, in *GAD2* have been predicted to be Ser, Ser, Ile, Ile, Asp, Ser, Ser and Lys which correspond to amino acid numbers 125, 126, 129, 208, 243, 246, 273 and 276, respectively (Marchler-Bauer et al., 2011). The Lys residue, which corresponds to the amino acid number 276, in addition to its co-factor binding role, was predicted to be catalytically active. These co-factor binding and catalytic residues are encoded by nucleotides in exon 3, 4 and 5. However, in the truncated *GAD2* transcript these exons are missing. In addition, a premature stop codon was inserted close to the junction between the 2nd and the 6th exon to further shorten the eventually translated protein. Therefore, it is very unlikely that the truncated protein would have a decarboxylase activity.

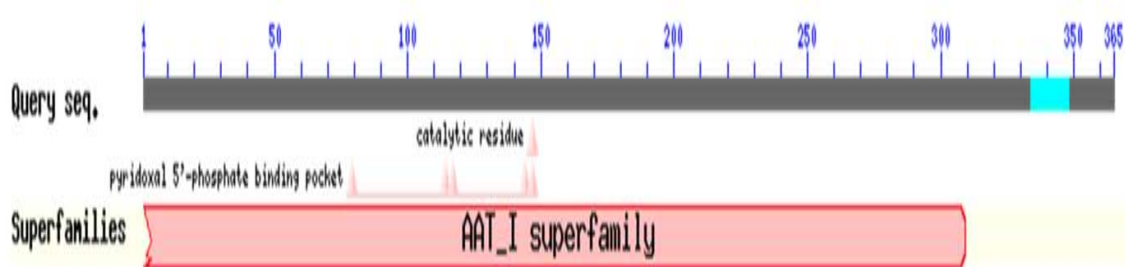


Figure 24. Schematic representation of *GAD2* protein with predicted catalytic residue and co-factor binding residues, Marchler-Bauer et al., 2011

The truncated *GAD2* transcript also seems to be stable and be expressed at a higher level than the corresponding native transcript. The molecular mechanisms controlling the stability of mRNAs have well been studied. The sequences upstream (5'-UTR) and downstream (3'-UTR) and poly(A) of the ORF were shown to be important in maintaining RNA stability (Chen et al., 2001; Parker and Sheth, 2007). The truncated *GAD2* transcript has indeed intact 5' and 3' UTR regions, and hence the stability of the transcript was not unexpected. The origin of the nine nucleotides (ATTTCCGG) that were inserted in between exon2 and exon6 is unknown. Sequences similar to the first six bases were identified in the intron region of the *GAD2* gene and also on the vector backbone of the T-DNA insertion. However, the exact source of this sequence is unknown.

4.2. GAD1 and GAD2 proteins synthesize most of the GABA in shoots and roots

GABA is mainly produced *via* the GABA shunt. However, there are reports which indicated the possible synthesis of GABA by the degradation of polyamines like spermidine, putrescine, etc. (Bouchereau et al., 1998; Fait et al., 2007). In *Arabidopsis*, five *GAD* genes have been identified each of which show a distinct expression pattern in tissues. *GAD1* and *GAD2* contribute more than 90% of the total *GAD* transcript in leaves and roots under normal growth conditions (Table 1). If the activity of glutamate decarboxylases is the only factor to determine the GABA pool in leaves and roots, then mutation in the two genes would dramatically reduce the GABA level. Indeed, simultaneous mutations of *gad1* and *gad2* decreased the GABA level by 10-fold in the shoot and 48-fold in the root compared to the wild type (Fig. 5; Table 3&4). Previously, the control of the GABA pool by GABA degradation has been reported. The *Arabidopsis pop2* mutant, defective in GABA degradation, accumulated a significantly higher amount of GABA in leaves and roots compared to the wild type (Palanivelu et al., 2003; Renault et al., 2010). Despite the control of GABA pool by its degradation, the synthesis appeared to be a major determinant. The significant reduction of the GABA level in the *gad1/2* plants (Fig. 3B) indicated that the major route for GABA production is the GABA shunt.

4.3. GABA plays a role in the normal development of *Arabidopsis*

The GABA-less *gad1/2* mutant plants showed a reduced rosette size compared to the wild type. To determine whether this was a growth and/or developmental problem, the cell density was determined and the result showed that there is no difference in the average cell size, thus excluding a growth defect. The overall reduced rosette size of *gad1/2* mutant plants was due to the reduced total number of cells which points towards a defect in cell division/proliferation, i.e. a defect in development. The question remains how GABA influences the division of a cell. In the mammalian system, the role of GABA in cell proliferation and differentiation has been reported (Watanabe et al., 2006). The underlying mechanism has been suggested to be the activation of the GABA receptors which in turn activates the receptor tyrosine kinases as shown in cancer cells (Yarden 2001). Tyrosine kinases catalyze the transfer of phosphate group onto the tyrosine residue of a protein thereby controlling many cellular processes including cell division (Radha et al., 1996). However, the presence of both GABA receptor and tyrosine kinase has not been reported in plants.

The increase in the GAD activity and the accumulation of GABA in colon cancer, breast cancer and gastric cancer cells indicated the role of GABA in cell proliferation (Maemura et al., 2003; Opolski et al., 2000; Matuszek et al., 2001). Mice defective in the two GAD genes (GAD 65/67) were completely lacked GABA and was born with cleft palate (Ji et al., 1999). Arabidopsis *gad1* plants contained less GABA in roots and exhibited a less developed root system (Bouche et al., 2004). Similarly, *gad1/2* plants showed a shorter root length when grown on soil. The root fresh weight, however, remained unchanged mainly due to the proliferation of many auxiliary roots. Although the GABA receptors have not been identified in plants, the involvement of GABA in plant cell proliferation and normal plant development cannot be ruled out.

4.4. The *gad1/2* mutant metabolite was differentially regulated under salt and drought stress.

The accumulation of glutamate, which plays a central role for the synthesis of almost all other amino acids, was significantly higher in *gad1/2* mutant compared to wild type under normal growth conditions (Tables 3 & 4). The single mutants also accumulated a significantly higher level of glutamate in leaves compared to wild type (Table 4). The higher glutamate content in the *gad1* mutant seems to be shoot-specific as similar glutamate levels in roots of wild-type and *gad1* mutant have been reported (Bouche et al., 2004). Glutamate can be converted to aspartate by transferring the amino group to oxaloacetate, and aspartate in turn is known to be the precursor for asparagine, lysine, threonine and isoleucine (Lea et al., 2007; Azevedo et al., 2006). After drought stress, the significant increase in the asparagine pool in *gad1/2* plants most likely resulted from the conversion of glutamate (Table 4). A relatively stable accumulation of glutamate compared to the other amino acids has been discussed by Forde and Lea (2007). However, the observation in this study showed a significant change in the glutamate pool which was not even observed for most of the other amino acids analyzed. Although there are arguments that indicate the tight control of the glutamate pool by its synthesis, i.e. glutamate synthase and glutamate dehydrogenase (Maschlaux-Daubresse et al., 2006), its degradation through the GABA shunt also seems to be important. Alanine is another amino acid which rapidly accumulates in Arabidopsis during drought stress (Allan et al, 2008). In this study, however, the accumulation of alanine did not increase in wild type, and even decreased in mutants following drought stress (Table 4). The decrease in the level of alanine in single and double mutants indicates the significant contribution of GABA-derived

alanine to the total alanine pool under drought stress. Similar results have been reported in *gad1* mutant that was subjected to hypoxic condition (Miyashita and Good, 2008).

A strong link between the TCA cycle and the GABA shunt has been discussed previously (Fait et al., 2007). Mutations in the TCA cycle upstream of succinate production have been shown to affect the general activity of the GABA shunt (Fait et al., 2007; Studart-Guimarães et al., 2007). In this experiment, the accumulation of all metabolites, except succinate, were significantly reduced in *gad1/2* plants compared to wild type under control conditions. This observation indicated the significant contribution of the GABA shunt to the TCA cycle metabolite pool. However, after 150 mM NaCl treatment, the accumulation of all analyzed metabolites was significantly reduced in wild-type plants, whereas in *gad1/2* plants the accumulation of malate, oxaloacetate and citrate significantly increased. This might be due to a feedback response from the accumulation of glutamate. The over-accumulation of glutamate in the double mutant may down-regulate the activity of glutamate dehydrogenase, which is responsible for the production of glutamate from α -ketoglutarate. This in turn may cause an over-accumulation of α -ketoglutarate and further upstream metabolites. The induction of the GABA shunt during stresses may suggest the limited activity of α -ketoglutarate dehydrogenase, which otherwise would convert its substrate to succinyl CoA more efficiently and reduce the substrates for the GABA shunt.

A dramatic increment of proline accumulation, which is 63-fold higher than the wild type, was observed under salt stress condition in *gad1/2* plants. This indicates that under stress the GABA shunt is a preferred route for the metabolism of glutamate. The GABA shunt in wild-type plants functions normally and the majority of glutamate was, therefore, metabolized via the GABA shunt. This is clearly demonstrated by the rapid increase of GABA and significantly less accumulation of proline in wild-type leaves compared to *gad1/2*. A preferential accumulation of GABA over proline has previously been reported in tobacco plants during water stress (Liu et al., 2011). This observation strongly suggests that GABA could play an osmo-protectant role which is the normal function of proline.

4.5. GABA accumulation during salt and drought stress is important to prevent dehydration

GABA accumulation has been shown to be rapidly induced and to account for a major proportion of total free amino acids during biotic and abiotic stresses (Bown and Shelp,

1997). Of many abiotic stresses that plants are exposed to, salt and drought stress are the most prominent ones. About 20% of the irrigated lands are adversely affected by salinity (Flowers and Yeo, 1995). The toxicity of high concentrations of salt is known to have two components. First, it causes an ionic stress by directly competing with the uptake of physiologically important ion i.e. potassium; second, it causes an osmotic stress by providing a hypertonic environment and thereby causing dehydration. The *gad1/2* plants treated with 150 mM NaCl exhibited a wilted phenotype under green house conditions which is a manifestation of the osmotic component of salt stress. Despite the element analysis showed a higher accumulation of Na⁺ in *gad1/2* shoots, it does not seem to be sufficient to elicit ionic specific-stress symptoms. Indeed, ionic stress-specific symptoms like chlorosis and necrosis have not been observed. Treatment with 10 mM LiCl, which is an osmotically inactive concentration, elicited leaf chlorosis and necrosis in both genotypes within one week after the treatment, indicating that *gad1/2* plants were not oversensitive to the ionic stress component of salt stress. The osmotic stress experiment further confirmed the rapid loss of water in *gad1/2* plants which subsequently led to a wilted phenotype.

GABA has been described to play several roles in plants including function it's as osmoprotectant (Bown and Shelp, 1997). The accumulation of GABA during stress may lead to osmotic adjustment, typical of many compatible osmolytes, which in turn prevents dehydration. However, *gad1/2* plants were unable to induce GABA accumulation during salt and drought stress and hence were subjected to loss of water. Wild-type plants almost doubled the GABA content in roots following the salt stress most likely to reduce the osmotic gradient against the soil. The drought stress phenotype was more dramatic under greenhouse conditions than in the growth chamber. This was most likely due to different growth conditions; for example, the relative humidity (RH) in the growth chamber was in the range of 60-70% during the experiment whereas in the greenhouse it was as low as 40%. Therefore, it is likely that the transpiration rate was higher in the greenhouse.

The *gad1* and *gad2* single mutants were also unable to promote the accumulation of GABA and hence, are sensitive to drought stress. This indicates that the two GAD isoforms are not redundant, since the mutation of *gad1* was not compensated by *GAD2* and vice versa. Indeed, previous work showed that mutation of *gad1* did not affect the expression level of *GAD2* (Bouche et al., 2004) and the activity of *GAD2* (Miyashita and Good, 2008). It is likely that the expression and activity of *GAD1* not to be affected in the *gad2* background. The

metabolic data provided here supports this idea and also suggests that *GAD1* and *GAD2* might be differentially regulated. Indeed, under salt stress the transcript of *GAD1* decreases with increasing salt concentration whereas *GAD2* transcript consistently increases in RNA extracts of Arabidopsis whole plantlets (Renault et al., 2010). Under hypoxic conditions, the expression of *GAD1* increases whereas *GAD2* expression decreases (Miyashita and Good, 2008) further confirming the different regulation. There is a striking difference in the calmodulin domain of the two proteins in that *GAD2* lacks all four serine and threonine residues which is present in the *GAD1* calmodulin domain (Bouche et al., 2004).

4.6. *GAD* mutations enhance the transpiration rate by affecting the stomata density

As shown in the result section, *gad1/2* plants were oversensitive to drought stress, and this was correlated to a rapid loss of water through transpiration. The increased transpiration rate was at least partially attributed to an increase in stomata density. The question remained whether GABA or a derivative of GABA play a role in stomata development. The role of SSA or derivatives of SSA in the leaf patterning and structure along the adaxial-abaxial axis has been reported previously (Toyokura et al., 2011). The authors showed that the external application of SSA gave an adaxial character to the abaxial side of leaves. The authors also showed a reduced but similar effect of GABA and succinic acid on the adaxialization of leaves. The *gad1/2* plants contained undetectable level of GABA in the shoot. Reduced GABA level most likely leads to a reduced level of SSA, and this subsequently could lead to the abaxialization of the adaxial side of a leaf. This eventually may lead to a higher stomata density. To determine the specificity of the phenotype to the absence of GABA, the *gad1/2* plants were irrigated with 5 mM GABA. However, the phenotype was not suppressed. In fact, the concentration of GABA detected in the *gad1/2* leaves after GABA feeding was very low compared to the GABA detected in the wild-type leaves grown under normal conditions. This can be explained in three different ways. First, the concentration of GABA used for irrigation was too low. Second, the GABA absorbed was immediately metabolized and could not therefore act as an osmolyte. Third, the GABA absorbed may be restricted to the root and not transported to leaves. Therefore, further investigation with a higher concentration of GABA is important to assess this issue.

There is another hypothesis linking the GABA shunt with stomata biogenesis. Plants open their stomata mainly for exchange of gases despite losing water. The conversion of

glutamate to GABA involves the uptake of protons (H^+) and the release of CO_2 . The produced CO_2 is most likely shuttled into the Calvin cycle, thus contributing to the total carbon fixed by the plant. When CO_2 from the GABA shunt cannot be provided, plants will increase the uptake of CO_2 from the atmosphere. This can be achieved by increasing either the stomata number or the stomata aperture. Stomata conductance measurements and stomata number showed an increment of stomata density and stomata aperture. However, the percent contribution of the GABA shunt to the total CO_2 fixation should be analyzed.

4.7. Stomata closure was partially impaired in *gad1/2* mutant

Plants take in CO_2 and release water through stomata, an opening on the leaf epidermal cells formed by two “bean shaped” cells called guard cells. The water potential status of the two guard cells determines the opening and closing of the stomata. In general, the opening and closure of stomata involves the influx and efflux of anions and cations mediated by channels (Schroeder and Hagiwara, 1989; Blatt and Armstrong, 1993). The most widely known anions include chloride and malate, whereas potassium is the only cation described to date. Several stimuli has been described to control the opening and closing of the stomata these include light, CO_2 , temperature, ABA etc.

In this study, the *gad1/2* mutant showed a defect in the stomata closure as shown in the light to dark transition experiment, and was oversensitive to drought stress. Stomata closure during drought stress involves the sensing of the drought, the induction of the ABA pathway, the release of calcium ion, activation of ion channels and efflux of ion and water. The inability of *gad1/2* leaves to close their stomata as quickly as a wild-type after 10 μM ABA treatment suggests that the defect was not in the ABA synthesis. Similarly, upon light to dark transition the stomata closure response of *gad1/2* mutant was slower than the wild-type, indicating that the defect was common for both light and ABA mediated stomata closure. The stomata closure induced by both dark and ABA involve the efflux of ions, and therefore; it is possible that the defect is on the efflux of the ions. The questions that remain unanswered are how the GABA shunt plays a role in the efflux of ions, which component of the GABA shunt is important and in which step it plays a role. Therefore, further investigations have to be performed.

4.8. GABA shunt plays a role in potassium homeostasis

The GABA-less *gad1/2* plants accumulated a significantly lower amount of potassium in shoots under normal growth conditions (Fig. 13). In contrast, high GABA accumulating *pop2-1* plants showed a significantly higher K^+ levels in the shoot (Renault et al., 2010). The two observations together indicate that there is a correlation between the proper functioning of the GABA shunt and K^+ homeostasis in the plant. The potassium uptake experiment on low potassium containing plates further indicated that GABA has an important function in K^+ uptake. The most likely mechanism would be the regulation of potassium channels *via* other regulatory proteins. For example, 14-3-3 proteins, well known regulatory proteins, have been reported to be regulated by GABA (Lancien and Roberts, 2006) which in turn could regulate potassium transporters like KAT1 (Sottocornola et. al., 2006).

The sustained growth of *pop2* plants on low potassium contrasts the previous observation by Renault et al. (2010). This is likely due to the difference in the experimental approach. In this experiment the seeds were first germinated on $\frac{1}{2}$ MS plate and then transferred to low potassium-containing plates. In the report by Renault et al., (2010), the seeds were germinated and grown directly on low potassium plates. Therefore, *pop2* plants may have accumulated sufficient potassium to allow growth under low potassium.

5. Conclusions

The rapid accumulation of GABA during biotic and abiotic stress is well documented. GABA is primarily synthesized from the decarboxylation of glutamate by glutamate decarboxylase (GAD), which exists in five copies in Arabidopsis genome. Despite its presence in multiple copies, *GAD1* and *GAD2* are the most abundantly expressed genes in leaves and roots. Knockout of the two genes reduced the GABA content dramatically in both tissues. This indicated that the GABA pool is mainly controlled by its synthesis. Phenotypic analysis of the GABA-depleted mutants revealed the sensitivity to salt, osmotic and drought stresses. The hypersensitivity of *gad1/2* plants to drought stress mediated by an increased transpiration rate confirms the involvement of GABA in leaf development and patterning. The wilting phenotype under salt stress showed the effect of the osmotic component of salt stress rather than the ionic stress. The dramatic increase of the already high GABA level in the root of wild-type plant indicates the importance of GABA as an osmolyte. The role of GABA as signaling molecule in the plant system should be further investigated.

Previous studies to identify the role of GABA in plants were carried out using only the high GABA accumulating *pop2* line. However, the results generated by using only *pop2* could not give conclusive information regarding the role of GABA. In this study, a GABA depleted *gad1/2* line was presented which in combination with the *pop2* line could be used to investigate the specific role of GABA in normal development and response to biotic and abiotic stresses.

References

- Akama K, Takaiwa F (2007)** C-terminal extension of rice glutamate decarboxylase (OsGAD2) functions as an autoinhibitory domain and overexpression of a truncated mutant results in the accumulation of extremely high levels of GABA in plant cells. *J. Exp. Bot.* 58: 2699-2707.
- Azevedo RA, Lancien M, Lea PJ (2006)** The aspartic acid metabolic pathway, an exciting and essential pathway in plants. *Amino Acids* 30:143–162.
- Bach B, Meudec E, Lepoutre JP, et al. (2009)** New Insights into γ -Aminobutyric Acid Catabolism: Evidence for γ -Hydroxybutyric Acid and Polyhydroxybutyrate Synthesis in *Saccharomyces cerevisiae*. *Appl. Environ. Microbiol.* 75(13):4231-4239.
- Baum, G., Lev-Yadun, S., Fridmann, Y., Arazi, T., Katsnelson, H., Zik, M. et al. (1996)** Calmodulin binding to glutamate decarboxylase is required for regulation of glutamate and GABA metabolism and normal development in plants. *EMBO J.* 15: 2988–2996.
- Blatt MR, Armstrong F (1993)** K⁺ channels of stomatal guard cells: Abscisic-acid-evoked control of the outward-rectifier mediated by cytoplasmic pH. *Planta* 191:330-341.
- Bouchereau A, Aziz A, Larher F, Martin-Tanguy J (1998)** Polyamines and environmental challenges: recent development. *Plant Science* 140:103-125.
- Bouché N, Lacombe B, Fromm H (2003)** GABA signaling: A conserved and ubiquitous mechanism. *Trends Cell Biol.* 13:607–610.
- Bown AW, Shelp BJ (1997)** The metabolism and functions of γ -aminobutyric acid. *Plant Physiol* 115:1–5.
- Bouche N, Fromm H (2004)** GABA in plants: just a metabolite? *Trends Plant Sci.* 9: 110–115.
- Chen CY, Gherzi R, Ong SE, et al. (2001)** AU binding proteins recruit the exosome to degrade ARE-containing mRNAs. *Cell* 107:451–464.
- Cousson A, Cotellet V, Vavasseur A (1995)** Induction of stomatal closure by Vanadate or a light/dark transition involves Ca²⁺-calmodulin-dependent protein phosphorylations. *Plant Physiol.* 109:491-497.
- Dubos C, Huggins D, Grant GH, Knight MR, Campbell MM (2003)** A role for glycine in the gating of plant NMDA-like receptors. *Plant Journal* 35:800-810.
- Fait A, Fromm H, Walter D, Galili G and Fernie AR (2008).** Highway or byway: the metabolic role of the GABA shunt in plants. *Trends in Plant Science* 13(1):14-19.
- Forde BG, Lea PJ (2007)** Glutamate in plants: metabolism, regulation, and signaling. *Journal of Experimental Botany* 58(9):2339–2358.

- Ji FY, Kanbara N, Obata K (1999)** GABA and histogenesis in fetal and neonatal mouse brain lacking both isoform of glutamic acid decarboxylase. *Neurosci. Res.* 33:187-194.
- Kim SA, Kwak JM, Jae SK, Wang MH, Nam HG (2001)** Overexpression of the *AtGluR2* gene encoding an Arabidopsis homolog of mammalian glutamate receptors impairs calcium utilization and sensitivity to ionic stress in transgenic plants. *Plant and Cell Physiology* 42:74-84.
- Kinnersley AM, Turano FJ (2000)** γ -Aminobutyric Acid (GABA) and Plant Responses to Stress. *Critical Reviews in Plant Sciences* 19(6):479-509.
- Lacombe B, Becker D, Hedrich R, et al. (2001)** The identity of plant glutamate receptors. *Science* 292:1486–1487.
- Lam HM, Chiu J, Hsieh MH, et al. (1998)** Glutamate-receptor genes in plants. *Nature* 12: 396 (6707):125-126.
- Lancien M, Roberts MR (2006)** Regulation of Arabidopsis thaliana 14-3-3 gene expression by γ -aminobutyric acid. *Plant, Cell & Environment* 29(7):1430-1436.
- Lea PJ, Sodek L, Parry MAJ, Shewry PR, Halford NG (2007)** Asparagine in plants. *Annals of Applied Biology* 150:1–26.
- Liu C, Zhao L, Yu G (2011)** The dominant glutamic acid metabolic flux to produce γ -amino butyric acid over proline in *Nicotiana tabacum* leaves under water stress relates to its significant role in antioxidant activity. *J. Integr. Plant Biol.* 53(8):608–618.
- Logemann J, Schell J, Willmitzer L (1987)** Improved method for the isolation of RNA from plant tissue. *Anal. Biochem.* 163:16-20.
- Maemura K, Yamauchi H, Hayasaki H, et al. (2003)** γ -Amino-butyric acid immunoreactivity in intramucosal colonic tumors. *J. Gastroenterol.Hepatol.* 18:1089-1094.
- Marchler-Bauer A, Lu S, Anderson JB, et al. (2011)** CDD: a Conserved Domain Database for the functional annotation of proteins. *Nucleic Acids Res.* 39(D):225-229.
- Masclaux-Daubresse C, Reisdorf-Cren M, Pageau K, et al. (2006)** Glutamine–glutamate synthase pathway and glutamate dehydrogenase play distinct roles in the sink source nitrogen cycle in tobacco. *Plant Physiology* 140: 444–456.
- Matuszek M, Jesipowicz M, Kleinrok Z (2001)** GABA content and GAD activity in gastric cancer. *Med. Sci. Monit.* 7:377-381.
- Miyashita Y, Good AG (2008)** Contribution of the GABA shunt to hypoxia induced alanine accumulation in roots of Arabidopsis thaliana. *Plant and Cell Physiology* 49(1):92-102.
- Opolski A, Mazurkiewicz M, Wietrzyk J, et al. (2000)** The role of GABAergic system in human mammary gland pathology and in growth of transplantable murine mammary cancer. *J. Exp. Clin. Cancer Res.* 19:383-390.

- Park DH, Mirabella R, Bronstein PA, et al. (2010)** Mutations in γ -aminobutyric acid (GABA) transaminase genes in plants or *Pseudomonas syringae* reduce bacterial virulence. *Plant J.* 64:318–330.
- Palanivelu R, Brass L, Edlund AF, Preuss D (2003)** Pollen tube growth and guidance is regulated by POP2, an *Arabidopsis* gene that controls GABA levels. *Cell* 114:47–59.
- Parker R, Sheth U (2007)** P bodies and the control of mRNA translation and degradation. *Mol. Cell.* 25:635–646.
- Radha V, Nambirajan S, Swarup G (1996)** Association of Lyn tyrosine kinase with the nuclear matrix and cell-cycle-dependant changes in matrix-associated tyrosine kinase activity. *Eur. J. Biochem.* 236(2):352-359.
- Renault H, Roussel V, Amrani A El, et al. (2010)** The *Arabidopsis pop2-1* mutant reveals the involvement of GABA transaminase in salt stress tolerance. *BMC Plant Biol.* 10:1–16.
- Renault H, Amrani A El, Palanivelu R, et al. (2011)** GABA accumulation causes cell elongation defects and a decrease in expression of genes encoding secreted and cell wall-related proteins in *Arabidopsis thaliana*. *Plant Cell Physiol.* 52(5):894-908.
- Schroeder JI, Hagiwara S (1989)** Cytosolic calcium regulates ion channels in the plasma membrane of *Vicia faba* guard cells. *Nature* 338:427-430.
- Shelp BJ, Bown AW, McLean MD (1999)** Metabolism and functions of gamma-aminobutyric acid. *Trends Plant Sci* 4:446–452.
- Shelp BJ, Bown AW, Faure D (2006)** Extracellular γ -Aminobutyrate mediates communication between plants and other organisms. *Plant Physiology* 142:1350-1352.
- Shimada S, Cutting G, Uhl GR (1992)** gamma-Aminobutyric acid A or C receptor? gamma-Aminobutyric acid rho 1 receptor RNA induces bicuculline-, barbiturate-, and benzodiazepine-insensitive gamma-aminobutyric acid responses *Xenopus* oocyte. *Mol. Pharmacol.* 41 (4): 683–687.
- Solomon PS, Oliver RP (2002)** Evidence that γ -aminobutyric acid is a major nitrogen source during *Cladosporium fulvum* infection of tomato. *Planta* 214:414–420
- Sottocornola B, Visconti S, Orsi S, et al. (2006)** The potassium channel KAT1 is activated by plant and animal 14-3-3 proteins. *Journal of Biological Chemistry* 281: 35735–35741.
- Steward FC, Thompson JF, Dent CE (1949)** γ -Aminobutyric acid: a constituent of the potato tuber? *Science* 110:439-440.
- Studart-Guimarães C, Fait A, Nunes-Nesi A, et al. (2007)** Reduced Expression of Succinyl-CoA Ligase Can Be Compensated for by Up-Regulation of the γ -Aminobutyrate Shunt in Illuminated Tomato Leaves. *Plant Physiology* 145(3):626-639.

Suliaman S, Schulze J (2010) Phloem-derived γ -aminobutyric acid (GABA) is involved in upregulating nodule N₂ fixation efficiency in the model legume *Medicago truncatula*. *Plant Cell Environ.* 33(12):2162-2172.

Takeuchi A, Onodera K (1972) Effect of bicuculline on the GABA receptor of the crayfish neuromuscular junction. *Nature New Biol.* 236 (63):55–56.

Toyokura K, Watanabe K, Oiwaka A, et al. (2011) Succinic semialdehyde dehydrogenase is involved in the robust patterning of arabidopsis leaves along the adaxial–abaxial axis. *Plant Cell Physiol.* 52(8):1340–1353.

Turano FJ, Fang TK (1998) Characterization of two glutamate decarboxylase cDNA clones from Arabidopsis. *Plant Physiol.* 117:1411-1421.

Watanabe M, Maemura K, Oki K, et al. (2006) Gamma-aminobutyric acid (GABA) and cell proliferation: focus on cancer cells. *Histol Histopathol* 21:1135-1141.

Yarden Y (2001). The EGFR family and its ligands in human cancer: signaling mechanisms and therapeutic opportunities. *Eur. J. Cancer* 37(4):3-8.

Zik M, Arazi T, Snedden WA, Fromm H (1998) Two isoforms of glutamate decarboxylase in Arabidopsis are regulated by calcium/calmodulin and differ in organ distribution. *Plant Mol. Biol.* 37:967–975.

Chapter Two: Investigation on GHB/SSA toxicity

1. Introduction

Gamma hydroxybutyric acid (GHB) is a naturally occurring compound and regarded as short chain fatty acid. In mammals, it is found in the brain, and was known to function as a neurotransmitter or neuro-modulator in the central nervous system (Poldrugo and Addolorato, 1998). These days the compound is used as a drug against sleeping disorders and also alcoholism. GHB has also been detected in various organisms including yeast (Bach et al., 2009) and plants (Allan et al., 2008) apart from mammals. The presence of GHB in plants was first reported almost a decade ago (Breitkreuz et al., 2003; Allan et al., 2003). GHB is known to accumulate in plants in response to environmental stresses most likely to prevent the resulting damage. Arabidopsis plants stressed with drought, salinity, heat and oxygen deficiency accumulated higher amounts of GHB (Allan et al., 2008). A dramatic increase in GHB levels from 10 to 155 nmol/g FW in soya bean sprouts, and from 273 to 739 nmol/g DW in green tea leaves after anoxia treatment has previously been reported (Allan et al., 2003). In yeast the existence of GHB and its subsequent metabolism to form polyhydroxybutyric acid (PHB) was demonstrated in 2009 (Bach et al., 2009); despite, the enzyme(s) responsible for converting SSA to GHB is still unknown.

Succinic semialdehyde (SSA) is also a naturally occurring γ -aminobutyric acid (GABA) shunt intermediate. Its accumulation increases in response to biotic and abiotic stresses (Bown and Shelp, 1997; Shelp et al., 1999). The compound is highly unstable, and therefore immediately oxidizes to succinate and enters the TCA cycle (Tuin and Shelp, 1994; Bouché et al., 2003) or reduces to GHB (Allan et al., 2008; Breitkreuz et al., 2003). SSA as an aldehyde group containing compound capable of reacting with nucleic acids, oxidizes membranes and alters the transcription of stress-related genes (Allan et al., 2008; Weber et al., 2004; Kotchoni et al., 2006). SSA and GHB are the direct and side products of the GABA shunt, respectively.

The GABA shunt in plants includes the decarboxylation of glutamate to GABA, catalyzed by the cytosolic glutamate decarboxylase (GAD), the import of GABA into mitochondria for the transamination into succinic semialdehyde (SSA), catalyzed by the GABA transaminase (GABA-T) and the final oxidation of SSA to succinate, catalyzed by the SSA dehydrogenase (SSADH). In addition, SSA can be converted into GHB in the cytosol by the cytosolic GHB

dehydrogenase / glyoxylate reductase (GHBDH1 / GR1) or in the chloroplast by plastidial GHBDH2 / GR2 (Allan et al., 2009). Two distinct GHBDH homologues (GR1 and GR2) have been identified in Arabidopsis. The proteins belong to the hydroxyisobutyrate dehydrogenase superfamily. GR1 has been described to exist in the cytosol whereas GR2 resides in the chloroplasts (Hoover et al., 2007a; Simpson et al., 2008). Both forms of GHB dehydrogenases have been shown to use SSA and glyoxylate as substrate with different affinities. GR1 and GR2 have a 250- and 350-fold higher affinity for glyoxylate than SSA, respectively (Hoover et al., 2007). Both forms of the GHB dehydrogenases have been demonstrated to convert SSA to GHB irreversibly in an *in vitro* experiment (Simpson et al., 2008). In contrast, in the mammalian system the conversion of GHB to SSA has been reported (Doherty et al., 1975). Some years later, cytosolic GHB dehydrogenase from the mammalian brain and liver, which is regulated by NADP⁺ and NAD⁺, has been reported to mediate the conversion of GHB to SSA (Kaufman and Nelson, 1981). Therefore, the conversion of GHB to SSA in the cytosol of plants in a concentration dependent manner cannot be ruled out.

Mutations in SSADH have been associated with developmental disorder. In mammals, deficiency in SSADH activity has been known to cause a disorder called GHB aciduria, which is manifested by an elevated level of GHB in the physiological fluids, like plasma and urine (Jacobs et al., 1981; Hogema et al., 2001). In Arabidopsis, deficiency in SSADH function causes stunted growth (dwarfism), necrosis on leaves and hypersensitivity to environmental stresses (Bouché et al., 2003). Furthermore, this abnormal growth phenotype was accompanied with an increased accumulation of GHB in the tissue. To our knowledge, so far it was not possible to measure the level of SSA in the tissue mainly due to the unstable nature of the compound. Hence, the sensitive phenotypes observed in *ssadh* mutants were associated to the elevated GHB.

Here, the toxicity of SSA and/or GHB as a causal agent for the abnormal phenotype of the Arabidopsis *ssadh* mutant was investigated. For that, a double mutant Arabidopsis line defective in the function of the two GHB dehydrogenases (GR1 and GR2) was generated. Then, the phenotype and chemotype of the double mutant were analyzed after externally feeding GHB and SSA.

2. Materials and Methods

2.1. Generation of mutant lines

A. Single mutants

Seeds of Arabidopsis plants heterozygously mutated for *ghbdh1* (At3g25530; SALK_057410 and GK_316D04), *ghbdh2* (At1g17650; GK_933D03) and At4g20930 (GK_911G06) were purchased from SALK and GABI-KAT stock centres. The lines were sown on soil and grown until the F2 seeds were produced. The F2 seeds were harvested from the individual plants and pooled. Similarly, the F2 seeds were sown and after two weeks of growth leaf samples were collected in 1.5 ml eppendorf tubes containing 3-4 glass beads and were immediately frozen in liquid nitrogen. For genotyping, the frozen samples were homogenized in a tissue lyser (Qiagen, Cat. No. 85220, S.N 127061203) and 200 µl of extraction buffer (0.2 M Tris HCl pH 7.5, 25 mM EDTA, 0.5 % SDS and 250 mM NaCl) was added. The mix was briefly vortexed and centrifuged at maximum speed for a minute. The supernatant (150 µl) was transferred into a new 1.5 ml eppendorf tube, and 100% isopropanol (150 µl) was added to it. The mix was homogenised by inverting the tube up and down 4 to 5 times and then incubated at RT for 5 minutes. The mix was centrifuged with a maximum speed for 5 minutes and the supernatant was removed. The pellet was air dried and dissolved with 100 µl milliQ water.

The selection of homozygous mutant lines was carried out first by performing a PCR with gene specific primers. Samples displaying no product after a PCR with gene specific forward and reverse primers were selected and verified by repeating the PCR with primer combinations of T-DNA specific (LB) and gene specific.

B. Generation of double and triple mutants

The seeds of homozygous single mutants were sown on soil and grown to flowering. First, *ghbdh1/2* was generated by crossing the respective single mutants. The mother plant was emasculated by removing the stamens and then the pollen from the male parent was brought into contact with the stigma using a forceps. The pollinated flowers were marked and the whole plant was covered with a plastic to which water is sprayed for about 24 hours. Selection of the homozygous double mutant in the F2 generation was carried out as described in section A. For the generation of a triple mutant, a similar procedure was followed. The knockout of

all three genes was also confirmed at transcript level. For that RNA was isolated from the mutant and wild type using a previously described protocol (Logemann et al., 1987)

2.2. Phenotypic analysis

The single (*ghbdh1*, *ghbdh2* and *at4g20930*), double (*ghbdh1/2*) and triple (*ghbdh1/2 X at4g20930*) mutants generated were characterized for the presence of an altered phenotype on soil and on plates containing either SSA or GHB. For phenotypic analysis on soil, seeds from the wild type (Col-0) and the respective mutants were sown on small pots. Ten days after sowing, single plants were transferred to six cm plastic pots. At least five plants from each genotype were included in the treatment. Two weeks after transplanting, the lines were treated without or with 150 mM NaCl. For NaCl treatment a perforated tray, on which five plants from each five mutant lines along with the wild type were placed on, was immersed into a tray consisting of either water or 150 mM NaCl for 1-2 hours. The treatment was repeated every three days at least three times during which the plants were monitored for any stress phenotype.

For SSA and GHB treatment, a ½ MS agar plates (2.23 g MS (Duchefa), 2% sucrose and 0.8% agar) was prepared and autoclaved at 121 °C). After the media was cooled down approximately to 60 °C, 0.3 mM SSA and 1.5 mM GHB were added. The seeds were surface-sterilized by fumigation (mixing 90 ml sodium hypochlorite and 10 ml of 37% HCl) under the fume hood for four to five hours. Five seeds were then put onto agar plates with and without SSA/GHB. The plates were placed in the cold room for 24 hours, and then transferred to a growth chamber (16/8 light/dark cycle, 23°C) in which the growth conditions were controlled. Pictures were taken after two weeks of growth.

2.3. Chemotypic analysis

For chemotypic analysis 60-100 mg leaf sample was collected and snap frozen in liquid nitrogen. The samples were stored at -80°C until further use. For metabolite extraction the frozen leaf materials in a 2 ml eppendorf tube were ground to fine powder using a pre-cooled electrical drill machine. Immediately, 300 µl methanol and 30 µl internal standard (0.3 mg/ml Ribitol dissolved in methanol, stored at -20°C) was added, vortexed and placed on ice until all samples were ready for the next step. Then, the samples were incubated at 70°C for 15 minutes during which the cap of the eppendorf tube was briefly opened after a minute to

release the pressure. Next, 200 μl chloroform was added, briefly vortexed and incubated at 37 $^{\circ}\text{C}$ for 5 minutes while shaking. Then 400 μl of HPLC grade water was added, vortexed and spun with 14000 rpm for 5 minutes. Finally, three times 160 μl of the upper phase was subtracted into 3 small glass bottles as technical replicates and dried in a Speed Vac for 90 minutes. The dried samples were stored at -20°C until further use. For derivatization 40 μl of MeOx (Methoxyamine, 20mg/ml dissolved in pyridine) was added to the dried sample, thoroughly vortexed and incubated at 30 $^{\circ}\text{C}$ for 90 minutes. Then 70 μl of MSTFA (*N*-methyl-*N*-trimethylsilyl trifluoroacetamid) was added, briefly vortexed and incubated at 37 $^{\circ}\text{C}$ for 30 minutes. Finally, 100 μl of the derivatized extract was added to a glass tube which in turn was placed in a glass bottle. The samples were finally measured for the metabolite content using GC-MS (gas chromatography coupled with mass spectrometry).

2.4. Enzyme activity assay

Approximately 200-300mg leaf samples were collected from four-week-old Wt and mutant plants and snap frozen in liquid nitrogen. The samples were stored at -80°C until further use. For total protein extraction leaf samples were ground to a fine powder using mortar and pestle. The extraction buffer (20 mM Tris HCl, pH 8, 0.05% triton X-100), containing PMSF (1mg/ml extraction buffer, stock 50mg/ml in ethanol) was added to the ground sample at 1ul/mg sample base. The mix was thoroughly homogenized and spun at 14000 rpm for 10 minutes at 4 $^{\circ}\text{C}$. Then the supernatant which constituted the total protein was transferred to a new eppendorf tube.

The quantification of the protein extract was carried out using the Bradford assay. For that 2 μl of the total extract was added to 998 μl of the Bradford reagent, which is diluted 1:5 in milliQ water. The mix was incubated for about 3-5 minutes and the absorbance of the samples was measured at wave length of 595 nm. The concentration of the proteins was then determined by comparing to the standard curve. Equal amount (40 μg) of protein extract from the Wt and mutants was loaded on a 10% native acrylamid gel (without SDS) in a cold room and was run for 120 minutes with 120 mA current. For the enzyme activity assay the gel was immersed into a 10 ml staining solution (50 mM K_2HPO_4 pH 8, 0.05% NBT, 3 mM NAD^+) in the presence or absence of 4 mM GHB as a substrate. The existence of an enzyme activity was monitored by the presence or absence of substrate-specific band.

2.5. Yeast strains and growth medium

Wild type (BY4742) and mutant yeast strains (*uga2*, *gnd1*, *gnd2*) were used to analyze the toxicity of GHB and SSA. The yeast strains were taken from the stock and streaked on fresh YPD plates (2% peptone, 2% glucose and 1% yeast extract) and incubated at 30°C overnight. For spot assay, few cells were picked up from the plate with tooth picks and inoculated into 5ml YPD medium and incubated at 30°C overnight while shaking with 220 rpm. The next day the density of the culture was measured. An initial $OD_{600} = 0.1$ and a three step ten-fold dilutions were prepared by diluting in distilled water. Then 7.5 μ l of the diluted samples were spotted on YPD plates with and without GHB/SSA. For a growth kinetics study, an overnight culture from each strain was diluted into 5 ml YPD medium with and without SSA to an OD_{600} of 0.1 in a glass test tube. The tubes were then incubated at 30°C while shaking at 220 rpm and growth data were collected by taking 100 μ l aliquots every 3 hours for a total of 21 hours. For each treatment five replications were used.

2.6. H₂O₂ analysis

For the analysis of H₂O₂ generation by fluorescent microscopy, overnight cultures of Wt and *uga2* strains were prepared and then diluted to an OD_{600} of ~0.2 in three replicates. The cultures were incubated for 5 hours while shaking until OD_{600} reaches approximately 1.0. Then 10 mM of SSA and 5 mM H₂O₂ were added to two sets (each three test tubes) of tubes and one set was kept as control. The cells were incubated for about 20 hours. Cells of OD_{600} equal to 1.0 were measured and taken as a sample and then 10 μ g DCF-DA (2',7'-dichlorofluorescein diacetate, from 2mg/ml stock in ethanol) was added and incubated for 2 hours. The cells were spun down and washed with 1x PBS buffer. Finally, the cells were dissolved in 300 μ l of 1x PBS buffer and analyzed under a fluorescent microscope.

2.7. Metabolite extraction and measurement

Metabolites were extracted from yeast wild type and *uga2* strains treated without and with 5 mM SSA and GHB. For metabolite extraction the protocol of Yoshida et al. (2010) has been used with minor modifications. Briefly, overnight cultures of wild type and *uga2* strains were prepared. The cultures were diluted into glass tubes containing 5 ml YPD medium without and with 5 mM SSA or GHB to an OD_{600} of 0.05. Next day, 2 ml of the overnight grown culture was spun and the cells were pelleted (~45 mg). The cells were washed once with 1x

PBS buffer, spun at 14000 rpm for 1 minute and the supernatant was removed. Next, the cells were frozen in liquid nitrogen for 5 minutes and then 20 μ l of fine glass beads were added. The cells were vigorously vortexed at 1200 rpm for 10 minutes at room temperature. Following that, 500 μ l of methanol, 30 μ l of ribitol (dissolved 20 mg/ml in methanol) and 200 μ l chloroform were added and incubated at 37°C for 30 minutes while shaking at 1200 rpm. Then, 400 μ l of pure HPLC grade water was added, mixed by inverting and then spun at 4°C for 5 minutes at 14000 rpm. Finally, 200 μ l of the supernatant was transferred into each three 2 ml glass bottles and then vacuum dried for 90 minutes. The derivatization and measurement of the metabolites was performed in the same way as for the plants.

3. Results:

3.1. *Arabidopsis thaliana*

3.1.1. Generation of *ghbdh1/2* double mutant

In an attempt to dissect SSA/GHB toxicity, two *ghbdh1/2* double mutant lines were generated. The first mutant was generated by crossing *ghbdh1* (SALK_057410) and *ghbdh2* (GK_933D03) which was then named as E27, and the second was generated by crossing *ghbdh1* (GK_316D04) and *ghbdh2* (GK_933D03) and was name as D7 (Fig 25A). In line E27, both genes have the T-DNA insertion in the intron of the open reading frame (ORF). In line D7, the *ghbdh1* has its insertion in the exon of the ORF. The homozygosity of the insertions was verified by PCR using primer combinations specific for the gene and the T-DNA. Furthermore, the absence of the respective transcripts in the mutant line was verified by PCR using two gene specific primers (Fig. 25B). For phenotypic and chemotypic analysis line E27 was used.

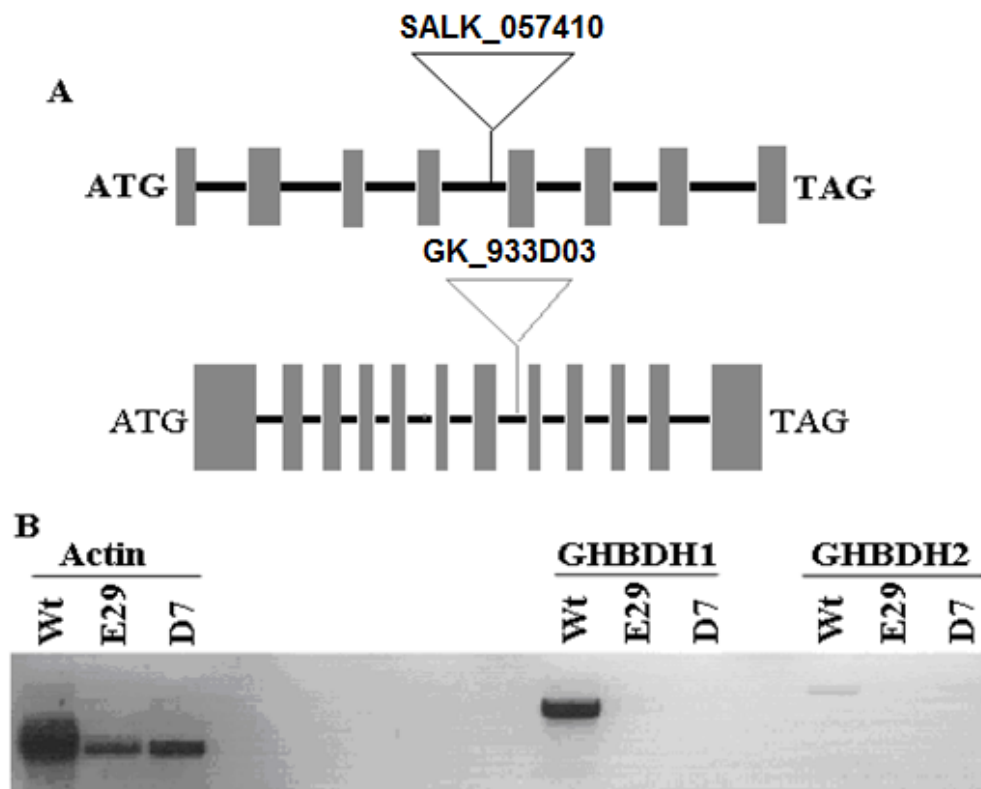


Figure 25. Schematic representation of the T-DNA insertion in the *GHB1* and *GHB2* genes (A); transcript analysis of *GHB1* and *GHB2* genes by RT-PCR using primers amplifying the full length transcripts (B).

3.1.2. Phenotypic and chemotypic analysis

Next, the effect of the *ghbdh1/2* mutations on the growth performance of the mutant plants was analyzed. The double mutant plants showed a similar phenotype compared to the wild type both on soil and agar medium (Fig. 27). To determine the effect of *ghbdh* mutations on the accumulation of metabolites, leaf extracts were analyzed for the content of GABA shunt and GABA shunt related metabolites from four-week-old wild type and *ghbdh1/2* plants.

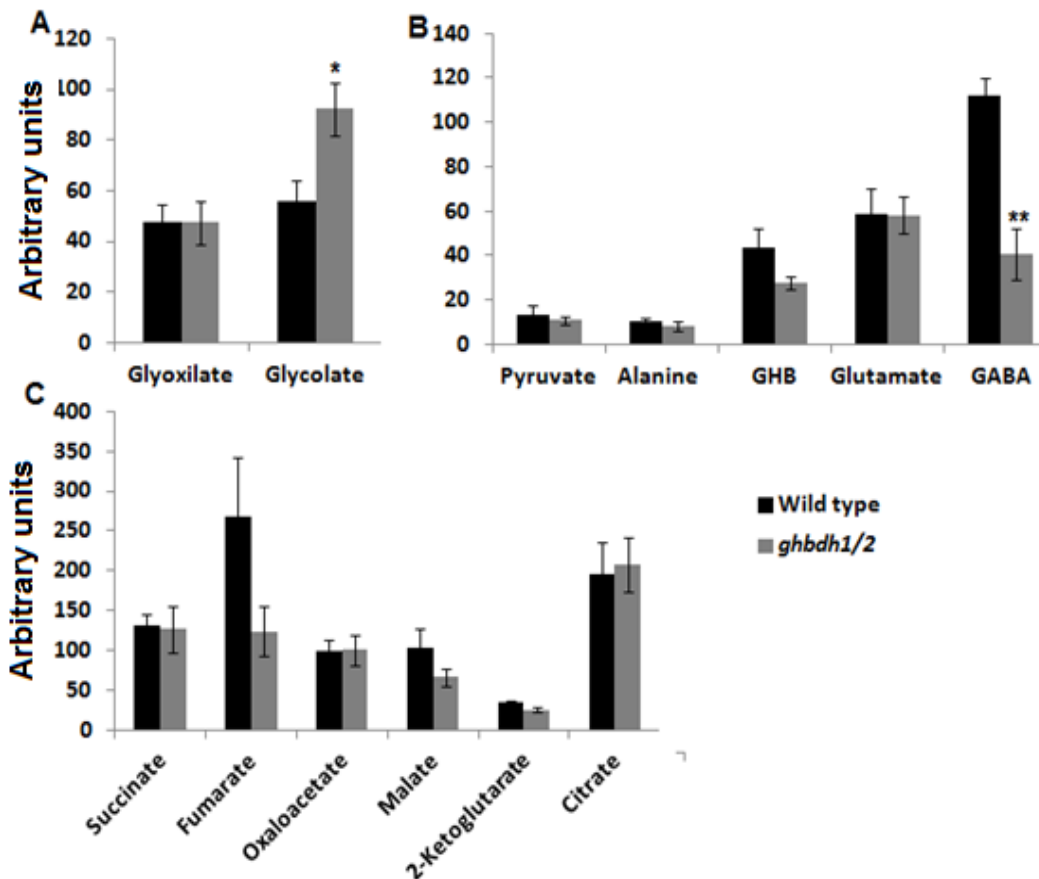


Figure 26. GC/MS analysis of major GABA shunt related (A), GABA shunt (B) and TCA cycle (C) metabolites from leaf extracts of four-week-old wild type and *ghbdh1/2* plants; error bars represent the standard error of means; n=5; * for P<0.05; ** for P<0.01.

The accumulation of glyoxylate, one of the substrates of GHBDH, did not change by the mutations of two glyoxylate dehydrogenases. However, glycolate which is the product of glyoxylate dehydrogenase was significantly increased in the mutant line (Fig. 26A). Most of the GABA shunt intermediates were unaffected by the knockout of the genes. However, a significant reduction in GABA level (P<0.01) was observed in *ghbdh1/2* line (Fig. 26B). The accumulation of GHB was also decreased slightly which was expected. Almost all TCA cycle intermediates were unaffected by the *ghbdh1/2* mutations (Fig. 26C).

To discriminate between SSA and GHB toxicity, *ghbdh1/2* double mutants along with wild type seeds were germinated and grown on ½MS plates containing either SSA or GHB. The assumption was that the double mutant cannot convert SSA to GHB and *vice versa*. Therefore, they were expected to show over-sensitivity to one of the two compounds compared to the wild type. However, external feeding of SSA and GHB, at both concentrations, did not show a contrasting phenotype between the mutant and the wild type (Fig. 27). However, the growth of both genotypes was severely affected by the treatment of 0.3 mM and 0.6 mM SSA which slightly resembles the bushy phenotype of the *ssadh* plants on soil. Feeding of 1.5 mM GHB, on the other hand, caused only a marginal sensitivity which was manifested only in the root growth (Fig. 27).

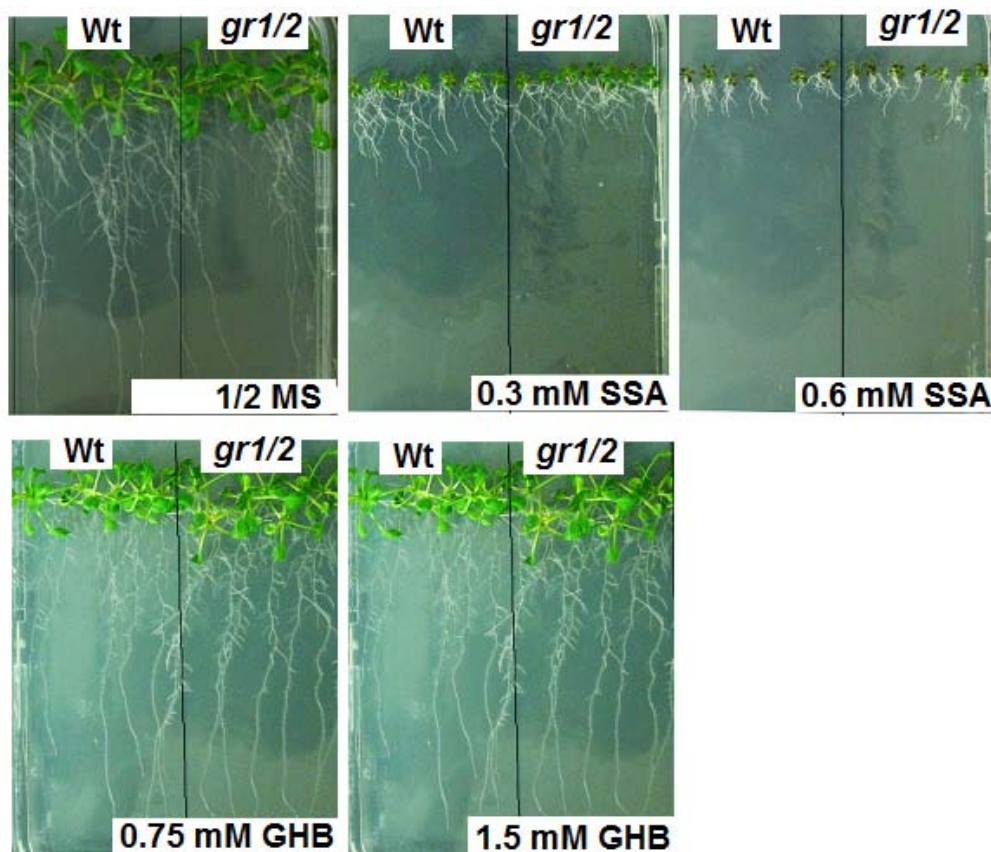


Figure 27. Phenotypic analysis of wild type and *ghbdh1/2 / gr12* double mutant; seeds of wild type and *ghbdh1/2* mutants were germinated and grown on plates without and with 0.3 mM SSA, 0.6 mM SSA, 0.75 GHB and 1.5 mM GHB. Pictures were taken after two weeks of growth.

Metabolic analysis revealed that most of the GABA shunt metabolites were not significantly different between the wild type and *ghbdh1/2* plants after external feeding of 0.3 mM SSA or 1.5 mM GHB. Unexpectedly, an increased level of GHB was detected in *ghbdh1/2* mutant

plants after feeding 0.3 mM and 0.6 mM SSA treatment (Fig. 28). After the two known *GHB*DHs are knocked-out, the accumulation of GHB was not expected in the double mutant. This observation indicated the existence of another homologue with putative dehydrogenase activity which utilizes SSA as a substrate to produce GHB.

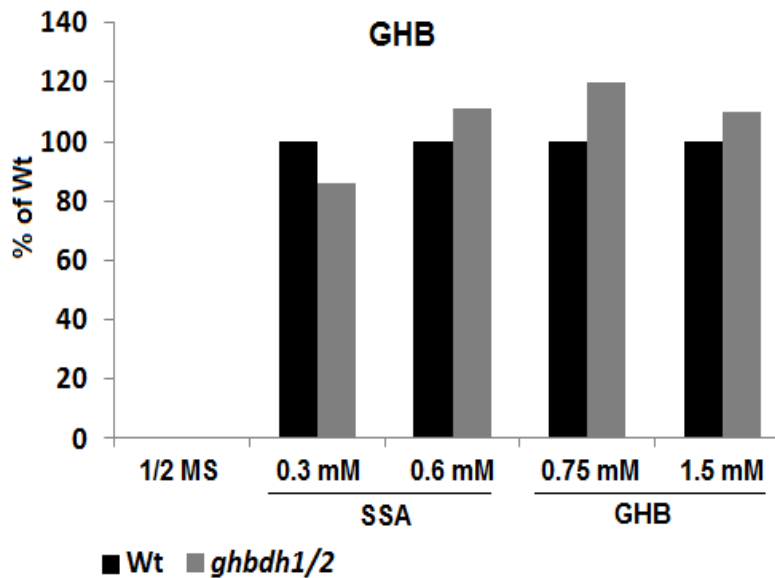


Figure 28. GC/MS analysis of GHB content in the leaf extracts of wild type and *ghb1/2* double mutant plants after SSA and GHB feeding; values are the average of at least three biological replicates.

To test the presence of a GHB to SSA conversion in the double mutants, a gel staining activity assay was performed using GHB as a substrate and NAD^+ as co-substrate. The principle of this test is, when there is an active enzyme with GHB dehydrogenase activity, it oxidizes GHB by removing hydrogen, and concomitantly reduces NAD^+ to NADH. The generated NADH in turn reduces the surrounding NBT (Nitro Blue Tetrazolium) which subsequently leads to the precipitation of the NBT at the position where the enzyme is located. Since, very long incubation leads to the precipitation of the NBT all over the gel, only precipitates in the first hour was taken for the picture. In the presence of a substrate, a unique band was observed (Fig. 29, arrow) which indicated the utilization of GHB as a substrate. This result showed that another homologue with a putative GHB dehydrogenase activity is capable of utilizing GHB as a substrate (Fig. 29). The other two bands on both gels with and without substrate are non-specific bands. The GC-MS measurement and enzyme activity assay data together may point towards the same enzyme catalyzing both forward and reverse reaction or towards two independent enzymes.

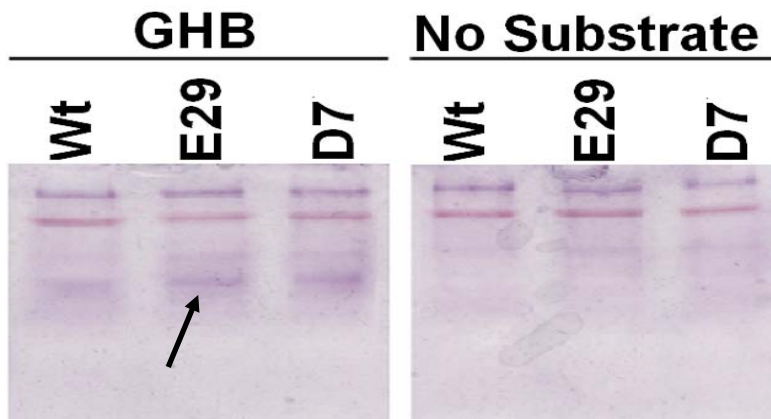


Figure 29. Enzyme activity assay on native gels with total protein extract; 40 μg of protein from each genotype was loaded on the gel. GHB was used as main substrate; NAD^+ was used as co-substrate in both cases; E29 and D7 represent two *ghbdh1/1* lines generated with two different *ghbdh1* insertion lines.

3.1.3. Searching of the third putative GHB dehydrogenase

The search of a third putative GHB dehydrogenase was performed by blasting the protein sequence of the GHBDH1/GR1 in the Arabidopsis protein data base (<http://www.ncbi.nlm.nih.gov>). Seven proteins which showed a variable degree of similarity to the GHBDH1 protein sequence were obtained. All identified proteins contain a conserved domain with a dehydrogenase activity.

To choose the best candidate, phylogenetic analysis was performed (<http://www.ebi.ac.uk/Tools/phylogeny/clustalw2/phylogeny/>), and the result revealed that At4g20930 was more recently diverged compared to the others (Fig. 30A). This gene is annotated in the database as gamma hydroxyisobutyrate dehydrogenase. Selection of this candidate gene was further strengthened by a co-expression analysis in which At4g20930 was found to be co-expressed with POP2 (At3g22200, GABA transaminase) and a plasma membrane GABA transporter (At1g08230) (Fig. 30B).

Sequence analysis revealed that At4g20930 protein shares a 44% identity with GHBDH1 at amino acid level over the entire length (Fig. 30C). Furthermore, the At4g20930 protein was predicted to contain an NAD binding domain and catalytically active domain which has a dehydrogenase activity (Marchler-Bauer et al., 2011). Unlike GHBDH1 which is cytosolic, the At4g20930 encoded protein was predicted to be mitochondrial. The first 37 amino acids, which do not align with GHBDH1 (Fig. 30C), could probably encode the signal peptide.

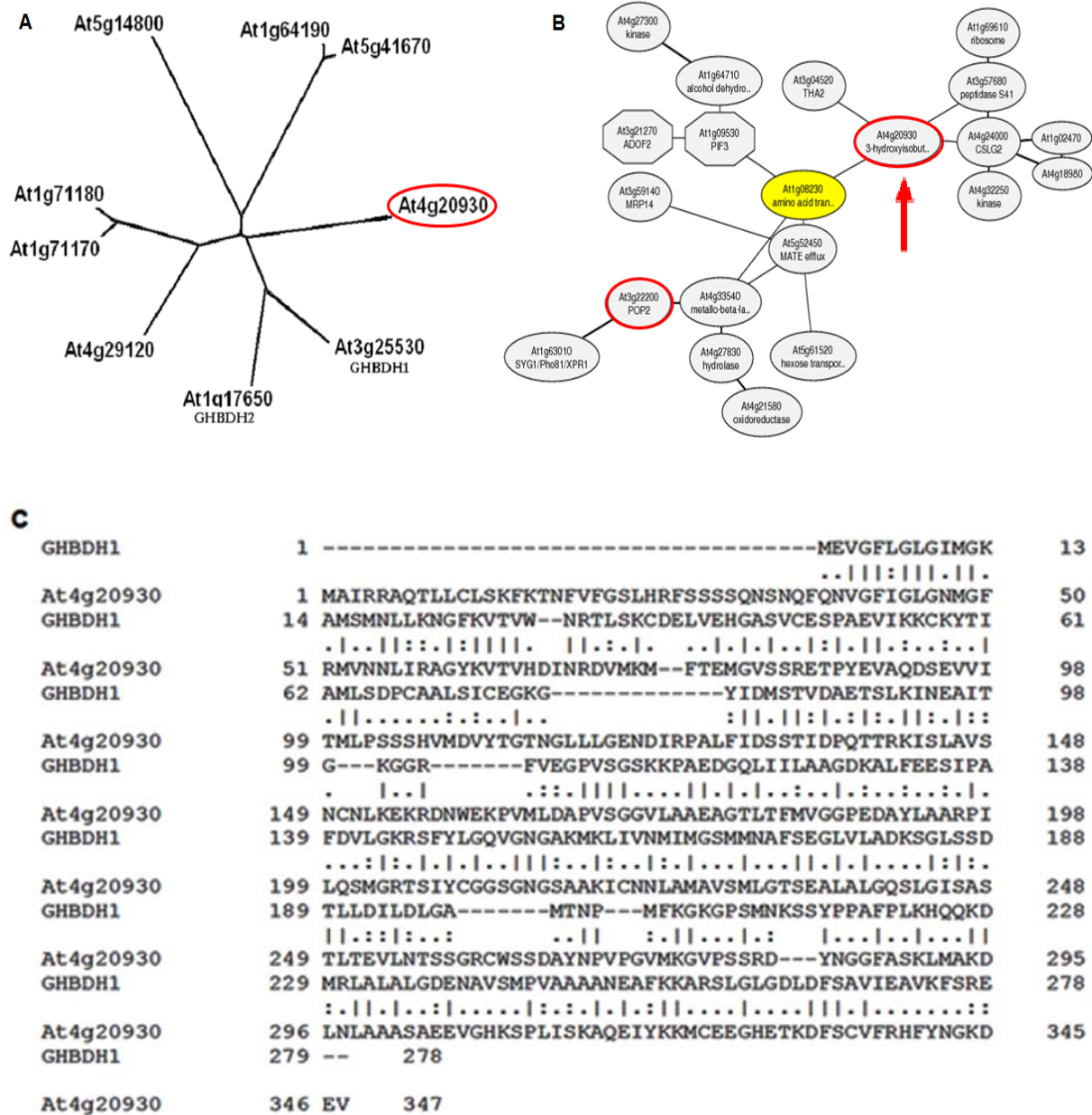


Figure 30. (A) Phylogenetic tree indicating the degree of divergence between GHBDH1 (At3g25530) and the remaining seven putative GHBDHs; (B) network showing co-expressed genes; the network was obtained by using At4g20930 as a node; (C) protein sequence alignment of GHBDH1 and At4g20930; sequence alignment was performed with the freely available web program (<http://www.ebi.ac.uk/Tools/msa/clustal/>).

3.1. 4. Generation of the *ghbdh1/2* x *at4g20930* triple mutant

The heterozygous At4g20930 line was purchased, selfed and the F2 generation was screened for the homozygosity. The homozygous *at4g20930* mutant did not show any abnormal growth phenotype on soil.

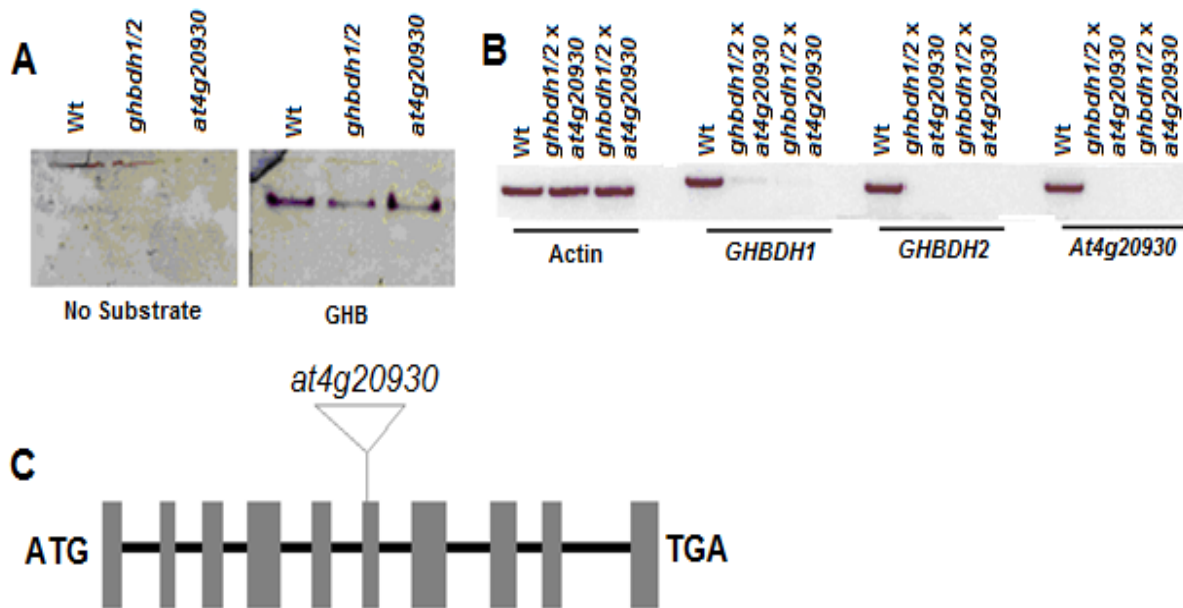


Figure 31. Enzyme activity assay for total protein extract from wild type, *ghbdh1/2* and *at4g20930* mutant lines (A); GHB and NAD^+ were used as a substrate; RT-PCR verification of *GHBDH1*, *GHBDH2* and *At4g20930* transcript in wild type and the triple mutant (B); DNase treated RNA was used to synthesize cDNA. Gene specific primers were then used to detect the presence of the respective transcript; Schematic representation of T-DNA insertion *At4g20930* (GK-911-G06) (C).

The protein extracts from *at4g20930* and the double mutant line were tested for the presence of GHBDH activity. Indeed, a unique single band was detected in the presence GHB as a substrate which was not unexpected in the *at4g20930* line (Fig. 31A). The triple mutant was then generated by crossing the *ghbdh1/2* (E29) line (Fig. 25A) with the *at4g20930* mutant (GK_911G06, Fig. 31C). After screening of about 100 F2 plants, no triple mutant was obtained. However, 12 lines which were homozygous for any of the two genes and heterozygous for the third gene were obtained. F3 plants, generated from the selfing of the above F2 plants, were screened for triple mutants, and four lines were obtained. The homozygosity of the knockout was verified at RNA level, and only very faint band for *GHBDH1* was detected with a higher cycle of amplification (Fig. 31B). Since the level of the transcript was very low compared to the wild type, the line was used for further phenotypic characterization and enzyme activity assay.

3.1.5. Phenotypic characterization and gel staining assay

Like the parental lines, the triple mutant also did not show an altered phenotype compared to wild type on $\frac{1}{2}$ MS plates supplemented without and with 0.1 mM SSA (Fig. 32C&D). Similarly, the triple mutant showed normal characteristics when grown on soil. Since the aim was to generate a mutant line which is deficient in GHB dehydrogenase activity, the protein

extract from the triple mutant, the parent lines and the wild type was analyzed for activity on a native gel. The gel staining assay, however, revealed the presence of a GHB activity in the triple mutant extract with the addition of 5 mM GHB as a substrate (Fig. 32A&B).

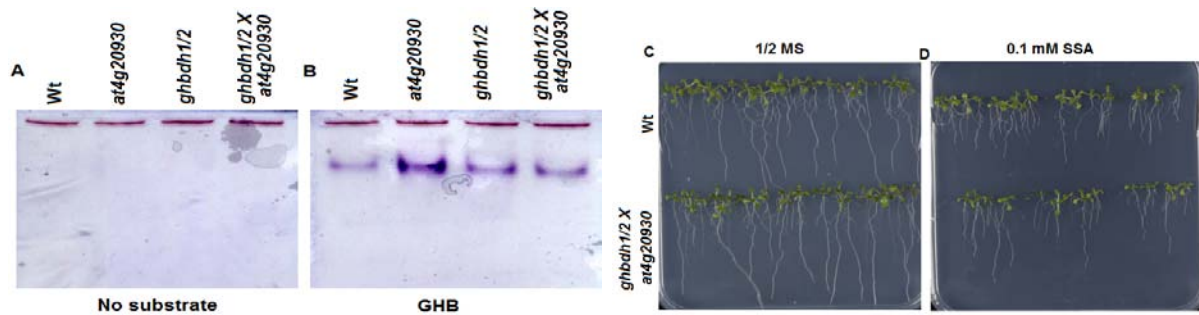


Figure 32. Enzyme activity assay for wild type, *at4g20930*, *ghbdh1/2* and *ghbdh1/2* x *at4g20930* lines on native gel containing substrate (B) and no substrate (A); Total protein was extracted and the activity assay was carried out as described above; phenotypic analysis of Wt and *ghbdh1/2* x *at4g20930* triple mutant on $\frac{1}{2}$ MS (C) and $\frac{1}{2}$ MS supplemented with 0.1 mM SSA (D). Seeds of wild type and the triple mutant were germinated and grown on $\frac{1}{2}$ MS plates without and with 0.1 mM SSA; Picture was taken after five days of incubation.

The accumulation of GHB in *Arabidopsis* and tobacco as a response to abiotic stresses and its regulation by the activity of glyoxylate reductase / GHB dehydrogenase (GRs / GHBDHs) has previously been reported (Allen et al., 2008). To test if the generated triple mutant would be sensitive to abiotic stress, wild type and the triple mutant seeds were germinated on $\frac{1}{2}$ MS plates. One-week-old plants were transferred on to $\frac{1}{2}$ MS plates containing 150 mM NaCl and grown for one more week. The triple mutant displayed a similar phenotype as the wild type (Fig. 33).

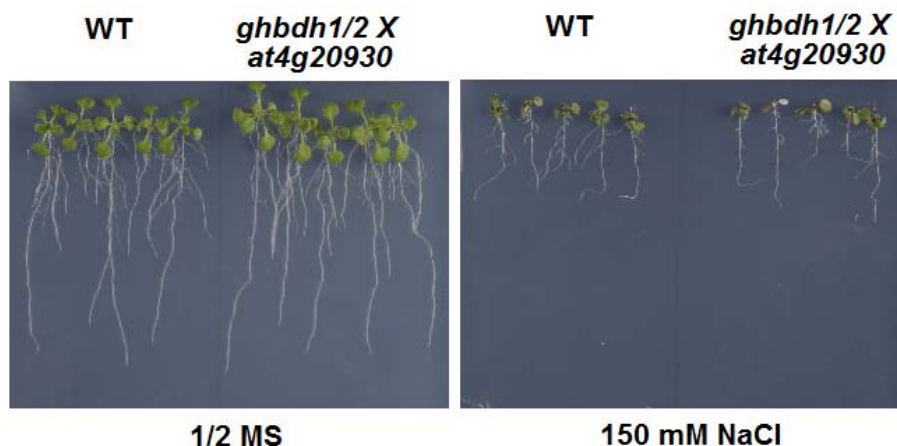


Figure 33. Phenotype of wild type and *ghbdh1/2* x *at4g20930* lines on $\frac{1}{2}$ MS plates without and with 150 mM NaCl; seeds were germinated on $\frac{1}{2}$ MS plates and one week later transferred on-to a plate containing no and 150 mM NaCl; pictures were taken one week after transfer.

3.2. *Saccharomyces cerevisiae*

3.2.1. The GABA shunt in yeast

The GABA shunt is also conserved in yeast, and the enzymes responsible for GABA metabolism have also been identified. Unlike the Arabidopsis GABA-T, the yeast UGA1 (GABA-T) converts GABA to SSA using alpha-ketoglutarate as a co-substrate, and generates SSA and glutamate (Fig. 34). Similar to Arabidopsis GABA-T, UGA1 is also encoded by a single copy gene. Mutants of *UGA1* showed an increased replicative life span (Kamai et al., 2011), and a decreased rate of vegetative growth (Ramos et al., 1985). A similar observation was reported when *GAD1* was deleted (Kamai et al., 2011).

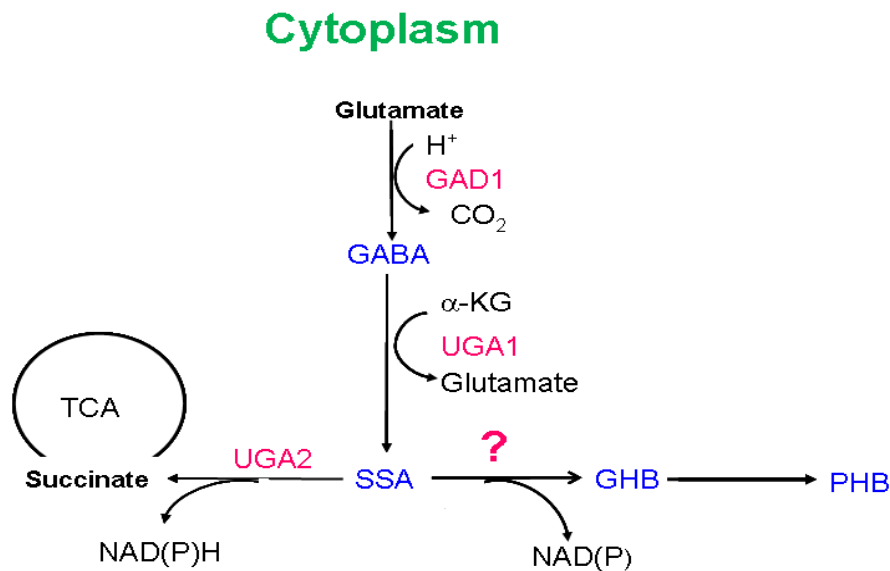


Figure 34. Schematic representation of the GABA shunt in yeast; GAD1 (glutamate decarboxylase 1); UGA1 (GABA transaminase); UGA2 (Succinic semialdehyde dehydrogenase); SSA (succinic semialdehyde); GHB (gamma hydroxybutyric acid); PHB (polyhydroxybutyric acid)

The apparent existence of multiple putative GHB dehydrogenases that play a role in the inter-conversion of SSA and GHB has made this specific study complicated in Arabidopsis plants. Therefore, the use of Baker's yeast (*Saccharomyces cerevisiae*) as an alternative model system was considered, despite, the GHBDH gene(s) is/are not identified yet. Owing to its smaller genome size compared to Arabidopsis, most enzymes in yeast are encoded by a single gene copy. Therefore, if there is a GHB dehydrogenase enzyme, then it is more likely to be encoded by a single copy gene. In yeast, GHB dehydrogenase activity has been reported previously; GHB has been detected when GABA was fed externally (Bach et al., 2009). However, the gene responsible for the dehydrogenase activity is not known yet.

3.2.2. Identification of the putative yeast GHB dehydrogenase

For identification of the putative yeast GHBDH, the Arabidopsis GR1 (GHBDH1) amino acid sequence was used for blasting. GR1 was selected for blasting because of its localization in the cytosol. The yeast GABA shunt is exclusively localized in the cytosol and the reduction of SSA to GHB also most likely takes place in the cytosol. Blasting of the Arabidopsis GR1 protein sequence in the yeast protein database identified two candidate proteins, GND1 and GND2, which are annotated as 6-phosphogluconate dehydrogenase proteins. Both GND1 and GND2 are localized in the cytosol and catalyze an NADPH regenerating reaction of the pentose phosphate pathway (Sinha and Maitra, 1992; Bro et al., 2004). GND1 is the major form of phosphogluconate dehydrogenase and accounts 80% of the total activity (Sinha and Maitra, 1992).

3.2.3. Phenotypic analysis of *gnd1* and *gnd2* mutants

Next, the mutant strains of *gnd1* and *gnd2* were obtained (kind gift of Prof. J. Dohmen) and subsequently used for the SSA/GHB toxicity analysis. To observe the toxicity of SSA, wild type and the two mutant yeast strains (*gnd1* and *gnd2*) were grown on YPD plates without and with 50 μ M SSA. However, all strains did not show any altered growth phenotype. It was evident that the *gnd1* strain exhibited a reduced growth even on the control plate. Therefore, the strains were treated with higher concentration of SSA (2 mM and 10 mM), and still the strains did not show any sensitive phenotype (Fig. 35B&C). Unexpectedly, the growth of *gnd1* was slightly but significantly ($T\text{-test}_{12h} = 0.0036$) stimulated by the addition of 1 mM SSA after 12 hours of incubation (Fig. 35E). Next, the sensitivity of these strains was tested on GHB containing plates. Concentration of GHB ranging from 0.5 mM to as high as 20 mM did not elicit sensitivity to all strains tested (Fig. 36 & 37). The question remained why the growth of the *gnd1* lines was stimulated by the addition of SSA. The growth stimulation of the *gnd1* strain by the addition of SSA might indicate two things: first, the involvement of *gnd1* in the catabolism of SSA, and second, the efficiency of UGA2 protein to effectively catabolize SSA to succinic acid, a TCA cycle intermediate.

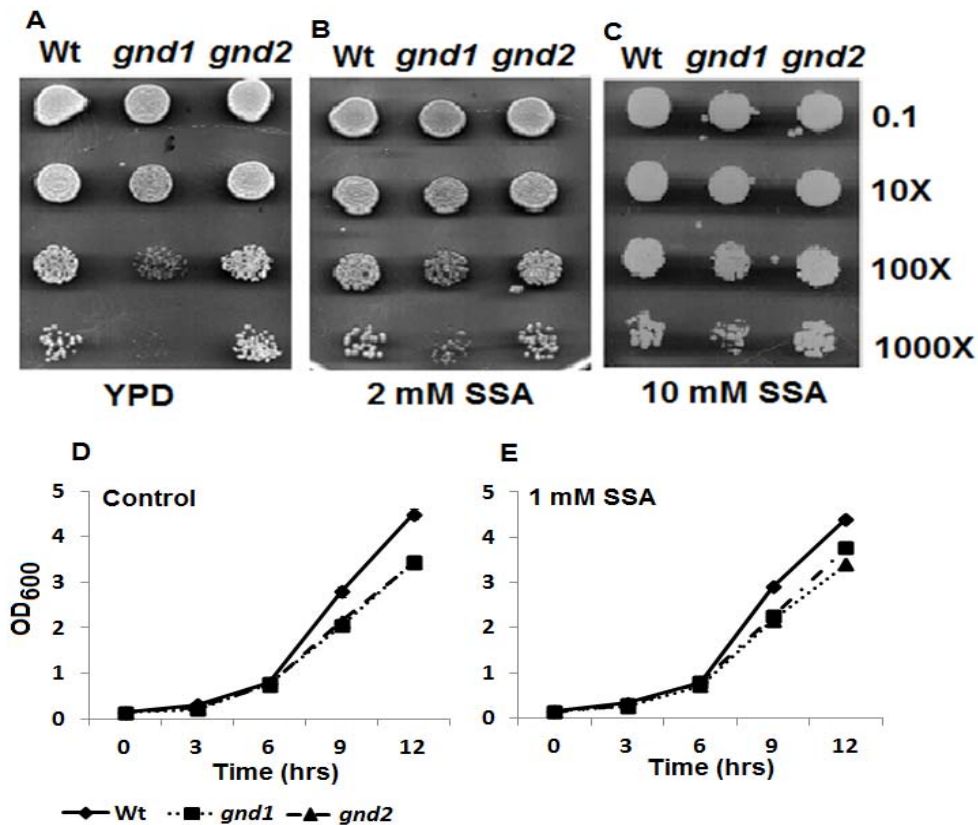


Figure 35. Overnight grown Wt, *gnd1* and *gnd2* strains were diluted to an initial OD₆₀₀ of 0.1 and three steps of 10-fold dilutions were prepared from it. 7.5 μ l of the samples were spotted on glucose containing YPD plates without (A) and with 2mM (B) and 10mM SSA (C). The plates were incubated at 30°C for two days before pictures were taken. For growth kinetics experiments, overnight cultures of Wt, *gnd1* and *gnd2* strains were diluted to an OD₆₀₀ of 0.1 in YPD medium without (D) and with 1mM SSA (E) and incubated at 30°C.

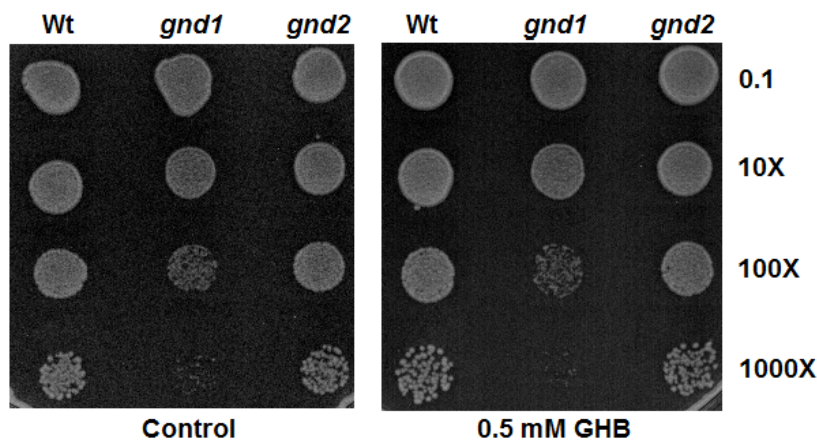


Figure 36. Overnight grown Wt, *gnd1* and *gnd2* strains were diluted to an initial OD₆₀₀ of 0.1 and three steps of 10-fold dilutions were prepared from it. 7.5 μ l of the samples were spotted on glucose containing YPD plates without (Control) and with 0.5 mM GHB. The plates were incubated at 30°C for two-days before pictures were taken.

Next, the contribution of UGA2 in the ability of the yeast to grow at very high concentrations of SSA was tested. As shown in Figure 27, 0.3 mM of SSA has severely affected the growth

of Arabidopsis plants. However, a 60-fold higher concentration of SSA appeared to be efficiently metabolized in yeast without causing any damage. Therefore, an *uga2* mutant strain was obtained (kind gift of Prof. J. Dohmen) and tested for SSA oversensitivity. Interestingly, the *uga2* mutant grows as good as the wild type at 2 mM SSA concentration (Fig. 37), and a similar observation was made when spotted on 6 mM SSA. However, increasing the SSA concentration to 10 mM almost completely inhibited the growth of the *uga2* strain (Fig. 37). A similar concentration of GHB did not inhibit the growth of the both strains.

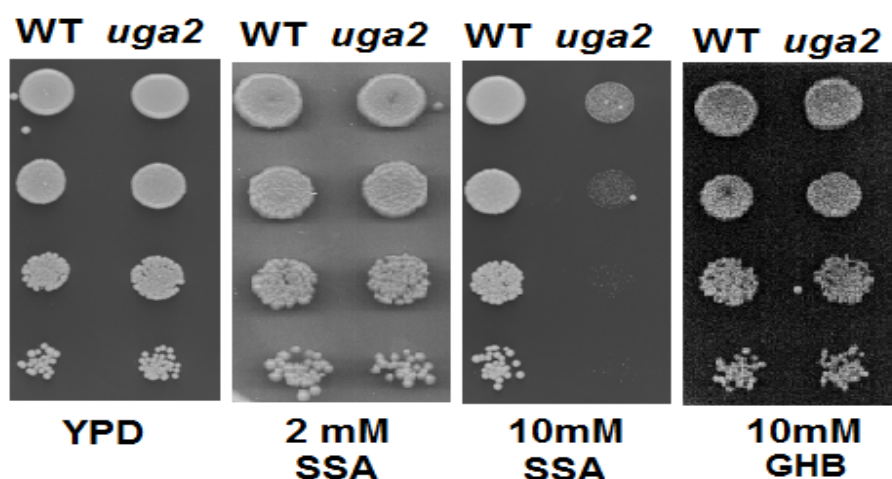


Figure 37. Overnight cultures of wild type and *uga2* strains were prepared and diluted to an initial OD_{600} of 0.1 and three steps of 10-fold dilutions were prepared from it. 7.5 μ l of the samples were spotted on YPD plates without and with SSA (2 mM and 10 mM) and GHB (10 mM). The plates were then incubated at 30°C for two days before pictures were taken.

3.2.5. Assessment of SSA/GHB as alternative carbon source

The stimulation of yeast *gnd1* strain growth on YPD plates containing 2 mM and 10 mM SSA raised the question whether SSA could be used as alternative carbon source. To address this question, wild type and mutant strains (*gnd1* and *gnd2*) were spotted on 20 mM SSA containing YP (2% pepton and 1% yeast extract) plate lacking glucose. Intriguingly, the strains grew better on SSA plates compared to growth on the control plate (Fig. 38A), suggesting that the cells were able to metabolize SSA for generating energy. To validate the observation, a growth kinetics experiment was conducted by inoculating the wild-type strain into 20 mM SSA or 20 mM GHB containing YP medium without glucose. Indeed, growth of the cells was promoted despite it took a longer lag phase (12 hours) which is by nine hours longer than the normal growth condition (Fig. 38B).

SSA generally could follow two metabolic routes, i.e. oxidation leading to succinate and/or reduction to GHB. To assess whether the route *via* GHB is responsible for the catabolism of the added SSA, the wild-type strain was inoculated into 20 mM GHB containing YP medium without glucose. Unlike SSA, GHB did not support growth of the cells better than the control within the specified incubation period (Fig. 38C). To confirm that the route *via* succinate is responsible for the degradation of SSA, *uga2* strains deficient for SSA dehydrogenase activity were spotted on YNB plates lacking sugar but containing 20 mM SSA as a sole carbon source. Expectedly, *uga2* strains were unable to grow on SSA as a sole carbon source while wild type does (Fig. 39). Both strains were able to grow slightly on YNB plate containing no sugar.

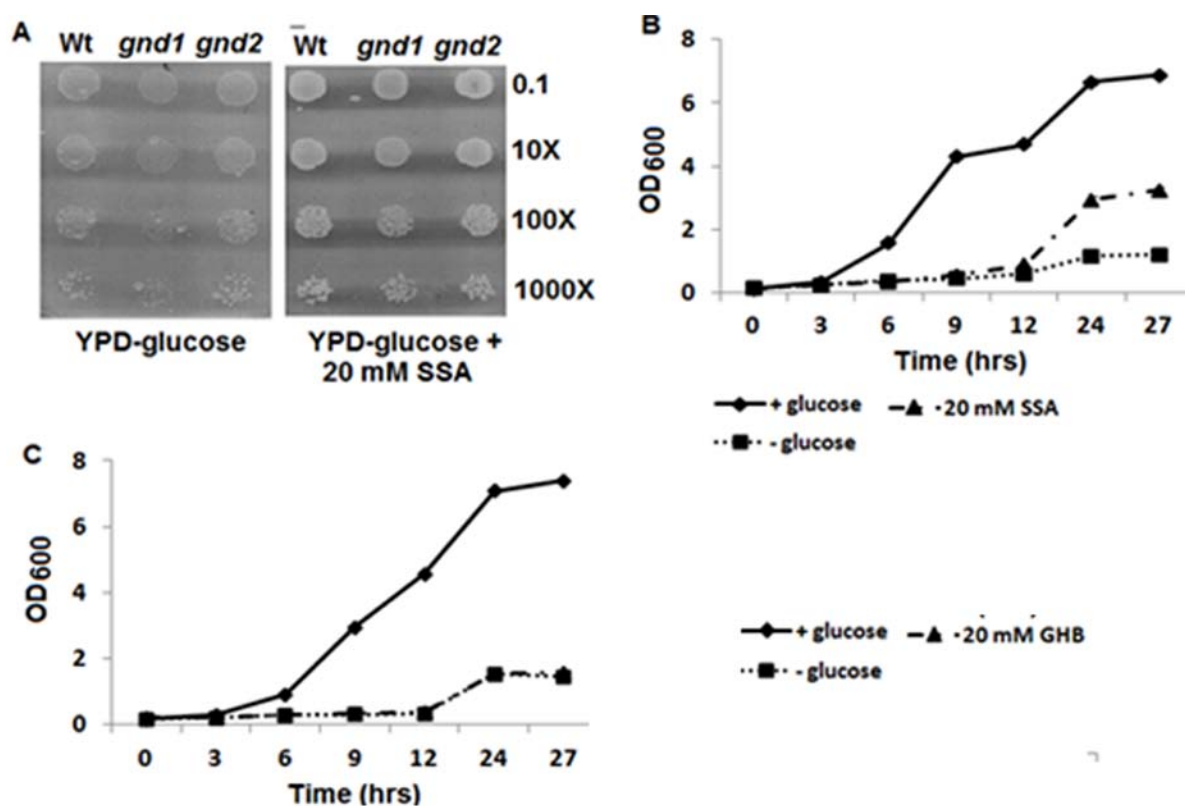


Figure 38. Overnight grown WT, *gnd1* and *gnd2* strains were diluted to an initial OD₆₀₀ of 0.1 and three steps of 10-fold dilutions were prepared from it. 7.5 μ l of the samples were spotted on YP plates without glucose and YP plate containing 20 mM SSA. Overnight grown wild type yeast was diluted to an initial OD₆₀₀ of 0.1 in 5 ml YPD medium containing 2% glucose, no glucose and 20 mM SSA (B) or 20 mM GHB (C). The cultures were incubated at 30°C while shaking at 220 rpm and samples were collected every 3 hours interval to measure the OD₆₀₀. Bars represent the standard error of four replicates.

To substantiate the utilization of SSA as a sole carbon source, but not GHB, with a metabolic data, wild type and *uga2* strains were fed with 5 mM SSA and 5 mM GHB. Then, metabolites were extracted and analyzed using GC-MS (Fig. 40). The content of alanine did not significantly change without or with treatment of SSA and GHB in both strains. Feeding of 5

mM SSA led to an increase in the metabolite level of GHB, succinate and GABA in both strains (Fig. 40B). After 5 mM SSA treatment, the level of GHB and GABA was more than three-fold higher in the *uga2* strains compared to wild type. However, the succinate level was more than three-fold less in the *uga2* strain compared to wild type (Fig. 40B). Treatment of 5 mM GHB has significantly increased only the accumulation of GHB but not succinate or GABA (Fig. 40C) perhaps indicating that there is no reverse reaction.

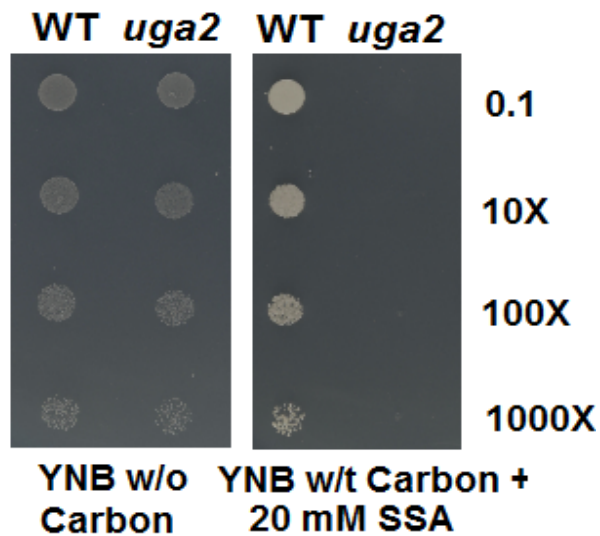


Figure 39. Overnight grown wild type and *uga2* strains were diluted to an initial OD₆₀₀ of 0.1 and three steps of 10- fold dilutions were prepared from it. 7.5 μ l of the samples were spotted on YNB plates without glucose and without SSA and with 20 mM SSA. The plates were incubated at 30°C four days before pictures were taken.

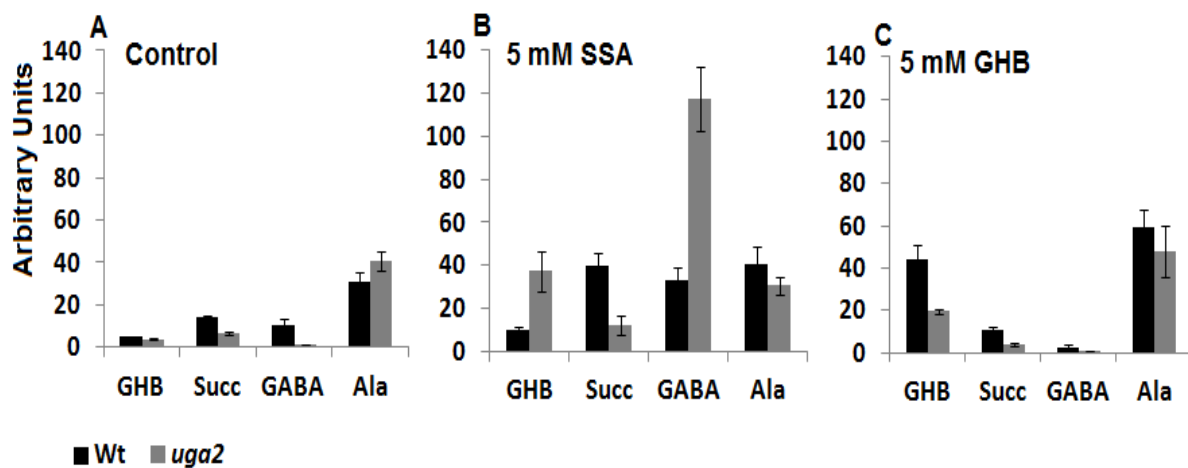


Figure 40. GC/MS analysis of GHB, Succinate (Succ), GABA and Alanine (Ala) from wild type and *uga2* yeast strains grown in YPD medium without (A) and with 5 mM SSA (B) or 5 mM GHB (C). Values are the mean of three biological replicates. Each sample was measured in three technical replicates; error bars represent the standard error of means.

3.2.6. Analysis of H₂O₂ induction

A recent publication showed that an aldehyde group containing compound, furan aldehyde (furfural), induced the accumulation of reactive oxygen species and thereby damaged the

cellular components of baker's yeast (Allen et al., 2010). The toxicity was associated to the reactive nature of the aldehyde group of the compound. SSA as an aldehyde group containing compound was hypothesized to cause a similar kind of damage and thereby inhibiting growth. To test this hypothesis, Wt and *uga2* strains were inoculated and grown to $OD_{600} \sim 1.0$ in three groups of five each. Then, 10 mM SSA was added to the first group, 5 mM H_2O_2 to the second group (positive control) and the third group maintained untreated (control). After overnight incubation, samples were collected and treated with a fluorescence dye (2' 7'-dichlorofluorescein diacetate (DCF-DA)). The data showed that SSA slightly induced the accumulation of H_2O_2 (Fig. 41). In Wt control cells, the green fluorescence signal is barely detectable indicating the absence of H_2O_2 (Fig. 41B).

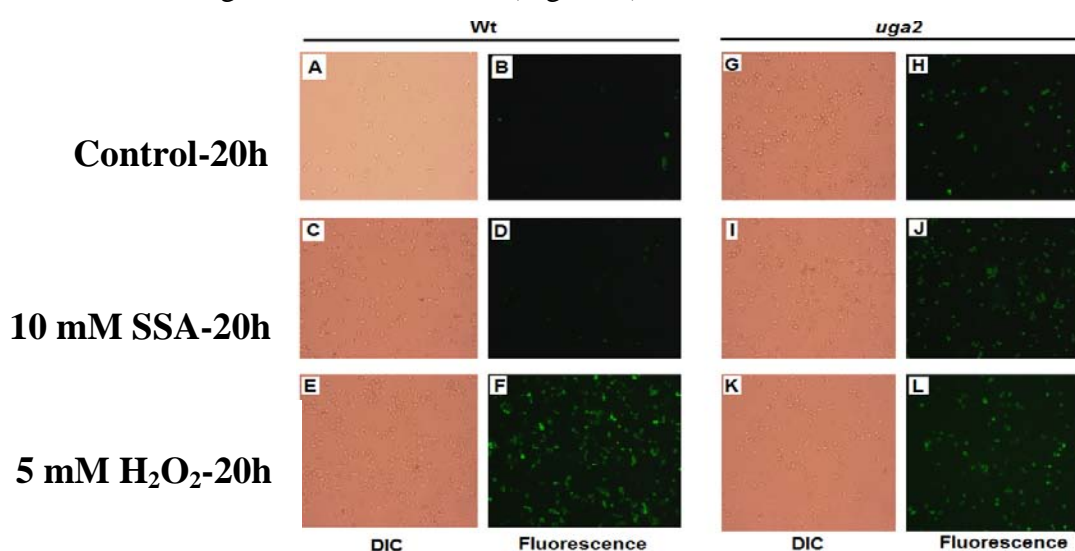


Figure 41. Analysis of the generation of H_2O_2 in wild type (BY4741) and *uga2* yeast strains after the treatment with 10 mM SSA for 20 hours.

With the addition of 10 mM SSA, there was a slight increase in the number of fluorescing cells, indicating the generation of hydrogen peroxide (Fig. 41D). This observation goes in line with the phenotypic data where there is no growth inhibition of the wild type in YPD media containing 10 mM SSA (Fig. 37). In contrast, *uga2* strains showed a considerable level of H_2O_2 accumulation under control condition and this was further increased by the addition of 10 mM SSA (Fig. 41 H&J). The higher H_2O_2 observed in *uga2* strain under control conditions suggests a role of UGA2 in preventing SSA induced ROS production. On the other hand, the increased H_2O_2 accumulation by 10 mM SSA indicates the contribution of SSA towards H_2O_2 accumulation.

4. Discussions

The *ghbdh1/2* plants did not show an abnormal phenotype under normal growth conditions perhaps indicating that these genes are not essential for the normal plant growth and development. The genes also seem to play a marginal role for the plants' response to abiotic stresses as the mutants displayed a similar phenotype under various stressful conditions. The metabolic analysis of leaf extracts from wild type and *ghbdh1/2* plants indicated the presence of another GHBDH / SSR (succinic semialdehyde reductase) because GHB was detected in the double mutant which is insignificantly different from the wild type. This observation suggests that the already identified GHBDHs (GR1 and GR2) may not be the main enzymes responsible for the reduction of SSA in the cytosol. Indeed, previous reports showed a more than 200-fold higher affinity of these two dehydrogenases for glyoxylate than for SSA (Simpson et al., 2008).

The attempt to discriminate between the GHB and SSA toxicity using Arabidopsis plants was not successful because of the presence of an enzyme that converts SSA to GHB and *vice versa*. However, treatment of plants with SSA as low as 0.3 mM produced a phenotype on plates which basically resembles the *ssadh* phenotype on soil. GHB, on the other hand, even at higher concentrations (up to 1.5 mM) did not elicit such a phenotype. Previous reports indicated GHB production as an escaping route for plants from the accumulation of SSA (Allan et al., 2009). The accumulation of GHB in tobacco and Arabidopsis during various abiotic stresses has been reported to serve as a stress tolerance mechanism (Allan et al., 2008). On top of that, several EMS (Ethylene Methyl Sulfonate) mutagenized *ssadh* lines have fully or partially rescued the abnormal *ssadh* phenotype despite the accumulation of relatively higher amount of GHB (Chapter Four). Taken together, the data suggests that SSA, but not GHB, is the major cause of the abnormal growth phenotype of the *ssadh* mutants.

In yeast, the toxicity of GHB was not observed even at concentrations as high as 10 mM (Fig. 34&36) indicating that GHB has no toxic effects. To ensure that GHB was taken up by the cells, metabolite analysis was performed. Indeed, GHB was taken up by the cells as shown by its increased accumulation in both genotypes (Fig. 40). However, the taken up GHB seemed not to be metabolized back to succinate or GABA (Fig. 40C) perhaps indicating that the GHB dehydrogenase from yeast does not perform a reversible reaction. This observation agrees with the inability of yeast to grown on GHB as a sole carbon source (Fig. 38C). The attempt

to visualize the reverse reaction using an enzyme activity assay on a native gel with GHB as substrate did not yield a band supporting the absence of a reverse reaction. In contrast, SSA was metabolized without causing any toxic effect even at relatively high concentrations. The toxicity was manifested only in *uga2* lines treated with 10 mM SSA or more. This observation suggested the higher efficiency of UGA2 enzyme compared to the plant homologue.

The question remained how the wild type strains managed to survive such a high concentration of SSA or how *uga2* lines survived a 60-fold high concentration of SSA whereas plants are sensitive to very low concentrations of it. One major difference between the GABA shunt in plants and in yeast is the cellular compartments in which it is localized. In plants, the SSA production step of the GABA shunt is localized in mitochondria. Mitochondria are known to be the power house of cells. Therefore, any damage caused by SSA in the mitochondrial proteins will affect the energy production used for plant growth and development. In yeast, this step is localized in the cytosol and such potential damages on mitochondria are not expected. In addition, the yeast genome encodes a cytosolic catalase which could detoxify the hydrogen peroxide produced upon induction by SSA. SSA induced hydrogen peroxide accumulation was shown by chemoluminescence (Fig. 41). This may explain why yeast is relatively tolerant to SSA. Metabolic analysis showed that SSA primarily was metabolized to succinate than to GHB. In wild type only a marginal increase in GHB was observed after treatment with 5 mM SSA. However, in the *uga2* strain the accumulation of GHB and GABA was increased by more than 5-fold because of the absence of SSADH activity.

5. Conclusion

So far, only two GHBDH (GR) homologues have been reported in Arabidopsis. However, the finding of this work revealed that these seem not to be the main GHBDHs and suggested the presence of another high affinity GHBDH/SSR. The attempt to discriminate the toxicity of GHB and/or SSA using the double (*ghbdh1/2*) and triple mutants (*ghbdh1/2* x *at4g20930*) indicated the presence of more than three *GHBDH* genes. It is possible that all seven putative GHBDH1 homologues identified in the data base could have a GHB dehydrogenase activity depending on their affinity to SSA and GHB. The use of yeast strains provided an alternative model system when studies in the plants are difficult because of multiple gene copies as in the case of GHBDH. The use of yeast provided an indication about the hydrogen peroxide mediated toxicity of SSA. In plant, as well, SSA could lead to the induction of H₂O₂ accumulation which then would lead to the damage of mitochondrial internal structures. This should be further confirmed by using electron-microscopic studies and by quantifying the level of reactive oxygen species (e.g. H₂O₂). A putative rescue of the *ssadh* phenotype by over-expressing catalase in mitochondria and cytosol would give further insight about the site of damage (mitochondria or cytosol) caused by SSA.

References

- Allan WL, Simpson JP, Clark SM, Shelp BJ (2008)** γ -Hydroxybutyrate accumulation in Arabidopsis and tobacco plants is a general response to abiotic stress: putative regulation by redox balance and glyoxylate reductase isoforms. *Journal of Experimental Botany* 59(9): 2555–2564.
- Allan WL, Peiris C, Bown AW, Shelp BJ (2003)** Gamma-hydroxybutyrate accumulates in green tea leaves and soybean sprouts in response to oxygen deficiency. *Canadian Journal of Plant Science* 83:951–953.
- Allan WL, Clark SM, Hoover GJ, Shelp BJ (2009)** Role of plant glyoxylate reductases during stress: a hypothesis. *Biochem. J.* 423:15–22.
- Bach B, Meudec E, Lepoutre JP, et al. (2009)** New Insights into gamma-Aminobutyric Acid Catabolism: Evidence for gamma-Hydroxybutyric Acid and Polyhydroxybutyrate Synthesis in *Saccharomyces cerevisiae*. *Applied and Environmental Microbiology* 75:4231–4239.
- Bouché N, Fait A, Bouchez D, Moller SG, Fromm H (2003)** Mitochondrial succinic-semialdehyde dehydrogenase of the γ -aminobutyrate shunt is required to restrict levels of reactive oxygen intermediates in plants. *Proc. Natl. Acad. Sci. U.S.A.* 100:6843–6848.
- Breitkreuz KE, Allan WL, Van Cauwenberghe OR, et al. (2003)** A novel γ -hydroxybutyrate dehydrogenase: identification and expression of an Arabidopsis cDNA and potential role under oxygen deficiency. *J. Biol. Chem.* 278:41552–41556.
- Bro C, Regenberg B, Nielsen J (2004)** Genome-wide transcriptional response of a *Saccharomyces cerevisiae* strain with an altered redox metabolism. *Biotechnol Bioeng.* 85(3):269-276.
- Bown AW, Shelp BJ (1997)** The metabolism and functions of γ -aminobutyric acid. *Plant Physiol* 115: 1–5.
- Doherty JD, Stout RW, Roth RH (1975)** Metabolism of (1-¹⁴C)-hydroxybutyric acid in rat brain after intraventricular injection. *Biochemical Pharmacology* 24:469-474.
- Hoover GJ, Van Cauwenberghe OR, Breitkreuz KE, et al. (2007)** Characteristics of an Arabidopsis glyoxylate reductase: general biochemical properties and substrate specificity for the recombinant protein, and developmental expression and implications for glyoxylate and succinic semialdehyde metabolism in planta. *Can. J. Bot.* 85:883–895.
- Hogema BM, Gupta M, Senephansiri H, et al. (2001)** Pharmacologic rescue of lethal seizures in mice deficient in succinate semialdehyde dehydrogenase. *Nat Genet* 29:212-216.
- Jacobs C, Bojasch M, Monch E, et al. (1981).** Urinary excretion of gamma-hydroxybutyric acid in a patient with neurological abnormalities. The probability of the new inborn error of metabolism. *Clinica Chimica ACTA* 111:169-178

Kamei Y, Tamura T, Yoshida R, et al. (2011) GABA metabolism pathway genes, UGA1 and GAD1, regulate replicative lifespan in *Saccharomyces cerevisiae*. *Biochem Biophys Res Commun.* 407(1):185-190.

Kaufman EE, Nelson T (1981). An overview of γ -hydroxybutyrate catabolism: The role of the cytosolic NADP1-dependent oxidoreductase EC 1.1.1.19 and of a mitochondrial hydroxyacid-oxoacid transhydrogenase in the initial, rate-limiting step in this pathway. *Neurochem. Res.* 16: 965–974.

Kotchoni SO, Kuhns C, Ditzer A, Kirch HH, Bartels D (2006) Overexpression of different aldehyde dehydrogenase genes in *Arabidopsis thaliana* confers tolerance to abiotic stress and protects plants against lipid peroxidation and oxidative stress. *Plant Cell Environ.* 29:1033–1048.

Marchler-Bauer A, Lu S Anderson JB, Chitsaz F, et al. (2011) CDD: a Conserved Domain Database for the functional annotation of proteins, *Nucleic Acids Res.*;39(D):225-229.

Poldrugo F, Addolorato G (1999) The role of gamma-hydroxybutyric acid in the treatment of alcoholism: from animal to clinical studies. *Alcohol and Alcoholism* 34(1):15-24.

Ramos F, el Guezzar M, Grenson M, Wiame JM (1985) Mutations affecting the enzymes involved in the utilization of 4-aminobutyric acid as nitrogen source by the yeast *Saccharomyces cerevisiae*. *Eur. J. Biochem.* 149:401–404.

Rinehart JA, Petersen MW, John ME (1996) Tissue-Specific and developmental regulation of Cotton Gene FbL2A. *Plant Physiology* 112:1331-1341.

Shelp BJ, Bown AW, McLean MD (1999) Metabolism and functions of gamma-aminobutyric acid. *Trends Plant Sci* 4:446–452.

Simpson JP, Di Leo R, Dhanoa PK, et al. (2008) Identification and characterization of a plastid-localized *Arabidopsis* glyoxylate reductase isoform: comparison with a cytosolic isoform and implications for cellular redox homeostasis and aldehyde detoxification. *J. Exp. Bot.* 59:2454–2554.

Sinha A, Maitra PK (1992) Induction of specific enzymes of the oxidative pentose phosphate pathway by glucono-delta-lactone in *Saccharomyces cerevisiae*. *J Gen Microbiol* 138(9):1865-1873.

Tuin LG, Shelp BJ (1994) *In situ* [¹⁴C]glutamate metabolism by developing soybean cotyledons. I. Metabolic routes. *J Plant Physiology* 143:1-7.

Weber H, Chetelat A, Reymond P, Farmer EE (2004) Selective and powerful stress gene expression in *Arabidopsis* in response to malondialdehyde. *Plant Journal* 37:877–888.

Chapter Three: Investigation of the fate of GHB

1. Introduction

In yeast the existence of GHB and its subsequent metabolism to form PHB was demonstrated previously (Bach et al., 2009). However, the enzyme responsible for converting SSA to GHB is still unknown. In mammals, GHB has been speculated to enter the mitochondrial fatty acid beta oxidation pathway (Struys et al., 2006). It has also been suggested that GHB could be converted to D-2-hydroxyglutarate in mammals (Struys et al., 2006). The metabolism of GHB appears to be very rapid. An aesthetic dose of GHB administered to rat brains revealed a very short half life time of one hour (Doherty et al., 1974). The authors also described degradation *via* succinic acid and then to the TCA cycle as the primary, if not the only, route for GHB metabolism. The conversion of GHB to GABA through SSA has also been reported (Doherty et al., 1974). The authors ruled out the direct conversion of GHB to GABA by transamination. In plants, the first report on the occurrence and accumulation of GHB was reported in 2003 (Allan et al.). However, the subsequent metabolism of GHB in the plants is still unknown.

Here, the major route of GHB metabolism in *Arabidopsis* was investigated. To test whether GHB can be considered as a short chain fatty acid and thus be degraded via the beta oxidation pathway, mutants deficient in peroxisomal fatty acid degradation were characterized. In mammals short chain fatty acids are metabolized via the mitochondrial fatty acid beta oxidation pathway. Fatty acid metabolism in plants has been associated primarily with peroxisomes (Fulda et al., 2002); however, evidence on the existence of a mitochondrial fatty acid beta oxidation is emerging. Graham and Eastmond (2002) showed the degradation of branched fatty acids in mitochondria. However, the complete set of genes involved in mitochondrial beta oxidation was not identified. Therefore, mutants of the peroxisomal beta oxidation pathways were used for the experiment. The possible degradation of GHB back to SSA and then to succinic acid was also investigated by using a mutant line deficient in the production of succinic acid.

The finding indicates that GHB is not metabolized via the peroxisomal fatty acid beta oxidation. However, the metabolism back to the GABA shunt appears to be the major route which supports the finding of Doherty et al. (1974).

2. Materials and Methods

2.1. Feeding of GHB

Seeds of wild type, *ghbdh1/2*, *pxa1*, *kat2* and *gs* (*gaba-t X ssadh*) lines were germinated and grown on ½ MS plates containing sucrose and 1.5 mM GHB. The *gs* line because of its GHB oversensitivity was germinated and grown on 0.1 mM GHB containing ½ MS plates. Two weeks old plantlets were transferred on to fresh ½MS plates or ½ MS plates containing 1.5 mM GHB. After two days of incubation on the fresh plates samples were collected for metabolite analysis using a GC-MS system. **GC/MS:** The sample extraction, derivatization and measurement were carried out as described in the material and method section of chapter one.

2.2. GHB extrusion and time course experiment

For GHB extrusion analysis, wild type seeds were germinated and grown on ½ MS plates containing 1.5 mM GHB. After two weeks of incubation, a part of the plants were harvested and frozen in liquid nitrogen and the remaining half part were transferred to 1ml of 10 times diluted ½ MS medium on 6-well culture plates. After 6 hours of incubation the plants were harvested, paper dried and frozen in liquid nitrogen. The medium was transferred into eppendorf tubes and vacuum dried. The pellet was then re-dissolved in 100 µl HPLC grade water. As a positive control, GHB was added to ½ MS medium to a final concentration of 1.5 mM and dried and re-dissolved; ½ MS alone was taken as a negative control. The metabolite extraction and derivatization was carried out as described in chapter one. The percent GHB content was calculated by comparing to the abundance measured in 1.5 mM GHB containing plate grown plantlets.

For the time course GHB degradation experiment wild type and *gs* lines were grown on 0.1 mM GHB containing ½ MS plates. Two weeks later the plantlets were transferred on to GHB-free ½MS plates. Then, samples were collected at 0, 3, 6 and 12 hours and the GHB content was analyzed as described before. The accumulation of GABA shunt-related metabolites was also measured and compared between the two genotypes.

3. Results

3.1. Analysis of GHB metabolism

The metabolism of GHB in plants is unknown. The question remains where does it end up after its synthesis; will it be stored in the tissue? To address this question, first the dynamics of GHB in the plant tissue was investigated. For that, wild type and *ghbdh1/2* mutant seeds were germinated and grown on $\frac{1}{2}$ MS plates containing 1.5 mM GHB for two weeks, and then the seedlings were transferred to GHB-free plates or to a fresh GHB plate. After two days of incubation, the level of GHB in the plants transferred to GHB free $\frac{1}{2}$ MS plates was nearly zero (Fig. 42). Expectedly, the GHB level remained the same in the plantlets transferred to a fresh $\frac{1}{2}$ MS plates containing 1.5 mM GHB

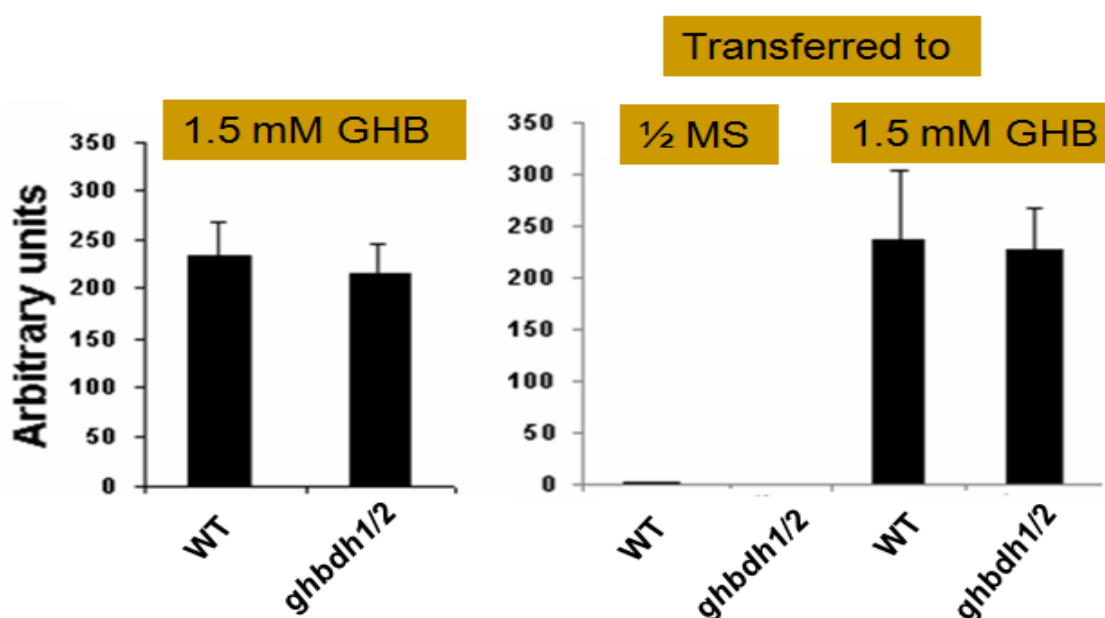


Figure 42. Analysis of GHB dynamics in wild type and *ghbdh1/2* mutant plants; seeds of wild type and *ghbdh* double mutants were germinated and grown on $\frac{1}{2}$ MS medium supplemented with 1.5 mM GHB. After two weeks of growth plants were transferred to 1.5 mM GHB containing fresh plates or on GHB-free $\frac{1}{2}$ MS plates. Sample preparation for GC/MS analysis from whole plantlets was carried out as described before. Error bars represent the standard error of means of five biological replicates.

This result indicated that GHB is converted to a yet unknown compound. To rule out the possibility that GHB is released back to the medium, wild type seeds were germinated and grown on 1.5 mM GHB containing plates. After two weeks, the plants were transferred to a liquid $\frac{1}{2}$ MS medium and incubated for six hours. Metabolite analysis indicates that only 3.5% of the GHB fed remained in the tissue and only 1% was excreted back to the medium (Fig. 43).

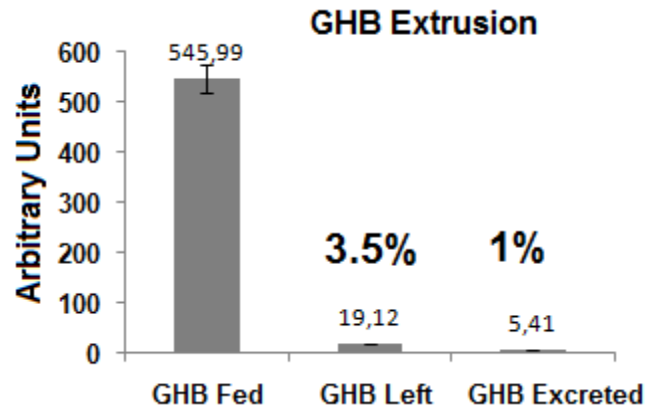


Figure 43. Extrusion of GHB back to the medium was analyzed by transferring plants grown on GHB containing plate to a GHB-free medium. The GHB concentration was determined in the medium and the plant using the procedure described in material and methods.

3.2. Analysis of GHB metabolism *via* peroxisomal fatty acid beta oxidation pathway

GHB sometimes is considered as being a short chain fatty acid, and has been hypothesized to be degraded *via* the fatty acid beta oxidation pathway (Struys et al., 2006). Here, the possible degradation of GHB *via* the peroxisomal beta oxidation pathway was analyzed. For that, two mutant lines (*pxa1* and *kat2*, kind gift of Dr. Gierth), which are deficient in the peroxisomal beta oxidation pathway, were used for the experiment. *PXA1* encodes a peroxisomal ATP-binding cassette transporter, and is known to transport fatty acids into peroxisomes. *KAT2* encodes a 3-ketoacyl-CoA thiolase that catalyzes the last step of the beta oxidation of fatty acids in peroxisomes.

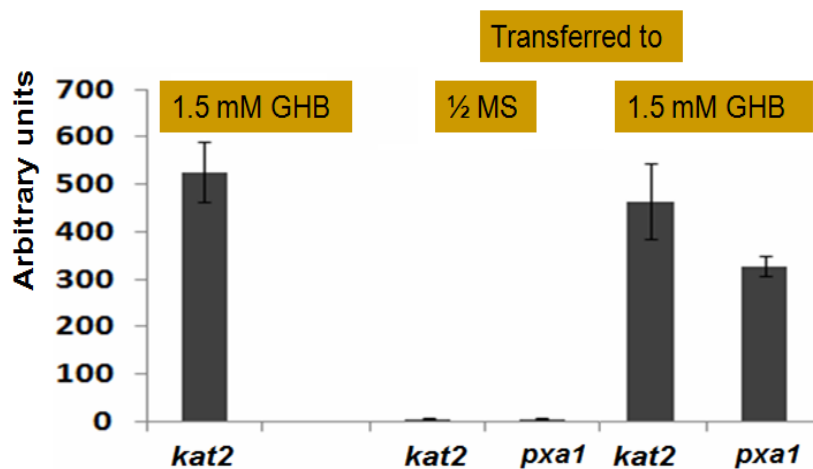


Figure 44. Analysis of the fate of GHB in *kat2* and *pxa1* mutants. All procedures were carried out as described before.

These two mutant lines were similarly treated with 1.5 mM GHB for two weeks and then transferred to a GHB-free plate. Two days after transfer to fresh plates, samples were collected for GC/MS analysis. Similar to the previous observations, GHB was hardly detectable after two days of incubation on GHB free medium (Fig. 44).

3.3. Analysis of GHB metabolism back to the GABA shunt

In the mammalian system the conversion of GHB to succinic acid and then to the TCA cycle has been previously reported (Doherty et al., 1974). In *Arabidopsis*, the only pathway for GHB metabolism known so far is the reverse reaction to SSA, and then to GABA and/or succinate. The attempt to verify this route as the major route by mutating the GHB dehydrogenases was not successful. Therefore, blocking the pathways upstream, at the SSA conversion to GABA and/or to succinate, was considered as an alternative approach. The line, described here as ‘gs’ (*gabat* X *ssadh* double mutants), was used to test this hypothesis.

The *gs* line, obtained by crossing *gaba-t* (GK_157D10) and *ssadh* (SALK_003223) (Fig. 45), was extremely sensitive to 0.5 mM GHB treatment, probably indicating the importance of this route (Ludewig et al., 2008).

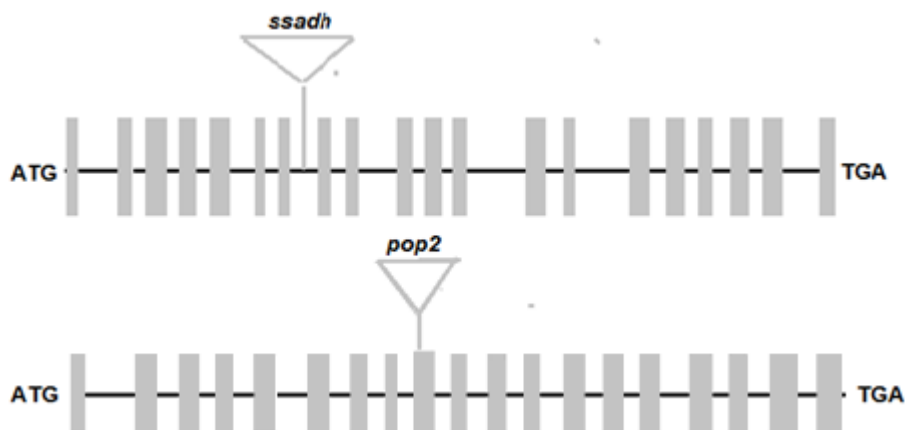
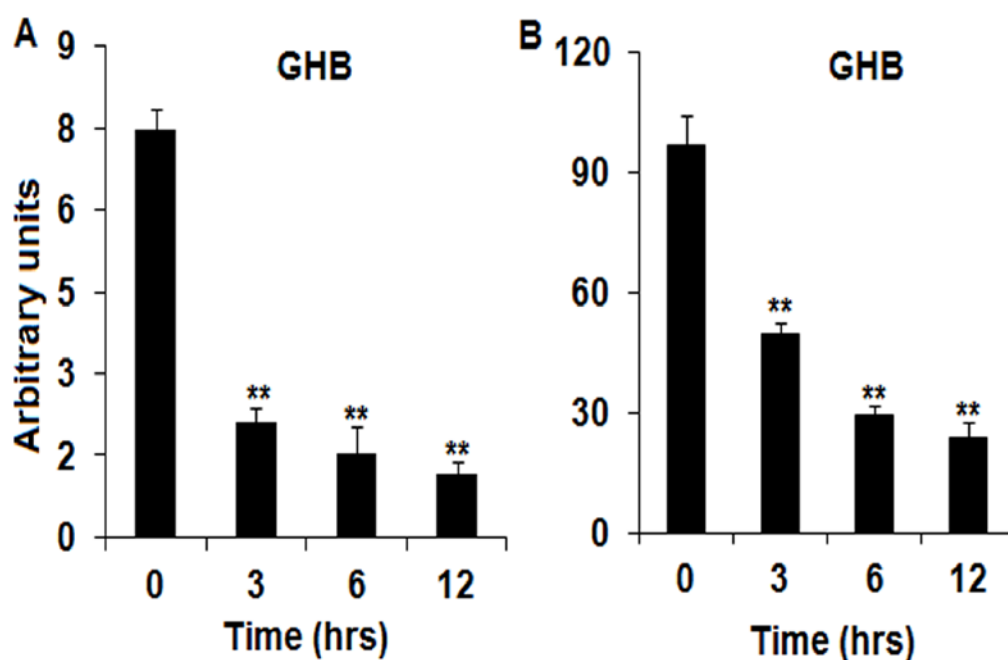


Figure 45. Schematic representation of the *ssadh* and *pop2* alleles used in the *gs* (*gaba-t* and *ssadh* double mutant) line. The triangles show the position of the T-DNA insertion; grey bars represent the exons of the ORF.

Therefore, GHB concentration that allows sufficient growth had to be identified in order to obtain sufficient material for GC/MS analysis. Indeed, the *gs* line grew better on 0.1 mM GHB containing ½MS plate than on 0.5 mM plates (Ludewig et al., 2008). Next, seeds of wild type and *gs* lines were germinated and grown on 0.1 mM GHB containing ½MS plates for two weeks. Then, 15 plants, pooled into five biological replicates, were harvested and

another 15 plants were transferred to each three fresh GHB-free ½ MS plates. Then, the samples were harvested after 3, 6 and 12 hours of incubation, extracted and analyzed for GHB content using GC/MS.



% GHB left after transfer to 1/2 MS				
	0hr	3hrs	6hrs	12hrs
Wt	100	28,11	20,34	15,26
<i>gs</i>	100	51,20	30,28	24,32

Figure 46. Analysis of GHB dynamics in the Wt (A) and *gs* (B) lines; Wt and *gs* seeds were germinated and grown on ½ MS containing 0.1 mM GHB and two weeks later the plants were transferred to GHB-free plates. Samples were collected after 3, 6 and 12 hours for GC/MS analysis; error bars represent the standard error of means; asterisks indicate statistically significant differences between time point 0 minute and other time points; ** (P < 0.01).

After three hours of incubation on GHB-free plates, GHB accumulation was reduced by 72% and 49% in wild type and *gs* lines, respectively, (Fig. 46). However, the difference in the amount of GHB left in the tissue narrowed with increasing time of incubation. To test whether the other GABA shunt metabolites show a similar trend at the above described time points, the accumulation was measured in both lines. GABA accumulation showed a time-dependent reduction in wild type until six hours after transfer to GHB-free plates (Fig 47A). However, GABA accumulation in the *gs* line, as expected, did not show any change after transfer to GHB-free plates (Fig. 47B). Pyruvate and alanine accumulation did not change significantly in Wt leaves after transfer to GHB-free plates, but alanine showed a slightly decreasing trend

in the *gs* line (Fig. 47C&D). Succinate, which did not significantly change in wild type, unexpectedly showed a significant reduction in the *gs* line after transfer on to GHB-free plate.

To test the effect of the externally fed GHB on the total succinate and GABA pool in the tissue, the accumulation of the respective metabolites was compared from Wt and *gs* lines grown on a plate supplemented without and with 0.1 mM GHB. For this, both lines were germinated and grown on 0.1 mM GHB containing ½MS plates for two weeks. Samples were harvested and extracted for GC/MS analysis.

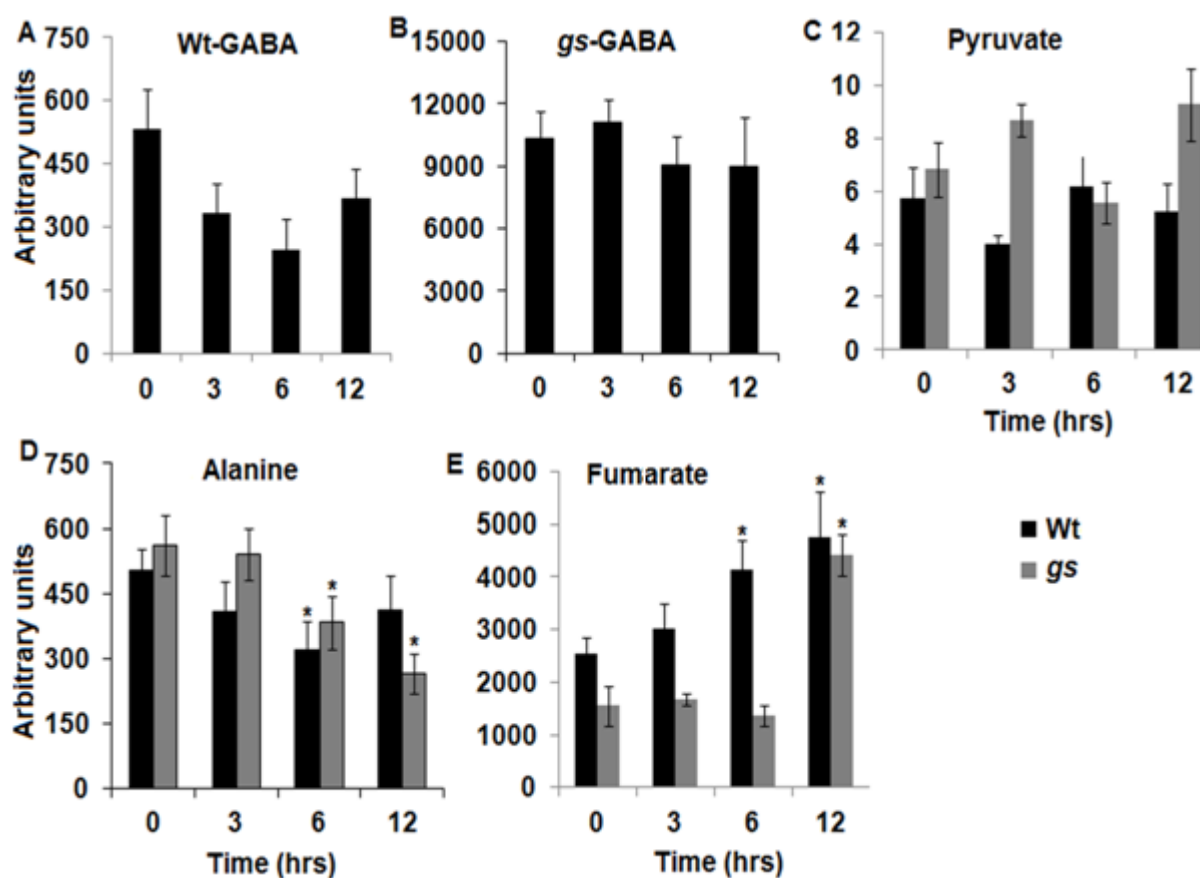


Figure 47. Analysis of time dependent change in accumulation of GABA-shunt metabolites after treatment with 0.1 mM GHB and then transfer to GHB-free ½ MS plates; measurement was made from samples taken at 0 (taken from GHB plate), 3, 6 and 12 hours; error bars represent the standard error of means of at least five biological repeats; asterisks indicate statistically significant differences between time point 0 minute and other time points; * (P < 0.05).

The accumulation GHB, succinate, GABA and alanine was significantly increased in wild type after two weeks of 0.1 mM GHB treatment (Fig. 48A&B). Interestingly, the accumulation of GABA and alanine did not change in *gs* indicating the absence of GABA-T activity (Fig. 48D). However, succinate showed an increased accumulation after 0.1 mM

GHB treatment which was unexpected. This raised the question whether SSADH is effectively knocked-out. PCR analysis of the transcript using full-length amplifying primers, however, showed the presence of a transcript for both GABA-T and SSADH genes although it was faint (Fig. 49). Therefore, new *gs* line (*gs1* in Fig. 49) was generated and no transcript was detected for both *GABA-T* and *SSADH* genes after PCR. Despite the presence of GABA-T transcript in *gs* line there was no change in the GABA accumulation. Therefore, repetition of the experiment using the newly generated *gs1* line is important.

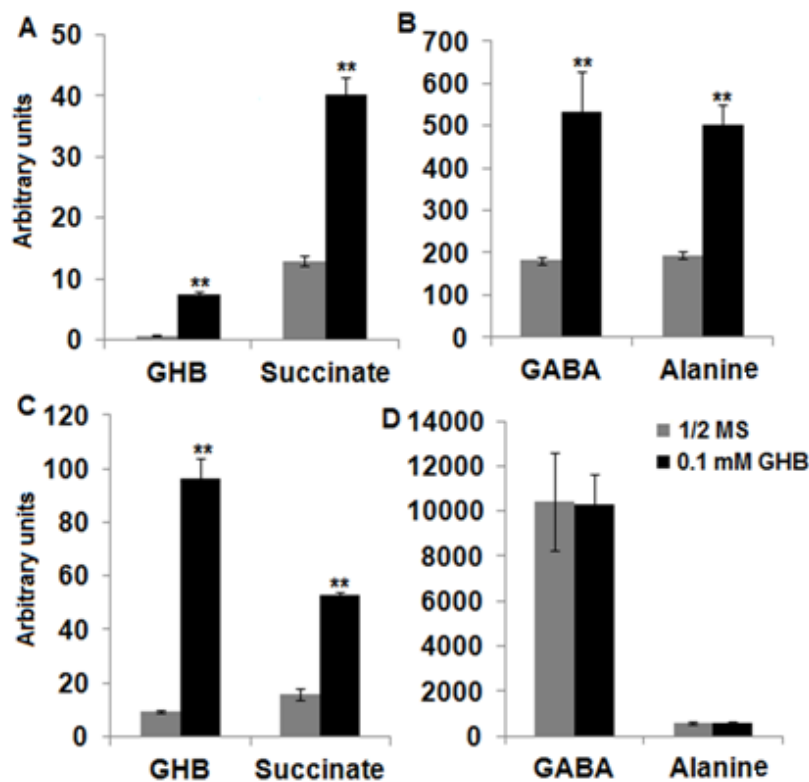


Figure 48. Analysis of GABA shunt-related metabolites in Wt (A&B) and *gs* (C&D) lines after treatment with 0.1 mM GHB for two weeks and transfer to GHB-free plates; error bars represent the standard error of means of at least five biological replicates; asterisks indicate statistically significant differences between time point 0 minute and other time points; ** (P < 0.01).

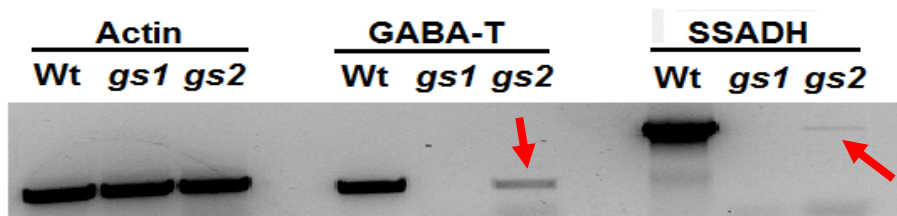


Figure 49. Total RNA was extracted from Wt and *gs* lines; *gs1* represents the newly obtained stock and *gs2* represents the seed stock used in the above experiment. cDNA was synthesized and the GABA-T and SSADH transcript was analyzed with RT-PCR.

4. Discussion

GHB metabolism in plants has not been studied so far. Here an attempt was made to discover the pathway that involves the metabolism of GHB in plants using *Arabidopsis* as a model organism. Before the pathway was investigated, the dynamics of GHB in plants was analyzed. The activity of the GABA shunt under normal growth conditions seems to be relatively weak, and hence, GHB accumulation is often not detectable in the shoot. To simulate the accumulation of GHB during abiotic stress, *Arabidopsis* plantlets were fed with exogenous GHB. The accumulation of GHB reduced to an undetectable level after 1.5 mM GHB fed plantlets were transferred to GHB-free plates. This indicated that GHB is not stored but rather metabolized to its product(s). A previous report in a mammalian model, indeed, showed a short half life (less than one hour) after GHB administration to the rat brain (Poldrugo and Addolorato, 1999).

Next, an attempt was made to unravel the route for GHB metabolism. Here, the metabolism via fatty acid beta oxidation, possible excretion in to the media and metabolism back to the GABA shunt was investigated. The analysis using mutants defective in the peroxisomal fatty acid beta oxidation revealed that GHB is not metabolized via this pathway. In mammals, the metabolism of small chain fatty acids is often carried out in the mitochondria (Wanders et al., 2010). In plants, the mitochondrial degradation of GHB may not happen for the following reasons: Firstly, the mitochondrial fatty acid beta oxidation in plants has not been clearly indicated and the components of the pathway are still not identified, despite there are some indications of its existence (Graham and Eastmond, 2002). Secondly, GHB synthesis and the GHB synthesizing enzyme, GHBDH1, are localized to the cytosol. Thirdly, no mitochondrial GHB transporter or receptor has been identified in plants. However, if any of the other unidentified GHB dehydrogenases would localizes to mitochondria, then its degradation via the mitochondrial beta oxidation could be possible. For example, *in silico* analysis of the At4g20930 amino acid sequence indicated the localization of the protein in mitochondria. However, this must be proven for example using fluorescent markers. The GHB extrusion experiment revealed that a small amount of GHB (1%) was excreted into the medium. Previous work in the mammalian model indicated a less than 2% excretion from the total GHB fed suggesting that it is metabolized within the cell but not excreted (Brenneisen et al., 2004).

The conversion of GHB back to GABA shunt metabolites seems to be the major pathway. Indeed, feeding of GHB enhanced the accumulation of GABA and succinate in wild type but not in the *gs* line. Increased accumulation of GABA and succinate after feeding of GHB has been demonstrated in the mammalian model system (Vayer et al., 1985; Hechler et al., 1997; Doherty et al., 1974; DeFeudis and Collier 1970). In this work, after three hours incubation of 0.1 mM GHB treated plants on to GHB-free plates, approximately 50% of the GHB was left in the tissue in contrast to the 28% in wild type. This is most likely due to the mutation of *gaba-t* and *ssadh* genes.

The question remains where the remaining 50% of the GHB fed has gone? The GHBDHs convert SSA to GHB and *vice versa* in a concentration-dependent manner. Hence, it is most likely that a part of the GHB is converted to SSA. The concentration of SSA then must have been very low to cause any toxicity. The polymerization of GHB to form polyhydroxybutyric acid (PHB) in yeast has been previously reported (Struys et al., 2006). Such a compound (PHB) is known to be present in plants like cotton (Rinehart et al., 1996) although the involvement of GHB is still unknown.

5. Conclusion

In comparison to SSA, GHB is chemically less toxic and hence, the damage caused by GHB accumulation would be very minimal, if any. Indeed, plants prefer to maintain the SSA level as low as possible to prevent any cellular damage and therefore, strict control of its level by adjusting its production and degradation is very important. SSA degradation occurs via two ways; first, via succinate which is energetically favourable, as it produces NADH, and second, via GHB which is energy consuming. Under normal growth conditions the activity of the latter way is negligible. But, under conditions of stress the activity of the GABA shunt increases, thereby increasing the production of SSA. Under such condition the plants maintain the SSA level low by converting to GHB which is virtually non-toxic. When the plants recover from the stress situation, the GHB produced would be metabolized back to SSA and then to succinate. This means that GHB could serve as a temporary non-toxic storage compound like GABA. Whether GHB can be used as an alternative source of carbon for plants remains to be investigated. But, in yeast, GHB did not support growth in the absence of another carbon source. From the above observations it is possible to conclude that in plants GHB is metabolized primarily to SSA by the reverse reaction catalyzed by GHB dehydrogenases and subsequently enter the TCA cycle.

References

- Allan WL, Peiris C, Bown AW, Shelp BJ (2003)** Gamma-hydroxybutyrate accumulates in green tea leaves and soybean sprouts in response to oxygen deficiency. *Canadian Journal of Plant Science* 83:951–953.
- Bach B, Meudec E, Lepoutre JP, Rossignol T, et al. (2009)** New insights into gamma-aminobutyric acid catabolism: evidence for gamma-hydroxybutyric acid and polyhydroxybutyrate synthesis in *Saccharomyces cerevisiae*. *Applied and Environmental Microbiology* 75:4231–4239.
- Brenneisen R, Elsohly MA, Murphy TP, et al. (2004)** Pharmacokinetics and excretion of gamma-hydroxybutyrate (GHB) in healthy subjects. *J Anal. Toxicology* 28:625-630.
- Defeudis, FV, Collier B (1970)** Conversion of γ -hydroxybutyrate to γ -aminobutyrate by mouse brain *in vivo*. *Experientia* 26:1072–1073.
- Doherty JD, Stout RW, Roth RH (1975)** Metabolism of (1-¹⁴C)-hydroxybutyric acid in rat brain after intraventricular injection. *Biochemical Pharmacology* 24:469-474.
- Fulda M, Shockey J, Werber1M, Wolter FP, Heinz E (2002)** Two long-chain acyl-CoA synthetases from *Arabidopsis thaliana* involved in peroxisomal fatty acid β -oxidation. *The Plant Journal* 32:93–103.
- Graham IA, Eastmond PJ (2002)** Pathways of straight and branched chain fatty acid catabolism in higher plants. *Prog. Lipid Res* 41:156–181.
- Hechler V, Ratomponirina C, Maitre M (1997)** γ -Hydroxybutyrate Conversion into GABA induces displacement of GABA_B binding that is blocked by Valproate and Ethosuximide. *The Journal of Pharmacology and Experimental Therapeutics*. 281(2):753-760.
- Poldrugo F, Addolorato G (1999)** The role of gamma-hydroxybutyric acid in the treatment of alcoholism: from animal to clinical studies. *Alcohol and Alcoholism* 34(1):15-24.
- Struys EA, Verhoevena NM, Jansen EEW, et al. (2006)** Metabolism of c-hydroxybutyrate to d-2-hydroxyglutarate in mammals: further evidence for d-2-hydroxyglutarate transhydrogenase. *Metabolism: Clinical and Experimental* 55:353–358.
- Vayer PH, Mandel P, Maitre M (1985)** Conversion of g-hydroxybutyrate to γ -aminobutyrate *in vitro*. *J. Neurochem.* 45:810–814.
- Wanders RJA, Ruiters JPN, IJlst L, Waterham HR, Houten SM (2010)** The enzymology of mitochondrial fatty acid β -oxidation and its application to follow-up analysis of positive neonatal screening results. *J. Inherit. Metab. Dis.* 33:479–494.

Chapter Four: Investigation on *ssadh* suppressor lines

1. Introduction

The GABA shunt involves the generation of potentially toxic intermediates like SSA. SSA, as an aldehyde group containing compound, is capable of damaging membranes, proteins and nucleic acids (Allan et al., 2009). Aldehyde group containing compounds cause cell toxicity by directly reacting to the cell components or by promoting the generation of reactive oxygen species (ROS). Fural aldehyde (Furfural) has been demonstrated to induce the accumulation of hydrogen peroxide and also cellular damage in *Saccharomyces cerevisiae* (Allan et al., 2010). In *Arabidopsis*, mutation in succinic semialdehyde dehydrogenase (SSADH), to which SSA is a substrate, has been shown to promote the accumulation of reactive oxygen intermediates (Fait et al., 2004; Bouché et al., 2003) which is most likely related to SSA accumulation.

A deficiency in SSADH activity has been associated with developmental disorder. In mammals, deficiency in SSADH activity has been known to cause a disorder called GHB aciduria, which is manifested by an elevated level of gamma hydroxybutyric acid (GHB) in the physiological fluids (Jacobs et al., 1981; Hogma et al., 2001). In *Arabidopsis*, deficiency in SSADH function caused a stunted growth (dwarfism), necrosis on leaves and hypersensitivity to environmental stress (Bouché et al., 2003). Furthermore, this abnormal growth phenotype was associated with an accumulation of GHB in the tissue. To our knowledge, so far it was not possible to measure the level of SSA in tissues mainly due to the unstable nature of the compound. Hence, the phenotypes observed in *ssadh* mutants were associated with elevated GHB levels. However, a previous report suggested that there is no correlation between GHB and the severity of the clinical features in mammals (Akaboshi et al 2003). External feeding of GHB as high as 2 mM did not cause a significant effect on the normal development of wild-type plants. However, 0.3 mM SSA was sufficient to be toxic and elicit a phenotype which resembles that of *ssadh* mutants on soil (Chapter two) perhaps indicating SSA is the most likely cause of the *ssadh* phenotype.

The *ssadh* inflicted disorder, GHB aciduria, in mammals is treated with several drugs. The most commonly used one is γ -vinyl- γ -aminobutyrate (Vigabatrin), a GABA analogue which irreversibly binds to the GABA transaminase and thereby prevents the degradation of GABA (Knerr et al., 2007) and ultimately prevents the accumulation of SSA/GHB. A similar rescue

of the *ssadh* phenotype has been reported in *Arabidopsis*. *Arabidopsis ssadh* plants treated with vigabatrin showed a reduced accumulation of ROS, reduced cell death and an improved growth compared to the *ssadh* itself (Fait et al., 2004). Taken together, these observations indicate that preventing the accumulation of the downstream toxic intermediates (SSA and/or GHB) by blocking degradation of GABA would significantly reduce the *ssadh* phenotype.

In this study, two different approaches have been used to rescue the abnormal *ssadh* phenotype. First, by knock out / knock down of glutamate decarboxylase expression which functions upstream of GABA-T, and second, by using a forward genetic approach after generating EMS-mutagenized suppressor lines. The detailed theoretical background of both approaches is described below.

1.1. Knock out/down of GAD expression

GAD (glutamate decarboxylase) is an enzyme that catalyzes the first step of the GABA shunt, i.e. the decarboxylation of glutamate to GABA in the cytosol. The *Arabidopsis* genome possesses five *GAD* genes which show differential expression patterns across organs. GABA is produced in the cytosol and transported to mitochondria for further degradation. *Arabidopsis* plants deficient in SSADH (converts SSA to succinate) grow abnormally (Bouché et al., 2003). However, the *ssadh* phenotype was suppressed by blocking the pathway upstream of SSA production. Ludewig et al. (2008) have reported the suppression of the *ssadh* phenotype by simultaneous knockout of the *POP2* gene whose product catalyzes the production of SSA. The suppression of the abnormal *ssadh* phenotype was most likely due to the prevention of SSA accumulation to a toxic level.

Here, it was hypothesized that the knockout of *GAD* genes likewise would reduce SSA accumulation, and thereby suppress the *ssadh* phenotype. However, it is almost impossible to generate a line deficient in all five *GAD* homologues. For example, *GAD3* and *GAD4* are closely located next to each other on chromosome 2. *GAD5*, on the other hand, shows an exclusive expression in pollen. Therefore, only *GAD1-4* genes were targeted for down regulation. *GAD1* and *GAD2* were knocked-out by T-DNA insertion where as *GAD3* and *GAD4* were targeted by artificial microRNA. Hereafter, the line is termed as *gad1/2-amigad3/4*.

1.2. EMS mutagenesis

Ethyl methanesulfonate (EMS) is a carcinogenic compound which is often used as a mutagen in biology. EMS induces a point mutation usually by substitution of bases. The ethyl group of the EMS reacts with the guanine residue of the DNA forming an abnormal O-6-ethylguanine. Then, upon DNA replication the polymerase attaches thiamine to O-6-ethylguanine instead of cytosine. With subsequent replications the GC pair will be replaced by AT causing a genetic change (Kim et al., 2006). Therefore, EMS mutagenesis has been widely used in forward and reverse genetics to identify functions of genes. Previously, Ludewig et al. (2008) have isolated a mutation in the *pop2* gene which rescued the *ssadh* phenotype. In that work, seeds of *ssadh* plants were treated with EMS and the F1 plants did not exhibit a rescued phenotype (Ludewig et al., 2008). However, in the second generation about 137 plants which show a better growth phenotype compared to *ssadh-2* mutants have been isolated (Ludewig et al., 2008).

Here, about 30 of the isolated lines were phenotypically characterized on plates. Out of these 30 lines, two lines, named 17J and 21H, were mapped for the mutation using a PCR-based system. For full-genome sequencing, two more lines, named 7D and 13J, along with the above two lines were used.

Using both approaches, the *ssadh* phenotype was partially suppressed. Suppression of the *ssadh* phenotype using the EMS approach was stronger than the *GAD* knock out/down method. Interestingly, the EMS suppressor lines accumulated GHB which was not detected in the *GAD* knock out/down lines. These two observations suggest that the *ssadh* phenotype was not caused by GHB. The PCR based mapping indicated the mutation of lines 17J and 21H to be in chromosome 5, and this brings more genes into play in the GABA shunt.

2. Materials and Methods

2.1. GADs Knock-out/down

2.1.1. Generation of the *gad1/2-amigad3/4* lines

First, the *gad1/2* double mutant was generated by crossing the single mutants as described in Materials and Methods of chapter one. Then, the artificial micro RNA construct targeting *GAD3* and *GAD4* were transformed by the flower dipping method. The preparation of the artificial micro RNA construct and the transformation method is described below.

2.1.2. Amplification of the amiGAD3/4 insert

The preparation of the artificial micro RNA construct was carried out using a web-based microRNA designer (<http://wmd2.weigelworld.org/cgi-bin/mirnatools.pl>). First, the primers that contain a sequence targeting the *GAD3* and *GAD4* transcripts and amplify the miRNA from the template were designed and the following primers were obtained: I. miR-s gaTATACTCTTAACCTACGGTAGtctctcttttgattcc II. miR-a gaCTACCGTAGGTTAA GAGTATAAtcaaagagaatcaatga III. miR*s gaCTCCCGTAGGTTATGAGTATTtcacaggtcg tgatatg IV. miR*a gaAATACTCATAACCTACGGGAGtctacatatattct. Primers flanking the miRNA i.e., primer A (CACCTGCAAGGCGATTAAGTTGGGTAAC) and primer B (GCGGATAACAATTTACACAGGAAACAG), were used for the amplification of the approximately 700 bp miRNA fragment from the template vector (pRS300). For the amplification of the final miRNA fragment targeting *GAD3* and *GAD4*, the following procedures were followed. First, three short fragments were amplified from the template vector using the following three primer combinations; primer A + primer IV, primer III + primer II and primer I + primer B. In the following step, primer A and primer B were used to amplify the full version of the miRNA using the combined PCR products obtained from the above three sets of primers as a template. In all cases a proof reading enzyme (pfu) polymerase was used.

2.1.3. Preparation of the Entry Clone

The full-length miRNA was cloned into the pENTR/D-TOPO vector according to the manufacturer's protocol with minor modifications (Invitrogen, Catalog No K2400-20). Briefly, 2 µl of the PCR product, 1 µl of salt solution and 0.2 µl of the entry vector (pENTR/D-TOPO) were mixed and filled to 6 µl with distilled water. The mixture was incubated for 15 minutes at room temperature. Then, the mix was added to chemically

competent TOP10 cells and incubated on ice for another 20 minutes. Next, the cells were heat-shocked in a water bath set at a temperature of 42 °C for one minute and then put back on ice for three minutes. Then, 500 µl of LB medium was added and incubated at 37 °C while shaking for one hour. Finally, the cells were collected by spinning down, re-suspended in 100 µl LB medium and spread on LB plate containing 50 µg/ml kanamycin. The colonies were screened for the presence of the construct by PCR. Overnight cultures were prepared from positive clones and the vector construct was harvested by miniprep. The entry clones were verified by digesting with Alw44I and NcoI restriction enzymes, and the positive clone was used for recombination with the destination vector.

2.1.4. Preparation of the expression clone

The correct entry clone was recombined with the pAMPAT destination vector according to the manufacturer's protocol with minor modifications (Invitrogen). Briefly, 4 µl of the entry clone (~100 ng/µl), 1 µl of destination vector (120 ng/µl) and 1 µl of LR Clonase were mixed and filled to 8 µl with TE buffer pH 8. The mix was incubated at room temperature for one hour, and then, the reaction was terminated by adding 1 µl of proteinase K solution. After incubating the samples for 10 minutes at 37 °C, the reaction was added to chemically competent TOP10 cells and incubated on ice for 30 minutes. Then, the cells were heat shocked for one minute at 37 °C, 500 µl LB added and incubated at 37 °C while shaking for one hour. Similarly, the positive clones were isolated by PCR, overnight culture prepared, and the construct was harvested by miniprep. Once again, the constructs were verified by digesting with restriction enzymes KpnI and NcoI. Then, the construct was transformed to the *Agrobacterium tumefaciens* GV3101 (pMP90RK) strain containing a helper plasmid. The transformants were selected on YEB plates containing 50 µM Rifampicin, 25 µM Gentamycin, 12 µM Kanamycin and 50 µM Carbenicillin. The positive clones were again selected by PCR based system. Then glycerol stocks were prepared from the positive clones by mixing 1 ml overnight culture and 1 ml glycerol and stored at -80°C.

2.1.5. Plant transformation

An overnight culture of the positive clone was diluted to an OD₆₀₀ of 0.2 in 50 ml YEB medium containing the selection antibiotics. Approximately after 6 hours the culture was added to a fresh YEB medium to a final volume of 500 ml. The culture was incubated at 28

°C for 20 to 24 hours while shaking until the OD₆₀₀ reached between 1 and 1.2, and then the cells were harvested by spinning down. Then, the transformation of four-week-old *gad1/2* plants was carried out by dipping the flowers as described before (Clough and Bent, 1998). Briefly, the cells were resuspended in 5% sucrose solution to which Silwet-77 was added to 0.02%. The flowers were then dipped into the solution for a maximum of 10 seconds. The transformed plants were laid horizontally, covered with a plastic bag and incubated in the dark for 24 hours. The transformed plants grew under green-house conditions and the F1 seeds were screened with BASTA.

2.1.6. Generation of a *gad1/2-amigad3/4-ssadh* line

First, the triple mutant *gad1/2-ssadh* line was generated by crossing the homozygous *gad1/2* line with a heterozygous *ssadh* line. In the F1 generation, individual plants were screened for the presence of the T-DNA insertions in all the three genes by PCR. Lines selected in the F1 generation were selfed, and in the second generation F2 plants were screened again for homozygous insertions of the T-DNAs by PCR. For the generation of the desired line, the *gad1/2-ssadh* homozygous triple mutant was crossed to a *gad1/2-amigad3/4* line generated before. F1 plants were screened for the presence of the T-DNA insertion in the *SSADH* gene and the presence of the artificial miRNA construct by PCR as the *gad1/2* mutations were homozygous in both parents. In the next generation, F2 seeds were sown on a tray and 5 days after germination, the seedlings were sprayed with BASTA to select the ones containing the artificial miRNA construct. Then, positively selected plants were screened for the homozygous insertion of the T-DNA in the *SSADH* gene by PCR on genomic DNA. Lines with homozygous T-DNA insertions in the *SSADH* gene were used for further phenotypic analysis.

2.1.7. Phenotypic analysis

The phenotype of the *gad1/2-ssadh* and *gad1/2-amigad3/4-ssadh* lines was compared with wild-type and *ssadh* homozygous plants. For that, the seeds of all four genotypes were sown on soil and allowed to grow. After four weeks, pictures were taken and the inflorescence length was measured. Number of siliques and number of auxiliary inflorescences were also counted. The leaf character, flowering and the general growth characteristics were visually monitored.

2.1.8. Metabolite and hydrogen peroxide (H₂O₂) measurement

The chemotype of the *gad1/2 x ssadh* triple mutant and the triple mutant over-expressing the artificial miRNA against *gad3* and *gad4* was compared to the Wt and the *ssadh* mutant. For that, six independent *gad1/2-amigad3/4* lines (L1, L11, L21, L31, L41 and L51) were selected and characterized for GABA content. A line with the lowest GABA content was selected and crossed to the *gad1/2-ssadh* triple mutant to generate the desired line. Three independent lines from both the triple *gad1/2-ssadh* and *gad1/2-amigad3/4-ssadh* mutants were selected and analyzed for GABA shunt metabolites and GHB using GC/MS. The general procedure for the metabolite analysis using the GC/MS and HPLC was described in the methodology section of chapter one. Then, the metabolite content was compared to the *ssadh* line.

For H₂O₂ measurement, wild type, *gad1/2 x ssadh* and *ssadh* lines were grown on soil, and after four weeks leaf samples were collected from wild type and the triple mutant. For the *ssadh* line the whole plant was used after five weeks of growth, as they were growing very slowly. The H₂O₂ measurement was performed using the Amplex Red enzyme assay (Invitrogen). For that, the frozen plant material was ground to powder using an electric drill machine, and 150 µl 1x reaction buffer (4 ml 5x reaction buffer + 16 ml H₂O) was added. The mix was thawed at room temperature and vortexed. Then, the mix was spun down at 14000 rpm for 15 minutes at 4°C. 50 µl of the supernatant was transferred to a microtitre plate. Next, 50 µl of the AR solution (1x reaction buffer + HRP solution + Amplex red dissolved in DMSO) was added to wells containing the samples, and mixed by gentle shaking. The mix was then incubated in the dark at room temperature for 30 minutes. Finally, the absorbance of the reaction mix at 590 nm was measured using a spectrophotometer. The absolute concentration of H₂O₂ in the samples was determined by comparing to the standard curve generated by running H₂O₂ of known concentrations.

2.2. EMS induced mutation

2.2.1. Generation and screening of EMS mutants

The generation of the EMS lines was performed as described in Ludewig et al. (2008). Briefly, seeds of *ssadh-2* mutant were incubated in water containing 0.23% ethylmethane sulfonate (EMS) for 12 hours at room temperature. Then, the seeds were washed several times with water and finally dried. The suppressor lines were isolated by visual observation after sowing the M2 seeds on soil.

2.2.2. Phenotypic characterization of EMS lines

Firstly, 32 EMS suppressor lines were selected and characterized phenotypically on agar plates. Seeds of these 32 lines were surface-sterilized, germinated and grown on ½ MS plates for two weeks. Then, the shoot weight of the individual plants was measured, and six outperforming lines were selected for further analysis. Seeds of six independent suppressor lines (7D, 13J, 17J, 21H, 29B and 30L) along with the *gs* (*gaba-t* X *ssadh*) line were surface sterilized and germinated on ½ MS plates supplemented without and with 0.3 mM SSA. Approximately, after two weeks of growth, pictures were taken and the root length and the shoot weights were compared. The growth of the plants was also assessed on soil. The best four lines (7D, 13J, 17J and 21H) were used for genome sequencing. Lines 17J and 21H were mapped for the mutation by classical PCR-based system on genomic DNA.

2.2.3. Isolation of mapping populations

For mapping of the EMS-induced mutation, the respective suppressor lines were crossed to *Landsberg erecta* (*Ler*) (wild type) plants. The F1 seeds were sown on soil and the resulting F1 plants were selfed. Next, the F2 plants were screened for homozygous insertion of the T-DNA in the *SSADH* gene and also for an improved growth. Those lines with homozygous *ssadh* mutation and improved growth were selected as mapping population. However, this procedure is very laborious, as only 1 out of 16 plants tested belongs to the mapping population. Hence, primary selections on plates were adopted. For that, sterilized F2 seeds were germinated and grown on ½MS plates. One week after germination, only yellowish plantlets were transferred to fresh ½MS plates. After another week, the plantlets were transferred to soil. Approximately, two weeks after transfer the plants were screened for the homozygous *ssadh* mutation.

2.2.4. Mapping of EMS-induced mutations

For mapping the mutation, genomic DNA was extracted from the mapping populations as described in the material and methods of chapter one. Primers discriminating between the Columbia (Col-0) and *Landsberg erecta* (*Ler*) fragments were designed on all five chromosomes. Then, PCR was performed on genomic DNA of the mapping population. The relative abundance of the Col-0 and *Ler* fragments was analyzed. A single band per lane corresponding to Col-0 or *Ler* is counted as two and double bands per lane counted one for each genotype. The number of bands was summed up and the percent of Col fragment was calculated as follows.

$$\% \text{ Col-0} = \text{No of Col-0 fragments} / \text{Total number of fragments} * 100$$

2.2.5. Genomic DNA extraction for whole genome sequencing

For genomic DNA extraction, seeds of lines 7D, 13J, 17J and 21H were germinated and grown on soil. After three weeks of growth, approximately 100 mg of inflorescence with flowers were collected from all four lines, and were immediately frozen in liquid nitrogen. The extraction of the genomic DNA was carried out using the DNeasy Plant Mini Kit (Cat. No. 69104). The concentration of the DNA was determined using a Nano Drop.

3. Results

3.1. GAD Knock out/down

3.1.1. Isolation of the triple *gad1/2-ssadh* mutants

The *gad1/2* line was crossed to heterozygous *ssadh* plants, as homozygous *ssadh* plants are difficult to use for crossing. The resulting F1 plants were selfed, and the F2 plants were screened for homozygosity. Out of 70 plants screened, no triple mutant was obtained. However, two lines homozygous for *gad1* and *gad2* and heterozygous for *ssadh* were obtained. These two lines were selfed again, and in the F3 generation out of 140 plants screened, about 25 independent lines were isolated with a triple homozygous mutation. The triple homozygosity of the lines was confirmed by PCR with gene specific primers (F+R), and a combination of gene specific and vector specific (LB) primers (Fig. 50). No product was amplified in all three genes with gene-specific primers whereas primer combination of LB and gene-specific primers yielded a product indicating that the insertion was homozygous (Fig. 50). Three out of 25 lines, assigned here as L1, L5 and L6, showed a superior phenotype compared to the rest, and therefore used for further analysis.

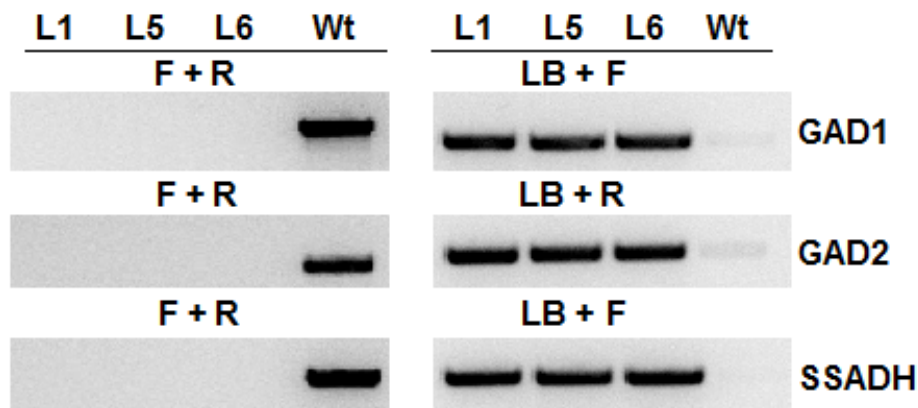


Figure 50. Screening of triple *gad1/2* x *ssadh* plants using gene-specific primers (F + R) and a combination of gene-specific and T-DNA-specific primers (LB).

3.1.2. Phenotypic analysis

Phenotypic analysis showed that *gad1/2-ssadh* plants grow much better than the corresponding *ssadh* plants. Indeed, the inflorescence length measurement revealed a ten-fold higher growth in four-week-old plants (Fig. 51A&B). However compared to the wild type, the triple mutants had a significantly shorter inflorescence length, indicating the incomplete suppression of the *ssadh* phenotype (Fig. 51A&B).

Further analysis was performed by counting the number of auxiliary inflorescences, and the number of siliques produced. Interestingly, after four weeks of growth the triple mutants initiated a higher number of auxiliary inflorescences compared with the *ssadh* mutant and the wild type (Fig. 51C) which gave the triple mutants a bushier look (Fig. 51A). The *ssadh* homozygous plants, however, did not even show a growth of the primary inflorescence. The count of siliques also revealed a higher number in the triple mutants compared to *ssadh* plants, and also were marginally higher compared to the wild type (Fig. 51D). However, the size of the siliques was very short compared to the wild type and somehow opens the fruit very quickly. The growth of the primary inflorescence did not change much in the triple mutant after the fourth week until the end of the life cycle. The leaves of the triple mutants also displayed a sign of burning and were died with increasing age. In some cases the tip of the inflorescence also wilted, and the early developing siliques prematurely died. However, the later developing siliques remained green. The siliques also showed a characteristic “dome” shape at the tip.

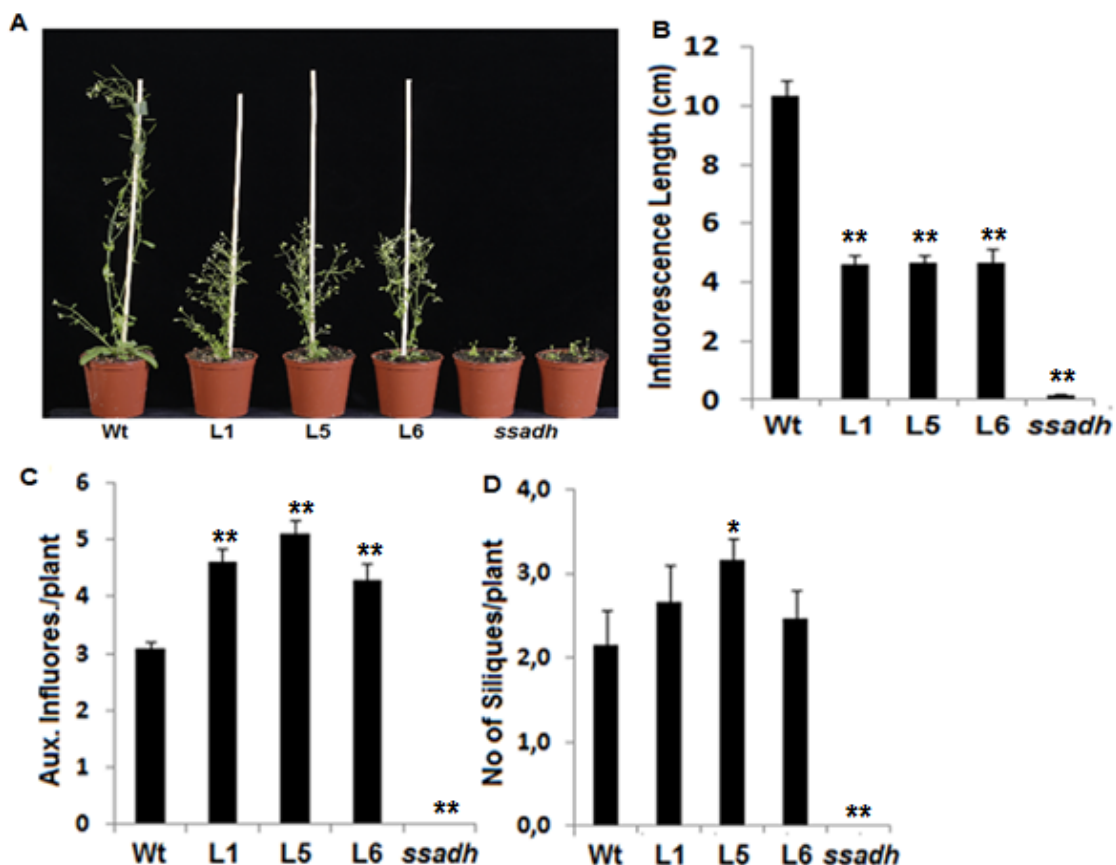


Figure 51. Growth phenotype of four-week-old wild type, *gad1/2-ssadh* and *ssadh* plants grown in pots filled with soil (A); shoot length of the triple mutant and *ssadh* plants (B); error bars represent the standard error of means of at least 13 plants per line; asterisks indicate statistically significant differences after student t-test; * ($P < 0.05$) and ** ($P < 0.01$).

3.1.3. Metabolic Analysis and H₂O₂ measurement

One of the major metabolic features of *ssadh* mutants is the accumulation of high levels of GHB which is considered to be responsible for the *ssadh* abnormal growth phenotype. Here, the presence of GHB in the leaves along with GABA shunt and TCA cycle intermediates were analyzed by GC/MS. A very high level of GHB has been detected in the *ssadh* line grown under normal conditions (Fig. 58B). Like in *gad1/2* double mutant plants, no GHB was detected in the leaves of *gad1/2 X ssadh* triple mutants although it was also hardly detected in wild type. Similarly, no GABA was detected in two (L1 and L5) of the triple mutants which is a typical feature of *gad1/2* mutants. Unexpectedly, line L6 contained detectable but low levels of GABA compared to the wild type and to the *gs* line. The *gs* line which rescued the *ssadh* phenotype by simultaneous GABA-T mutation, accumulated very high level of GABA, an observation that goes in line with that of Ludewig et al. (2008) (Fig. 52A).

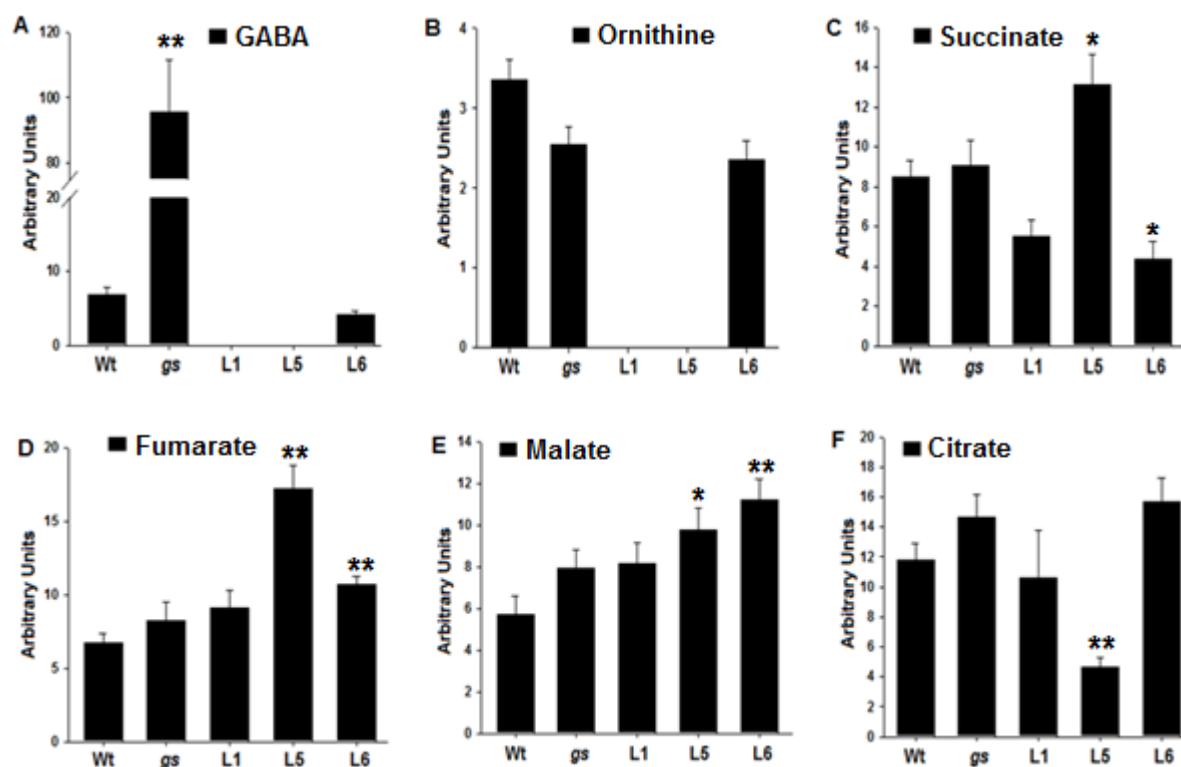


Figure 52. Metabolic analysis of GABA shunt and TCA cycle intermediates in the four-week-old wild-type, *gs* and *gad1/2Xssadh* triple mutants; bars are the mean of at least six biological and three technical replicates; error bars represent the standard error of means, n=5; asterisks indicate statistically significant differences between the wild type and the mutants; * (P<0.05) and ** (P<0.01).

The accumulation of TCA cycle intermediates do not seem to be consistent among the triple mutants. With respect to succinate, L1 and L6 showed a reduced accumulation in contrast to L5 which accumulated a significantly higher amount in the shoot (Fig. 52C). The amounts of

fumarate and malate were generally increased in all three triple mutants compared to wild type, a chemotype that seems intermediate between the *gad1/2* and *ssadh* plants. The level of citrate was different among the triple mutants compared to the wild type (Fig. 52F), perhaps indicating the presence of individual variations.

One feature associated with cell death in *ssadh* plants is the accumulation of reactive oxygen species like hydrogen peroxide (Fait et al., 2004). To test if the partial suppression of the *ssadh* phenotype by *gad1/2* mutations was due to a reduced H₂O₂ level, the hydrogen peroxide content in the triple mutants was compared to that of the *ssadh* mutant. Unexpectedly, there was no difference in the hydrogen peroxide content among the lines, despite L5 and L6 contained relatively lesser amounts (Fig. 53).

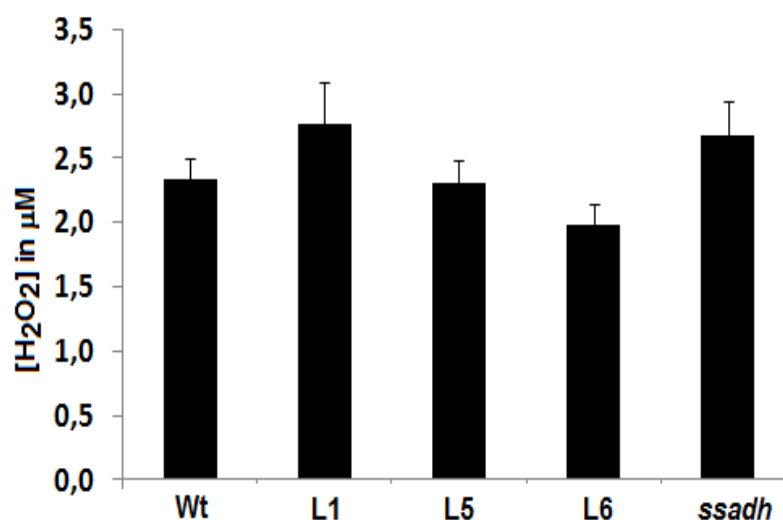


Figure 53. Measurement of hydrogen peroxide in the plant extracts of wild type, *gad1/2* x *ssadh* triple mutants (L1, L5 and L6) and *ssadh* lines. For each line five biological replicates were used, and each measurement was made in duplicates.

3.1.4. Generation of the *gad1/2-amigad3/4-ssadh* line

The incomplete suppression of the *ssadh* phenotype by simultaneous mutation of the two most abundantly expressing *GAD* genes (*GAD1* and *GAD2*) may be explained by the compensatory effect of the other three homologues. Indeed, *GAD4* transcript has been up-regulated in the shoot and root (Chapter one). The two genes (*GAD3* and *GAD4*) reside next to each other on chromosome 2, and obtaining the two mutations in one plant is almost impossible. Therefore, knock down of the *GAD3* and *GAD4* genes was targeted by an artificial miRNA. After BASTA selection, more than hundred positive plants were generated. To select a line which should be crossed to the *gad1/2-ssadh* triple mutant, metabolic analysis was performed to measure the GABA content.

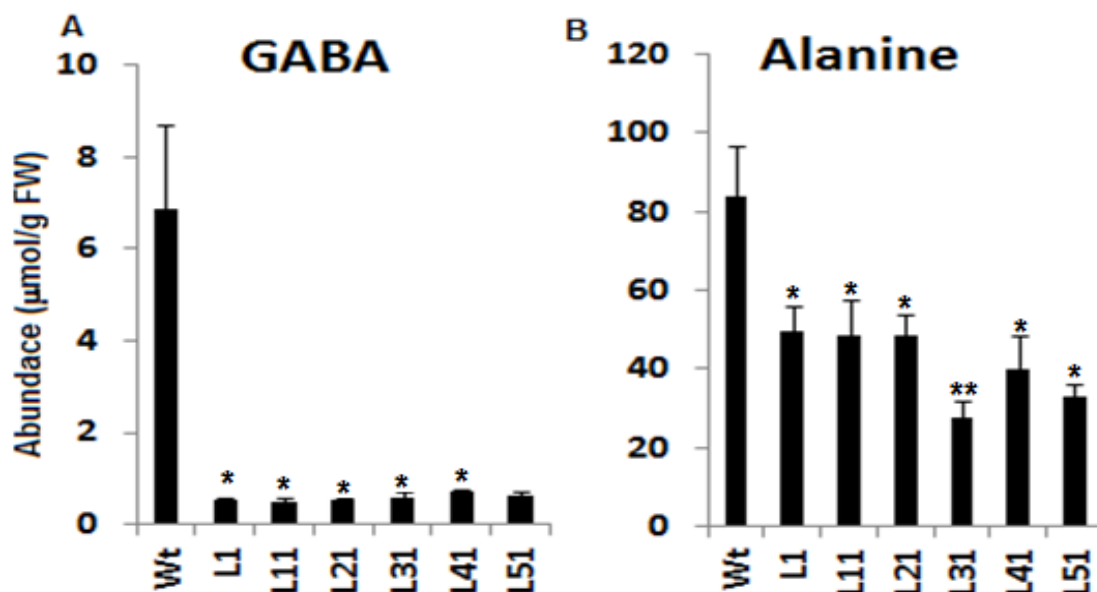


Figure 54. HPLC measurement of GABA (A) and Alanine (B) from wild type and six *gad1/2-amigad3/4-ssadh* lines; error bars represent the standard error of means, n=5; asterisks indicate statistically significant differences between the wild type and the mutants; * (P<0.05) and ** (P<0.01).

For metabolite analysis, six independent lines (named L1, L11, L21, L31, L41 and L51) along with the wild type were germinated and grown on soil, and leaf samples were collected from four-week-old plants. HPLC measurement of the amino acids revealed that the GABA content was reduced by 14-fold in line L11 and by about ten-fold in the remaining five lines (Fig. 54A). Similarly, the GABA degradation product, alanine, was also reduced in all mutant lines (Fig. 54B). Therefore, based on the chemotypic data, line L11 was selected and was crossed to the *gad1/2-ssadh* triple mutant L6. In the F2 generation, about eight independent lines which were resistant to BASTA and thus homozygously mutated for *gad1*, *gad2* and *ssadh* were isolated. Three of the eight lines had fertility problems, and only five of them were able to produce seeds. Preliminary observation of these eight plants did not show a further improved growth compared to the *gad1/2 x ssadh* triple mutants; however, the following generations need to be investigated.

3.2. Suppression of the *ssadh* phenotype by EMS mutation

3.2.1. Preliminary selection of the EMS suppressor lines

In the previous report of Ludewig et al. (2008), more than 130 lines have been reported to show better growth compared to the parent *ssadh-2* line. Some of these lines had fertility problems and could not pass to the next generation, and some more lines also were lost because of germination problems. To select few lines for mapping of the EMS mutation, a preliminary screening was performed by measuring the shoot weight (Fig. 55). For that 32 independent *ssadh* suppressor lines were germinated and grown on ½MS plates for two weeks.

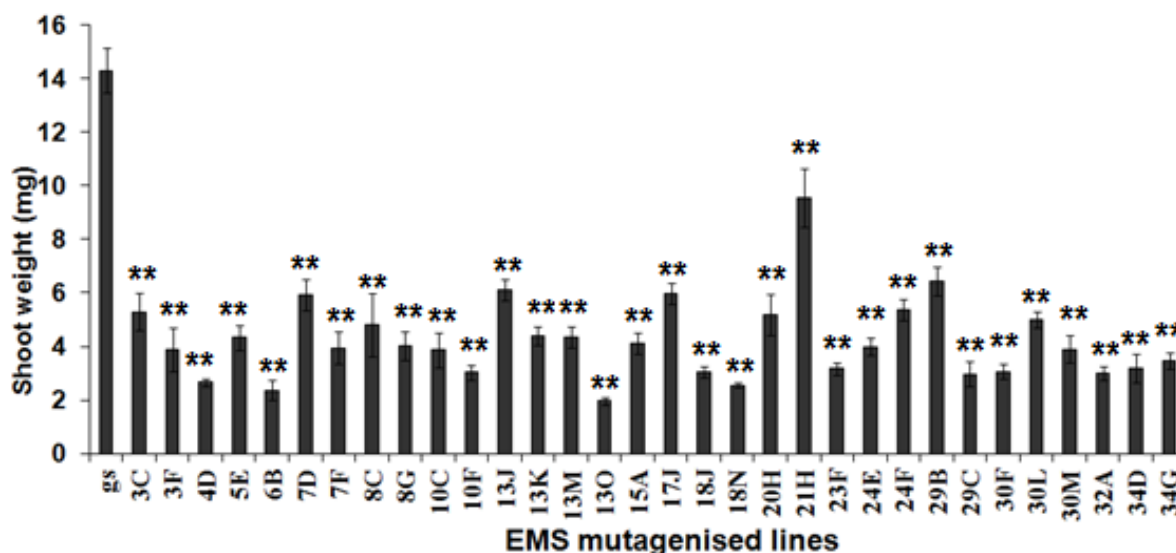


Figure 55. Phenotypic analysis of EMS suppressor lines germinated and grown on ½ MS plate for two weeks; error bars represent the standard error of means; for each line at least 7 plants were measured; asterisks represent statistically significant differences between the wild type and EMS lines; ** (P<0.01).

Six lines (7D, 13J, 17J, 21H, 29B and 30L) showed a better shoot growth compared to the rest (Fig. 55). Therefore, these six lines were further characterized on ½ MS plates without and with 0.3 mM SSA.

3.2.2. Phenotypic characterization of selected EMS suppressor lines

The *ssadh* mutant phenotype could be rescued either by preventing the accumulation of the toxic intermediate or by promoting the removal of the toxic intermediate. The idea was that, if the mode of EMS suppression is preventing the accumulation of the toxic intermediate like in

gs line, the exogenous application of SSA would make them oversensitive, and the other way round, if the mode of suppression is promoting the degradation of the toxic intermediate. Therefore, the suppressor lines along with the positive control, the *gs* line, were characterized for shoot weight and root length on ½ MS plates containing 0.3 mM SSA. The analysis revealed a comparable shoot and root growth of 21H and 29B to the positive control on ½ MS plates (Fig. 56). However, line 30L had a lower shoot weight and root length compared to the *gs* line. The shoot and root development of 13J was also lower compared to the control *gs* line (Fig. 56). Treatment with 0.3 mM SSA significantly reduced the shoot and root growth of all genotypes (Fig. 56C&D), perhaps indicating that the mechanism of *ssadh* phenotype suppression was not by an enhanced removal of the toxic compound. Except 17J and 29B, the remaining four lines had a similar shoot growth compared to the control *gs* line (Fig. 56C).

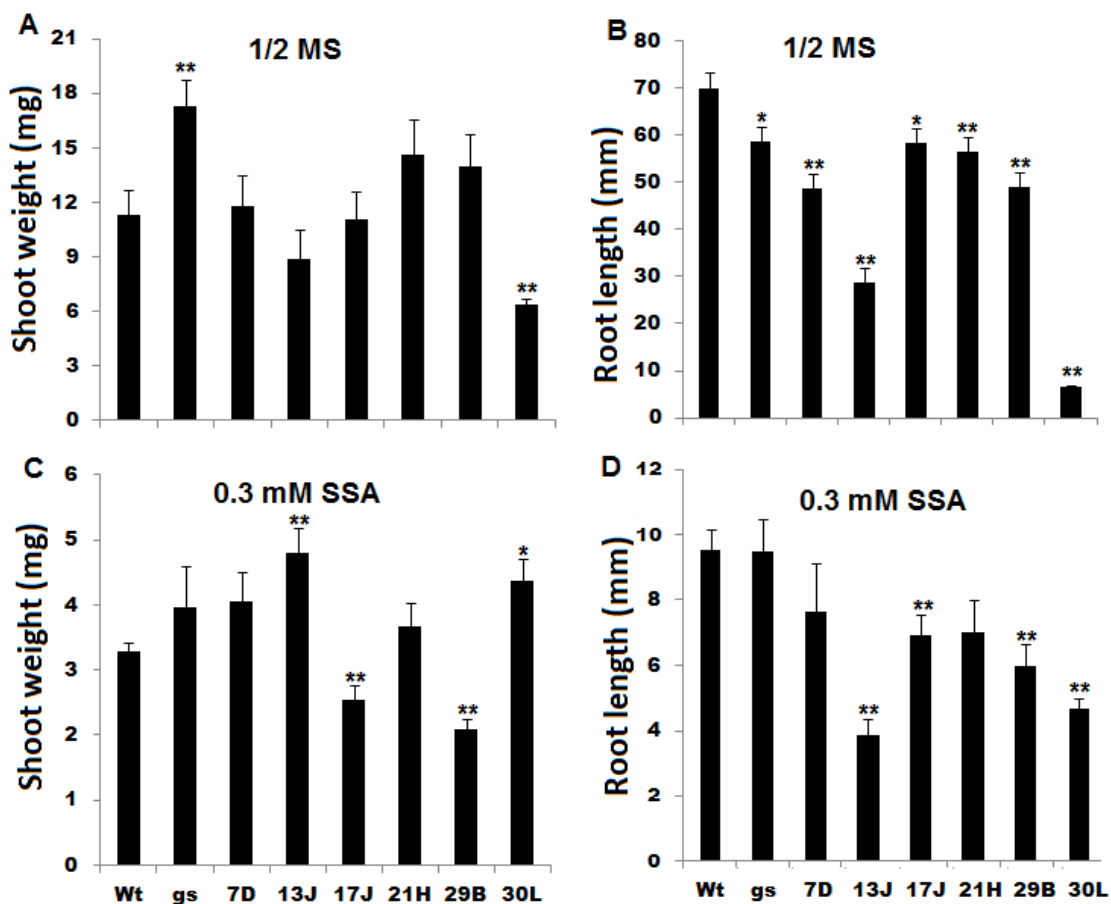


Figure 56. Seeds of *gs* and EMS mutagenized lines (7D, 13J, 17J, 21H, 29B and 30L) were germinated and grown on ½ MS plates without and with 0.3 mM SSA. Shoot fresh weight (A&C) and root length (B&D) were measured after two weeks of growth; bars represent the standard error of means; n=5; asterisks represent statistical significance after student t-test; * (P<0.05) and ** (P<0.01).

For mapping of the EMS mutations four lines (7D, 13J, 17J and 21H) were finally selected based on the phenotype. Line 30L was omitted because of its poor performance under normal growth condition (Fig. 56A&B), whereas line 29B was omitted because of its phenotypic similarity with 17J and 21H.

These selected lines were further characterized on soil (Fig. 57A). To rule out any seed contamination, plants from each line were genotyped for homozygosity of the *ssadh* mutation. PCR analysis with gene-specific primers (F+R) yielded a band only in the wild type (positive control), but not in the mutant lines (Fig. 57B). T-DNA-specific (LB) and gene-specific primer combinations yielded a product only in the mutants (Fig. 57B) indicating that the mutation was homozygous. After three weeks of growth the EMS mutants showed an improved phenotype compared to the *ssadh* parental line, and similar growth compared to the wild type (Fig. 57A). Line 7D, unlike the other three, was shorter and looked deep yellow throughout the growth period (Fig. 57A).

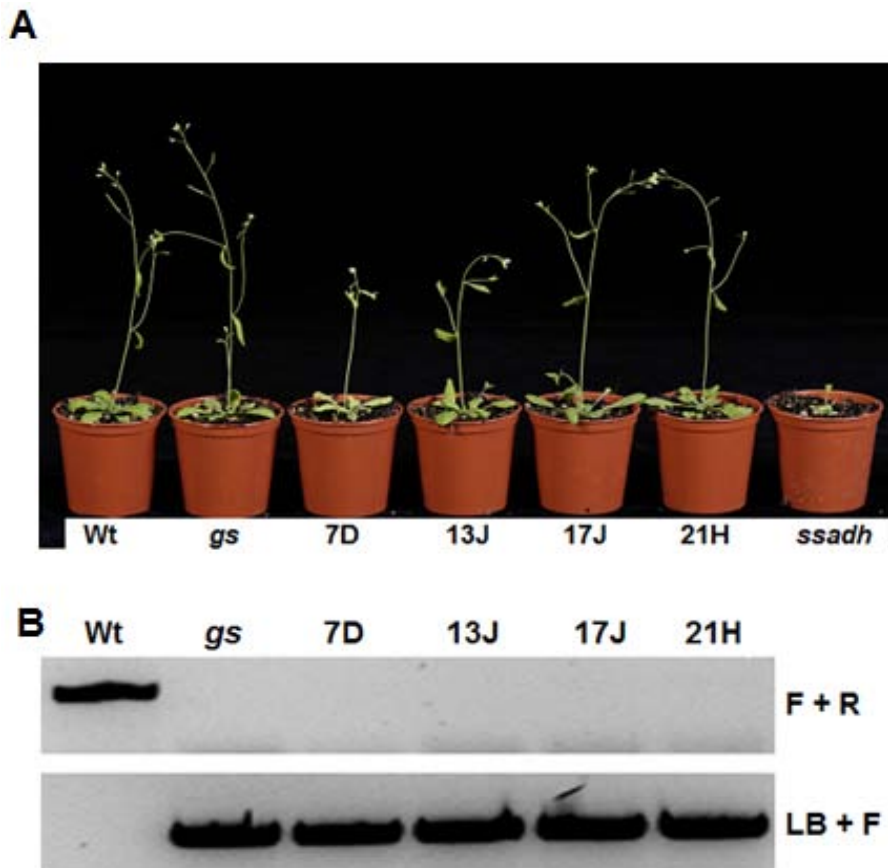


Figure 57. Phenotype of three-week-old Wt, *gs*, 7D, 13J, 17J, 21H and *ssadh* plants grown on soil under normal condition (A); The homozygosity of the EMS lines was confirmed by RT-PCR using gene-specific primers (F+R) and gene-specific and T-DNA-specific primer (LB + F) (B).

3.2.3. Metabolic analysis of the EMS suppressor lines

The abnormal phenotype of *ssadh* mutant plants has been associated with the accumulation of toxic intermediates like SSA and GHB. One feature of the *gs* line which rescued the *ssadh* phenotype is the prevention of GHB accumulation. To get an insight into the mode of suppression of the *ssadh* phenotype by the EMS mutations, the accumulation of GHB, GABA shunt and some of the TCA cycle intermediates were analyzed in the EMS lines compared to the controls. The accumulation of GABA in leaf extracts of the *gs* line was higher compared to the wild type, an observation that goes in line with the previous report (Ludewig et al., 2008; Fig. 58). As expected, no GHB was detected in leaf extracts of the *gs* line, an observation that resembles the wild type. A higher level of GABA compared to the wild type could be detected in all EMS lines 7D, 13J 17J and 21H (Fig. 58A).

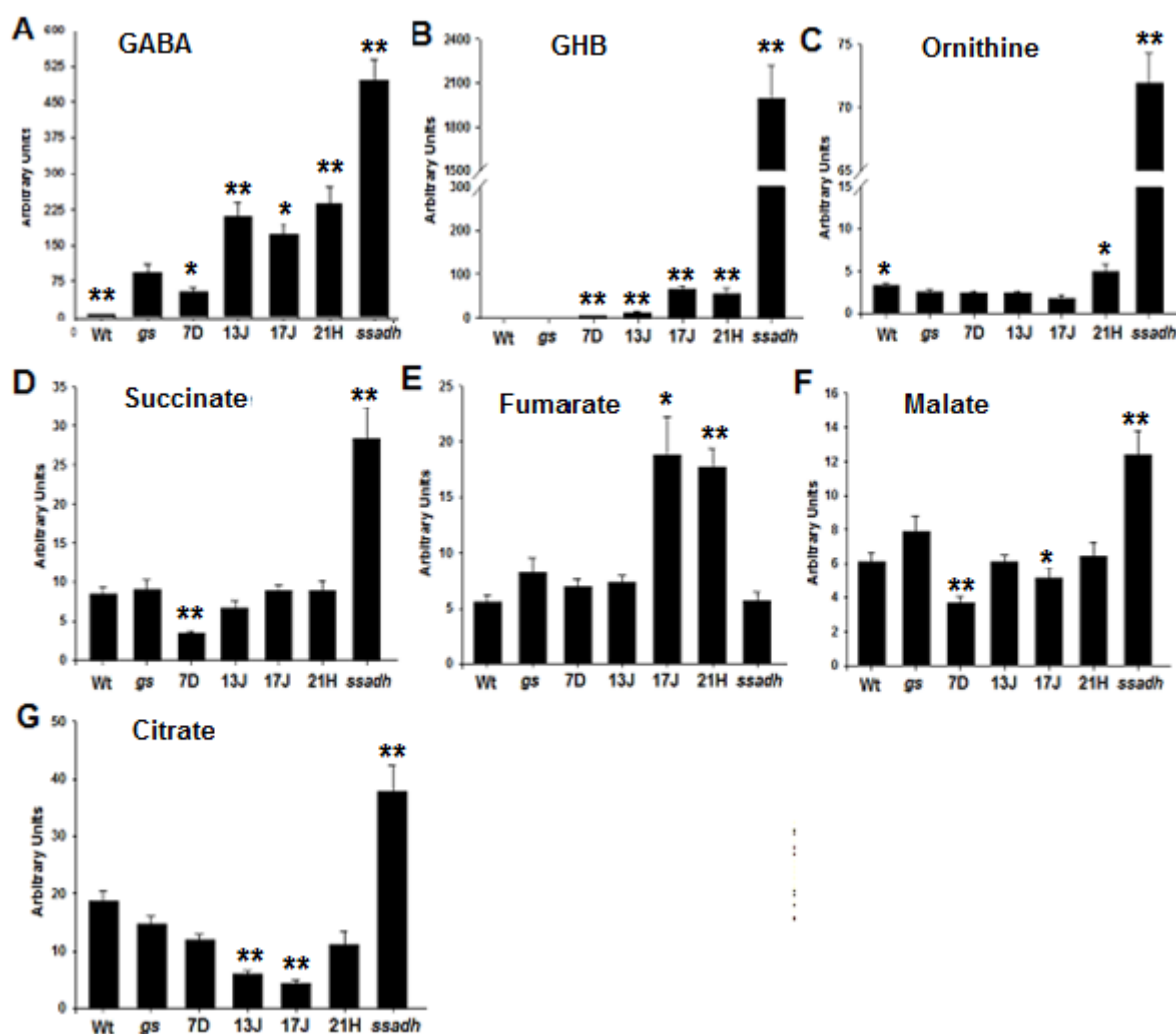


Figure 58. GC/MS analysis of major GABA shunt and TCA cycle intermediates in shoot extracts of wild-type, *gs*, 7D, 13J, 17J, 21H and *ssadh* lines; bars are the mean of ten biological and three technical replicates; error bars represent the standard error of means; asterisks indicate statistically significant differences between the *gs* and the EMS lines; * (P<0.05) and ** (P<0.01).

The GABA level in EMS lines 13J, 17J and 21H was even higher than in the control *gs* line. Unlike the wild type and *gs* line, the EMS lines appeared to contain a detectable level of GHB (Fig. 58B). Specifically, line 17J and 21H contained a significantly higher level of GHB compared to 7D, 13J as well as the controls. As expected, the leaf extract from the *ssadh* line contained GHB approximately 30-fold higher compared to the 17J and 21H EMS suppressor lines (Fig. 58A&B). The GABA content in the *ssadh* line was also 2 to 3-fold higher compared to the EMS lines. Unexpectedly, it was also 5-fold higher than that measured in *gs* leaf extract. The level of ornithine, which shares a structural similarity with GABA, was the same in the EMS lines and controls. However, the level in the *ssadh* plant leaf extract was significantly higher compared to the rest (Fig. 58C).

A striking difference between the controls and the EMS lines for the TCA cycle intermediates was not observed except for fumarate. The level of fumarate appeared to be higher in lines 17J and 21H compared to the rest (Fig. 58E). Lines 17J and 21H exhibited similar metabolic characteristics including the GHB content perhaps suggesting a similarity in mode of suppression of the *ssadh* phenotype. The content of TCA cycle intermediates remained higher in the plant extracts of the *ssadh* line except for fumarate.

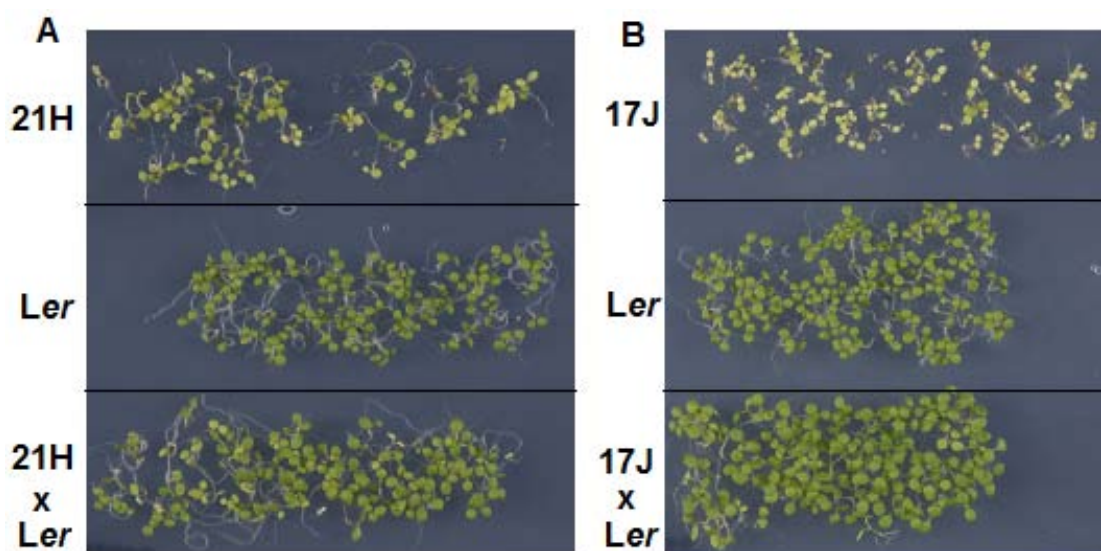


Figure 59. Preliminary screening of the 21H x *Ler* (A) and 17J x *Ler* (B) F2 population on 1/2 MS plates; seeds of *Ler*, 21H, 17J, 21H x *Ler* and 17J x *Ler* were germinated and grown on 1/2 MS plates; pictures were taken approximately one week after germination.

3.2.4. Generation of mapping populations

Isolation of the mapping population from plants germinated and grown on soil was not efficient for the following reasons; first, the lines belonging to the mapping population grew very slowly, perhaps because of late germination. Hence, mass sowing and germination of the F2 seeds on pots, and later transfer of individual seedlings were biased to plants which did not belong to the mapping population.

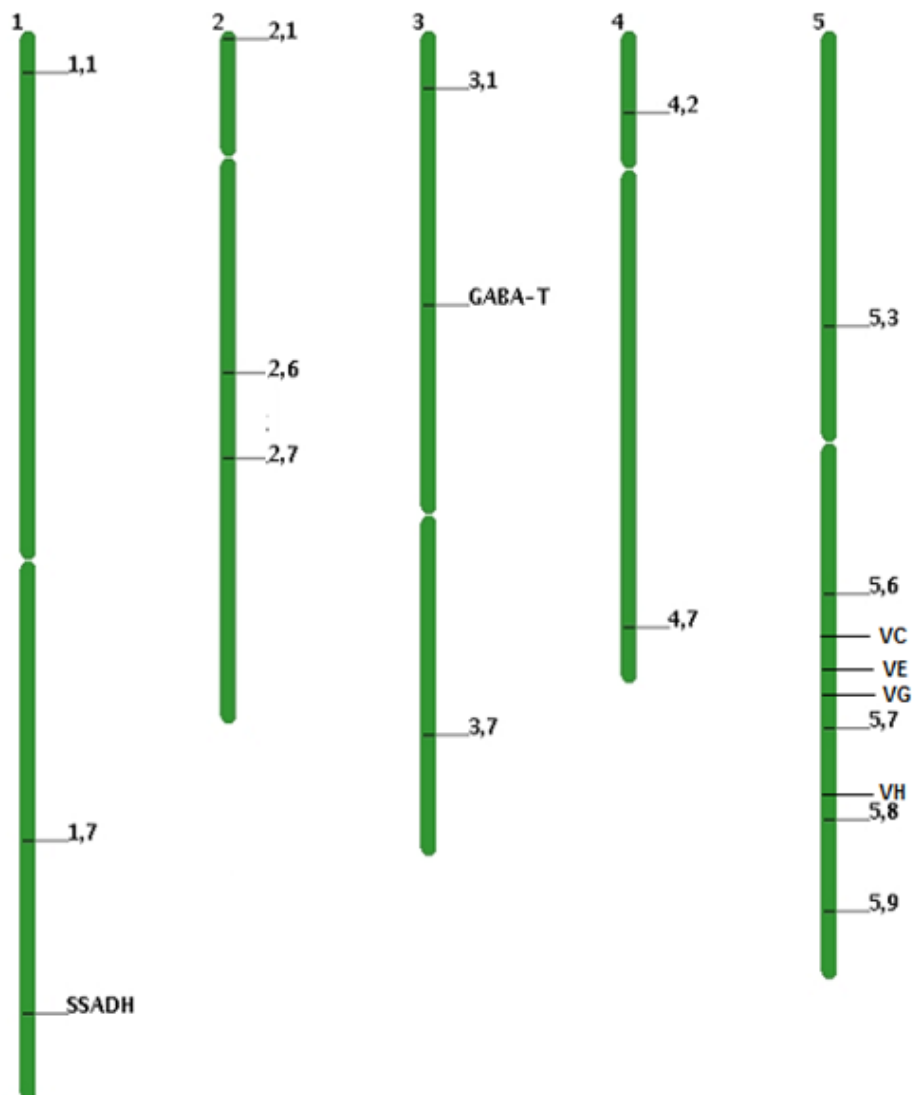


Figure 60. Schematic representation of the positions of markers designed to map the position of the EMS mutation on each chromosome; the numbers and letters represent the name of the markers used for mapping; the positions of the SSADH and GABA-T genes were also shown.

The desired lines remained at the bottom of the densely grown seedlings, and therefore, the chance of picking these plants was minimal. Second, theoretically only one out of 16 plants belongs to the respective mapping population. This made the selection procedure with PCR

very laborious. Hence, preliminary screenings were performed on ½MS plates. The EMS lines exhibit a yellow phenotype during the early stages of growth (Fig. 59). Therefore, this characteristic was taken to perform a primary screening on agar plates. Indeed, the lines belonging to the mapping populations exhibited a yellowish shoot phenotype (Fig. 59), and these plants were transferred to soil for further PCR-based screening. The yellowish phenotype was clearly visible only at the earlier stages of growth (up to two weeks); however, after being transferred and grown on soil, the plants got greener.

3.2.5. PCR-based mapping of the EMS mutations

After screening, 80 to 100 lines belonging to the mapping population were isolated from both EMS lines (17J and 21H). For mapping the mutation, several primers spanning all five chromosomes were designed (Fig. 60). For rough mapping, 20 lines were used and the percent Col-0 fragment was calculated based on the size of the PCR product obtained with each primer. In both lines, primers 2.6 and 5.9 yielded the highest percentage of the Col-0 fragment (Table 5).

Table 5. Rough mapping of EMS-induced mutation in lines 17J (A) and 21H (B) after crossing to *Ler* ecotype

A				B			
Chromosome	Primer name	% Col	No of plants	Chromosome	Primer name	% Col	No of plants
1	1.1	38.8	20	1	1.1	50.0	20
	1.8	88.8	20		1.8	91.0	20
2	2.1	47.2	20	2	2.1	44.0	20
	2.6	94.1	20		2.6	100	20
	2.7	33.0	20		2.7	33.0	20
3	3.1	41.6	20	3	3.1	41.0	20
	3.7	52.7	20		3.7	63.3	20
4	4.2	22.2	20	4	4.2	50.0	20
	4.7	44.4	20		4.7	61.0	20
5	5.3	66.6	20	5	5.3	67.0	20
	5.9	100	20		5.9	88.0	20

The highest percentage of Col-0 fragment using primer 1.8 was due to the *ssadh* mutation which is in the Col-0 background. This indicated that the mutations are situated in chromosome 2 and 5. To ensure that these regions are the correct positions, the PCR was repeated with an increased number of lines from the mapping population. Indeed, this region was rich in Col-0 fragments in both lines (Table 6). This also suggested that both lines might have been rescued by two mutations. The proportion of the mapping population obtained by selection of the F₂ generations points towards the rescue of the phenotype by more than one gene.

Table 6. Mapping of EMS-induced mutations in lines 17J (A) and 21H (B) with chromosome 2 and 5-specific primers

A				B			
Chromosome	Primer name	% Col-0	No. of plants	Chromosome	Primer name	% Col-0	No. of plants
2	2.6	95.2	72	5	5.7	94.0	70
5	5.8	89.5	72		5.8	89.3	70
	5.9	91.5	72				
	VG	95.0	72				

3.2.6. Full genome sequencing of 7D, 13J, 17J and 21H EMS lines

Full-genome sequencing helps to identify mutations that are induced by the EMS treatment. Here, the genome of four EMS-rescued *ssadh* lines (7D, 13J, 17J and 21H) were completely sequenced. Identification of the right EMS-induced mutation that rescues the *ssadh* phenotype is difficult as there are thousands of SNP's induced all over the genome. However, such difficulties can be eased by performing a PCR-based classical mapping which at least helps to determine the chromosome in which the EMS induced mutation resides. Here in lines 17J and 21H, the position of the EMS-induced mutation was mapped to chromosome 2 and 5 by the classical PCR-based system. Therefore, the sequences from chromosome 2 and 5 of line 17J and 21H were analyzed for searching the candidate mutations. Since no such mapping was performed for line 7D and 13J, the sequences from these two lines were not analyzed further.

A) Analysis of chromosome 5

Following the complete-genome sequencing, 113 and 119 single nucleotide polymorphisms (SNPs) in line 17J and 21H, respectively, was found to be different from the reference allele

within the chromosomal region of interest. However, about 44 and 66 of the predicted SNPs in lines 17J and 21H, respectively, were common for all four genotypes (7D, 13J, 17J and 21H), which is unlikely, and therefore rejected. From the remaining mutations, 6 SNP's from line 17J, none from 21H, were rejected because the call was biased towards the reference allele. About 52 SNP's were common between the lines 17J and 21H. There are 9 SNP's which are unique to Line 17J and 1 SNP which is unique to line 21H. Further analysis on these SNP's resolved 24 and 18 SNP's as intergenic, 15 and 11 SNP's as intronic, 30 and 23 SNP's as exonic in lines 17J and 21H, respectively. The possible change in amino acid due to exonic SNP's was also analyzed. The analysis revealed 13 and 9 SNP's as mis-sense, 8 and 7 SNP's as silent, 2 and 1 SNP's as non-sense mutation in line 17J and 21H, respectively (Table 7 &8).

SNP's induced mis-sense mutations were further analyzed for the possible changes in the property of the amino acids. Out of the 13 SNP's that induced mis-sense mutations in line 17J, 7 SNP's involved a net change in the charge of the amino acids (Table 9; shaded with green). For example, the substitution of glutamic acid by lysine in the protein encoded by the locus At5g44860 involves the replacement of a negatively charged amino acid by a positively charged one. Three substitutions were found to be synonymous mutation, i.e., the replacement of amino acid of the similar property. For example, the substitution of alanine by valine which involves the substitution of amino acid with non-polar and neutral side chains by the same non-polar and neutral side chained amino acid (Table 9; shaded yellow). The other group of substitutions are amino acids of the same charge but different polarity. For example, the substitution of alanine by threonine which involves the replacement of non-polar amino acid with polar amino acid (Table 9; shaded blue). The position of such substitutions on in the protein determines the activity of the protein.

Table 7. Mutations obtained in chromosome 5 of line 17J

Position on chromosome	Gene ID	Total reads	Ref./non - ref. alleles	Ratio	Codon change	Amino acid change	Gene Annotation in the data base
17802085	At5g44200	74	36 / 37	0,97	GAT to AAT	Asp to Asn *	CAP-Binding Protein 20, AtCBP20
18012564	At5g44640	61	28 / 33	0,85	GTC to GTT	Val to Val	Beta Glucosidase 13
18045658	At5g44730	64	30 / 32	0,94	GCT to GTT	Ala to Val	Haloacid dehalogenase-like hydrolase
18111023	At5g44860	65	28 / 36	0,78	GAG to AAG	Glu to Lys *	unknown protein
18141625	At5g44930	49	22 / 24	0,92	GAA to TAA	Glu to stop codon	Arabinan Deficient 2, ARAD2
18725607	At5g46190	72	26 / 44	0,59	AGG to AGA	Arg to Arg	RNA-binding KH domain-containing protein
18786752	At5g46310	70	32 / 37	0,86	TCC to TCT	Ser to Ser	WRKY family transcription factor
19003401	At5g46830	47	20 / 27	0,74	TCC to TTC	Ser to Phen	Calcium-binding transcription factor
19036529	At5g46890	46	19 / 26	0,73	GTT to ATT	Val to Ileu	Bifunctional inhibitor/lipid-transfer protein
19170353	At5g47210	39	3 / 35	0,12	CGC to TGC	Arg to Cys *	Hyaluronan / mRNA binding family
19198812	At5g47300	67	23 / 43	0,77	ATC to ATT	Isoleu to Isoleu	F-box domain-containing protein
19646544	At5g48485	69	13 / 55	0,24	GAT to AAT	Asp to Asn *	Defective in Induced Resistance 1
20491674	At5g50340	78	10 / 68	0,15	AAG to AAA	Lys to Lys	ATP-dependent peptidases
20544376	At5g50450	49	10 / 38	0,26	TGG to TAG	Trp to stop codon	HCP-like superfamily protein
20866484	At5g51340	51	0 / 51	0,00	ATC to ATT	Isoleu to Isoleu	Tetratricopeptide repeat superfamily protein
20974014	At5g51630	48	2 / 45	0,04	GAC to GAT	Asp to Asp	Disease resistance protein faminy
20986043	At5g51660	51	2 / 46	0,04	CCT to CTT	Pro to Leu	Cleavage and Poly(A) specificity Factor 160
21121925	At5g52010	71	8 / 62	0,13	GGA to AGA	Gly to Arg *	C2H2-like zinc finger protein
21273114	At5g52400	54	0 / 52	0,00	CCA to TCA	Pro to Ser	Cytochrome P450, Family 715
21556231	At5g53150	61	2 / 59	0,03	GGG to AGG	Gly to Arg *	DNAJ heat shock domain-containing protein
21795476	At5g53660	83	5 / 77	0,06	GAG to GAA	Glu to Glu	Growth-Regulating Factor 7
21817419	At5g53750	52	3 / 41	0,07	GCA to ACA	Ala to Threo	CBS domain-containing protein
21912469	At5g53970	54	4 / 49	0,01	GGG to GAG	Gly to Glu *	Tyrosine Aminotransferase 7

* Only mutations occurred in the exon were presented here; green shaded cells show amino acid changed; yellow shaded cells show silent mutations with no amino acid changes; red shaded cells show mutations where premature stop codon was induced; asterisks in the “amino acid change” column represent a net change of charge on the side chain of the substituted amino acid.

Table 8. Mutations obtained in chromosome 5 of line 21H

Position on chromosome	Gene ID	Total reads	Ref./non - ref. alleles	Ratio	Codon change	Amino acid change	Gene Annotation in the data base
17802085	At5g44200	46	4 / 42	0,10	GAT to AAT	Asp to Asn *	CAP-Binding Protein 20, AtCBP20
18012564	At5g44640	34	6 / 28	0,21	GTC to GTT	Val to Val	Beta Glucosidase 13
18111023	At5g44860	36	8 / 28	0,29	GAG to AAG	Glu to Lys *	unknown protein
18141625	At5g44930	36	5 / 31	0,16	GAA to TAA	Glu to stop codon	Arabinan Deficient 2, ARAD2
18725607	At5g46190	44	14 / 29	0,48	AGG to AGA	Arg to Arg	RNA-binding KH domain-containing
19003401	At5g46830	27	3 / 23	0,13	TCC to TTC	Ser to Phen	Calcium-binding transcription factor
19170353	At5g47210	28	6 / 22	0,27	CGC to TGC	Arg to Cyst *	Hyaluronan / mRNA binding family
19198812	At5g47300	32	6 / 24	0,25	ATC to ATT	Ileu to Ileu	F-box domain-containing protein
19646544	At5g48485	32	6 / 26	0,23	GAT to AAT	Asp to Asn *	Defective in Induced Resistance 1
20491674	At5g50340	51	0 / 51	0,00	ATC to ATT	Isoleu to Isoleu	Tetratricopeptide repeat protein
20544376	At5g50450	49	10 / 38	0,26	TGG to TAG	Trp to stop codon	HCP-like superfamily protein
20866484	At5g51340	39	12 / 26	0,46	AAG to AAA	Lys to Lys	Tetratricopeptide repeat protein
21121925	At5g52010	38	7 / 30	0,23	GGA to AGA	Gly to Arg *	C2H2-like zinc finger protein
21556231	At5g53150	37	9 / 27	0,33	GGG to AGG	Gly to Arg *	DNAJ heat shock domain-containing
21795476	At5653660	34	4 / 30	0,13	GAG to GAA	Glu to Glu	Growth-Regulating Factor 7
21817419	At5g53750	29	9 / 15	0,60	GCA to ACA	Ala to Threo	CBS domain-containing protein
21912469	At5g53970	36	6 / 29	0,21	GGG to GAG	Gly to Glu *	Tyrosine Aminotransferase 7

* Only mutations occurred in the exon were presented here; green shaded cells show amino acid changed; yellow shaded cells show silent mutations with no amino acid changes; red shaded cells show mutations where premature stop codon was induced; asterisks in the “amino acid change” column represent a net change of charge on the side chain of the substituted amino acid.

Table 9. Analysis of SNP's that resulted in amino acid substitutions

Gene ID	Amino acid changes	Amino acid property	nucleotide sequence near to the mutation
At5g44200	Asp to Asn	polar negative to polar neutral	GATGATCGGAAGAGAAGATCTTAA
At5g44730	Ala to Val	non polar neutral to non polar neutral	GCTGGAGCCATTGTGCTTCCAGA
At5g44860	Glu to Lys	polar negative to polar positive	GAGTTGCTTAATGGAAGAATA
At5g46830	Ser to Phen	polar neutral to non polar neutral	TCCAAATATTTTCTGGAGCCCC
At5g46890	Val to Ile	non polar neutral to non polar neutral	GTTCTTGGTATCAACCTTAA
At5g47210	Arg to Cys	polar positive to non polar neutral	CGCCGTGGTGGAGTTGC
At5g48485	Asp to Asn	polar negative to polar neutral	GATCTCTGCGGCATGAGCC
At5g51660	Pro to Leu	non polar neutral to non polar neutral	CCTGCTGCTTTAAATTCCTCTGGTAG
At5g52010	Gly to Arg	non polar neutral to polar positive	GGAAGGCATGCTGATTTGTGG
At5g52400	Pro to Ser	non polar neutral to polar neutral	CCATTTGGAAACCTTAATGACATG
At5g53150	Gly to Arg	non polar neutral to polar positive	GGGAGAAGAAGACAGTACGAA
At5g53750	Ala to Thr	non polar neutral to polar neutral	GCATTAACCCTTTTGTCTCACGAATT
At5g53970	Gly to Glu	non polar neutral to polar negative	GGGACCGCGGTGGGGCTGAA

* Green shaded cells represent amino acid changed that involve a net change of charge; yellow shaded cells represent amino acid substitutions of the same kind, synonymous mutation; blue shaded cells represent amino acid changes that involve in change in side chain polarity.

B) Analysis of chromosome 2

Similarly in chromosome 2, 84 SNP's and 143 SNP's were identified in line 17J and 21H, respectively, and 58 SNP's were common for the two lines. Only mutations that occurred solely in each of the two lines and mutations that occurred in only these two lines were selected. Next, based on the number of the alternative allele calls (non-reference allele), mutations that was called less number of times compared to the reference allele were disqualified. Following this, mutations that occurred within the intronic regions or intergenic regions were omitted. After these screenings, only 22 SNP's which are common for both lines were identified. Further analysis on the nucleotide substitution revealed that one of the mutations was a false positive. The remaining 21 SNP's were characterized for a possible change in the amino acid. Out of 21 SNP's, fifteen of them induced an amino acid change (Table 10), and one of them induced a premature stop codon. The remaining 5 SNP's did not cause an amino acid change (Table 10). Analysis of the amino acid substitutions revealed two changes which involved a net gain or loss of charge. For example, the substitution of arginine with glutamic acid involves the substitution of a positively charged amino acid with a negatively charged one (Table 11), although both of them have a similar hydropathy index (Kyte and Doolittle, 1982). Finally, one mutation that induced a premature stop codon was also identified. Whether these substitutions affect the activity of the protein depends on the position on the protein. If the substitution occurs within the catalytic domain or transmembrane domain of a protein, then most likely there will be a change in the activity of the protein.

Table 10. Mutations obtained in chromosome 2 of line 17J and 21H.

Position on chromosome	Gene ID	Total reads	Ref./non - ref. alleles	Ratio	Codon change	Amino acid change	Gene Annotation in the data base
10588170	at2g24860	72	6 / 61	0,098	AGG to AAG	Arg to lys	Heat shock protein
10598647	at2g24910	55	3 / 49	0,061	CCG to TCG	Pro to Ser	Pseudo gene transposable element
10659314	at2g25052	64	5 / 58	0,086	GGT to AGT	Gly to Ser	Actin binding protein
10793777	at2g25340	43	2 / 40	0,050	AGC to AAC	Ser to Asn	vesicle associated membrane proteins
10863443	at2g25530	74	4 / 66	0,061	CCC to TCC	Pro to Ser	AFG1-like ATPase family protein
10927134	at2g25660	65	2 / 63	0,032	CGA to CAA	Arg to Glu *	embryo defective 2410
11002492	at2g25790	71	3 / 67	0,045	CCT to CTT	Pro to Leu	protein serine/threonine kinase activity
11219205	at2g26350	64	4 / 58	0,069	GGA to GAA	Gly to Glu *	Zinc-binding peroxisomal membrane protein
11956640	at2g28070	59	4 / 54	0,074	TCT to TTT	Ser to Phe	ABC-2 type transporter family protein
12425476	at2g28930	63	2 / 60	0,033	CCT to TCT	Pro to Ser	product protein kinase 1B
12485802	at2g29065	44	0 / 39	0,000	CTT to TTT	Leu to Phe	GRAS family transcription factor
12680164	at2g29660	41	1 / 38	0,026	GAC to GAT	Asp to Asp	zinc finger (C2H2 type) family protein
12718714	at2g29780	62	6 / 54	0,111	AAG to AAA	Lys to Lys	Galactose oxidase/kelch repeat family protein
12920880	at2g30300	47	1 / 43	0,023	TCC to TCT	Ser to Ser	Major facilitator superfamily protein
13379904	at2g31370	57	0 / 57	0,000	CCA to TCA	Pro to Ser	Basic-leucine zipper (bZIP) transcription factor
13437277	At2g31560	64	3 / 59	0,051	CAA to TAA	Gln to stop	Protein of unknown function
13531171	at2g31820	59	4 / 52	0,077	CCT to CTT	Pro to Leu	Ankyrin repeat family protein
13726180	at2g32310	67	1 / 64	0,016	TTC to TTT	Phe to Phe	CCT motif family protein
13754913	at2g32400	62	4 / 57	0,070	TTG to TTA	Leu to Leu	glutamate receptor 5
13880889	At2g32730	49	1 / 45	0,022	CTT to TTT	Leu to Phe	26S proteasome regulatory complex
13997859	at2g32980	47	3 / 41	0,073	GCG to TCG	Ala to Ser	unknown protein

* Only mutations occurred in the exon were presented here; green shaded cells show amino acid changed; yellow shaded cells show silent mutations with no amino acid changes; red shaded cells show mutations where premature stop codon was induced; asterisks in the “amino acid change” column represent a net change of charge on the side chain of the substituted amino acid.

4. Discussion

4.1. GAD Knock out/down

4.1.1. Simultaneous mutation of *gad1/2* genes partially rescued the *ssadh* phenotype

The abnormal phenotype of *ssadh* plants was rescued by simultaneous knock out of the GABA-T (POP2) gene (Ludewig et al., 2008) suggesting that the metabolic intermediate(s) (SSA and/or GHB) produced between the two steps (SSADH and GABA-T) is responsible for the damage. Here, it was hypothesized that other mutations upstream of the SSADH step would reduce the accumulation of these toxic intermediates, thereby suppressing the *ssadh* phenotype. Hence, the glutamate decarboxylases acting upstream of the GABA-T were targeted for mutation. As described in the previous section, the *Arabidopsis* genome contained five copies of *GAD* genes. Since *GAD1* and *GAD2* are the most abundantly expressing *GAD* genes, both of them were knocked out by T-DNA insertion. The resulting double mutant contained only low amounts of GABA (Chapter one).

Crossing of the *gad1/2* double mutant and the *ssadh* heterozygous plants yielded triple mutants which have an improved growth compared to the *ssadh* plants. However, the rescued phenotype was not as good as the *gaba-t* rescued *ssadh* (*gs*) plants. The *gs* line has been reported to completely rescue the vegetative phenotype (Ludewig et al., 2008). Indeed, the *Arabidopsis* genome contained only one *GABA-T*, and therefore knockout of this single gene was sufficient to block the downstream pathways. Contrastingly, the gene targeted in this study exists in five copies, and only two of them (*GAD1* and *GAD2*), which are the most abundantly expressing isoforms, have been targeted for mutation. Therefore, the pathway was not completely blocked and the production of the suspected toxic compounds could not be completely prevented.

A notable feature of the *gad1/2* x *ssadh* plants was the burning and senescence of leaves, inflorescence tips and occasionally siliques. The plants germinated and grew normal during the first two weeks. Then, the curling and burning of the leaf tips started. This was most likely related to the generation of the toxic intermediate. At the early stage of plant development, the activity of *GAD3* and *GAD4* appeared to be very low thereby reducing the production of GABA. However, with increasing age of the plant, the activity of *GAD3* and *GAD4* seems to increase and more GABA was produced, which provides more substrate for GABA-T to

produce SSA. Indeed, the expression levels of *GAD3* and *GAD4* increase when the plants are getting older (Winter et al., 2007). Another observation was that some leaves on the same plant look quite healthy whereas one or two other leaves look curled and burned. This might be correlated to the leaf-specific expression pattern of *GAD3* and *GAD4* genes. For example, expression of *GAD4* was higher in leaf number four compared to leaf number one or two (Winter et al., 2007).

4.1.2. The *ssadh* phenotype is not correlated to the GHB levels

One feature of the *ssadh* plants is the accumulation of high GHB levels. Previously, GHB has been considered as the main cause of the *ssadh* phenotype, although the level of SSA has not been measured. In this study, the absence of GHB in the *gad1/2* x *ssadh* triple mutant was evident similar to the *gs* plants. However, the *ssadh* phenotype was only partially rescued unlike the *gs* lines. This observation suggests that GHB was not the primary reason for the *ssadh* phenotype. If the GHB level had been the major reason for the *ssadh* phenotype, the *gad1/2* x *ssadh* would have grown like wild type. Further knockdown of *gad3* and *gad4* transcripts with artificial miRNA did not improve the phenotype. This suggests that the elimination of GHB was not sufficient to rescue the phenotype. However, the bottleneck is still the inability to measure SSA in plant extracts. Another visible metabolic difference between the *gs* and *gad1/2* x *ssadh* triple mutant was the accumulation of GABA. In the *gs* line a very high level of GABA has been detected but not in the triple mutants (Fig. 51). GABA may have played some role in alleviating the *ssadh* phenotype. For example, GABA might be involved in the detoxification of reactive oxygen species like H₂O₂ which otherwise could inhibit the activity of the TCA cycle enzymes. Liu et al. (2011) showed the ability of GABA in scavenging O₂⁻ and H₂O₂. High H₂O₂ accumulation is a hallmark for *ssadh* plants (Fait et al., 2004). Unlike the previous report, a similar level of hydrogen peroxide has been measured in *ssadh* plants compared to wild type. This observation raises a question of whether H₂O₂ levels also contribute to the *ssadh* phenotype.

4.2. Suppression of the *ssadh* phenotype by EMS mutation

4.2.1. EMS mutation improved the growth of *ssadh* plants

Forward genetics is one tool in functional genomics to identify the function of unknown genes. In forward genetics a random mutation is induced artificially by chemicals or rays, and a phenotype is looked for. In this work, chemical mutagenesis has been induced to suppress the phenotype of an *ssadh* mutant. EMS mutagenized F1 *ssadh* plants did not show an improved phenotype whereas in the F2 generation few lines have been isolated with a better growth, indicating that recessive mutation rescued the phenotype (Ludewig et al., 2008). Finally, after successive screenings, four lines (7D, 13J, 17J and 21H) have been selected and characterized at the phenotypic level both on plates and soil.

All four lines grew much better than the *ssadh* itself (Fig. 55). Generally, there will be three mechanisms for the rescue of the *ssadh* phenotype. First, by preventing the generation of the toxic intermediate; this can be achieved by mutations upstream of the SSADH. Mutation in GABA transaminase is a good example. It can also be achieved by mutation in the mitochondrial high affinity GABA transporter (Michaeli et al., 2011) which subsequently prevents the import of GABA in the mitochondria. Second, by promoting the rapid degradation of the toxic intermediates; for example, one of the toxic compounds detected in *ssadh* plants was hydrogen peroxide. The EMS-induced mutations may enhance the activity of enzymes which are involved in the detoxification of this toxic intermediate. Third, the accumulation of the toxic compounds remains there but the plant develops other mechanisms to tolerate the toxic effect. However, a detailed analysis of the EMS-affected genes by obtaining the mutant lines is crucial for complete understanding of the underlying mechanism.

4.2.2. The *ssadh* phenotype is unrelated to the GHB level

Metabolic analysis emerged as a functional genomics methodology that contributes to the understanding of molecular interactions in biological systems (Hall et al., 2002; Bino et al., 2004). The over-accumulation of GHB and the inability to determine the SSA level in *ssadh* plants led to the speculation that GHB might be the reason for the abnormal phenotype. The complete rescue of the *ssadh* phenotype by simultaneous mutation in the *GABA-T* gene, in the *gs* line, which accumulated no GHB, further supported this speculation. To support or reject the speculation, further investigation on the correlation between GHB content and the *ssadh*

phenotype was needed. Hence, the level of GHB and other GABA shunt and TCA cycle intermediates were measured in the leaf extracts of the EMS suppressor and *ssadh* lines.

As expected, the level of GHB in the *gs* line was below the detection limit which is similar to the wild type (Fig. 56B). In contrast, the GHB level in *ssadh* plants was very high, an observation that goes in line with the previous report (Fait et al., 2004). The EMS suppressor lines contained variable levels of GHB. Line 17J and 21H contained a significantly high level of GHB compared to the *gs*, 7D and 13J lines (Fig. 56B). However, the phenotype of 17J and 21H was better than line 7D and 13J and was similar to the *gs* line. In addition to that, the *gad1/2* x *ssadh* plants (reported in the section before) contained no detectable GHB but did not rescue the *ssadh* phenotype to the level of 17J or 21H. Taken together, these data confirm that GHB is not the toxic compound that caused the *ssadh* phenotype. Measurement of other GABA shunt and TCA cycle intermediates revealed a similar chemotypic profile of line 17J and 21H except for GABA. This observation suggests that the two lines may have a similar mode of *ssadh* phenotype suppression.

The accumulation of GHB in the EMS lines, unlike in the *gs* line, suggests that the GABA shunt was not blocked upstream to prevent the accumulation of the downstream toxic intermediates. At the same time, the GABA chemotype resembles that of the *gs* line. Taken together, one may think the mutation to be within the *GABA-T* gene. But, sequencing of the *GABA-T* ORF ruled out the mutation within the coding region. Furthermore, the PCR-based mapping pointed the mutation not to be in chromosome 3 where *GABA-T* is located.

4.2.3. Full genome sequencing identified seven candidate genes

Centimorgan (cM) is a unit of measuring the linkage between genes on the same chromosome. By default a distance of one cM corresponds to a 1% crossover per generation (<http://www.isogg.org/wiki/Centimorgan>). In other words, two genes separated by one cM have a 1% chance of being separated in 100 chromosomes undergoing genetic recombination. In diploid species, like Arabidopsis, one plant in every 50 plants would contain the two genes separated from each other following crossing over during meiosis. Using the PCR-based mapping system, it was found that approximately 5% crossing over has occurred between the marker (VG) and the EMS induced mutation in line 17J. In line 21H, a 6% crossing over has occurred between marker 5.7 and the EMS mutation as shown by the percent of *Ler* fragment

(Table 6). From the above definition, it follows that the marker and the EMS mutation are 5 cM and 6 cM apart in line 17J and 21H, respectively.

The conversion of cM to base pairs is not easy, as it depends on the position over the chromosome. Generally, in heterochromatic regions of the chromosome where the DNA is tightly packed around the histones, the chance of crossing over is minimum compared to the euchromatic region. The region of interest in this analysis is the lower arm of chromosome 5. The average base pairs corresponding to one cM in this chromosome was calculated to be 2003800 (<http://www.arabidopsis.org/servlets/mapper>). Different softwares estimated the size of chromosome 5 differently in terms of base pairs or centimorgan. Here, the average numbers in both units was taken and divided to get the factor. Once this factor is determined, it was multiplied by the values obtained above. For line 17J, the physical distance between the VG marker and the EMS mutation is $5 \times 203800 = 1019000$ bp; and for 21H the distance between marker 5.7 and the EMS mutation is $6 \times 203800 = 1222800$ bp. The first nucleotide of the forward primers for markers VG and 5.7 correspond to the bases 18022267 and 19829939 on chromosome number 5, respectively. To identify the mutation that rescued the *ssadh* phenotype, mutations within 5 cM and 6 cM from the marker VG and 5.7, respectively, were screened from both directions. Roughly, mutations within the position of 17500000 and 22000000 were used for further analysis. Mutations that occurred at the same position in all four lines were rejected as it is most unlikely; whereas mutation that occur only in line 17J and 21H were considered for two reasons. Firstly, it has a 50% probability of being true; second, the phenotypic and chemotypic data of these two lines is very similar. In addition, the PCR-based mapping pointed the mutation to be in the same region. Therefore, it is possible that the two lines are clones.

The classical PCR-based mapping also indicated a Col-0 rich fragment in chromosome 2. Similar to the mutation in chromosome 5, the EMS induced mutation was mapped within 5 cM of the marker 2.6. The first base of the forward primer of marker 2.6 corresponds to the position 12273294th nucleotide on the chromosome 2. The estimation of 1 cM on this chromosome was about 208595 base pairs, and for 5 cM region about one million base pairs up and down of the marker (2.6) were evaluated.

Sequence analysis revealed that 13 and 9 SNP's induced mis-sense mutation in chromosome 5 of line 17J and 21H, respectively. The question would be whether these mutations would

lead to a change in protein properties. Some substitutions are not real changes in terms of the amino acid properties and do not change the function of the protein. It has been shown that substitution of leucine for isoleucine (both have non polar and neutral side chain) did not lead to a functional change in a protein, and hence described as synonymous (silent) mutation (Alberts, 2008). Three such substitutions in line 17J and one substitution in 21H have been identified and this reduces further the number of candidate genes. For example, the substitution of alanine to valine as in the case of At5g44730 is synonymous mutation, as both amino acids have non-polar and neutral side chain. In chromosome 2 the most plausible candidates were three; two of which involved a net change of charge of the amino acid chain and one involved the induction of a premature stop codon. The effect of the premature stop codon on the functions of these three proteins indentified in chromosome 2 and 5 was briefly discussed below.

At5g44930

The locus of At5g44930 has an open reading frame (ORF) of three exons. The encoded protein has a length of 443 amino acids and a calculated molecular weight of 51 kDa. AT5g44930 encoded protein belongs to the glycosyltransferase family 47 proteins (Harholt et al., 2006). The gene is annotated as a putative arabinosyl transferase (ARAD 2) coding protein in the NCBI protein database. The protein shares a domain similar to the exostosin family proteins (Marchler-Bauer et al. 2011) which involve in the suppression of tumor formation (Lind et al., 1998). The stop codon induced by EMS mutation in this protein leads to a 173 long polypeptide. This mutation is within the stretch of the predicted domain that resembles to the domain of the exostosin family protein. To date, no functional characterization has been made for this protein. However, mutants of its closest homologue ARABINAN DEFICIENT 1 (ARAD 1) showed a largely reduced amount of arabinose, although there was no sever phenotype (Harholt et al., 2006). The premature insertion of a stop codon in this ARAD2 protein most likely leads to a reduced level of arabinose. The question remains, how this mutation could be integrated to the GABA shunt deficient phenotype. Further analysis by isolating homozygous mutant and crossing the *ssadh* deficient mutants is important.

At5g50450

The Locus of At5g50450 has an ORF consisting of three exons. The translated protein has a size of 336 amino acids with a calculated molecular weight of 37 kDa. Analysis of conserved

motifs in the protein identified two domains; the zinc finger MYND (Myeloid, Nervy, DEAF-1) and the Tetratricopeptide (TPR) domains. The MYND domain consists of clusters of cysteine and histidine amino acids that provide a potential motif for zinc binding (Gross and McGinnis, 1996). The premature stop codon induced by EMS mutation reduces the protein size just to 80 amino acids. The predicted functional domains on the native protein reside within the 80th and 200th amino acid for TPR domain and within 260th and 300th amino acid for MYND motif. The truncated protein will miss both domains and most likely will not have a normal function. The TPR motif of the At5g50450 encoded protein predicted to be similar with the SEL1 subfamily proteins (Marchler-Bauer et al. 2011). This family of proteins was described to involve in the transport of sulfate and selenium (Rouached et al., 2009). However, the function of this protein has not been studied and reported.

At2g31560

The locus of At2g31560 has an ORF consisting of 2 exons. The protein encoded by this gene has a size of 202 amino acids and has a calculated molecular weight of 22.1 kDa. Unlike the previous two candidates, this protein did not have a domain which corresponds to the previously identified ones. The function of the protein is also unknown. The premature stop codon induced by the EMS mutation reduces the protein size by only 11 amino acids. Whether this mutation would have significant effect on the function of the protein remains to be identified.

Conclusion

Mutation in the *SSADH* gene caused abnormal phenotypes in plants, humans, mice etc. Understanding the underlying mechanism of this abnormal phenotype would help in discovering new targets for alleviating the problem. The attempt to rescue the *ssadh* phenotype by simultaneous knock out of the abundantly expressing *GAD1* and *GAD2* genes was only partially successful. The presence of multiple copies of *GAD* genes made the blocking of the pathway nearly impossible. However, blocking of the pathway alone doesn't seem to be sufficient for rescuing the *ssadh* phenotype. Because the absence of GABA with this approach will have an additional effect as GABA is playing many roles in the normal growth and development of an organism. The rescue of the *ssadh* phenotype by Vigabatrin in human GHB aciduria treatment, and by simultaneous mutation of *GABA-T* in *ssadh* plants is a cumulative effect of two things; first, prevention of the accumulation of the downstream toxic intermediate, likely SSA, and second, the accumulation of GABA. However, further studies must be conducted to assess the exact nature of the *ssadh* phenotype. Measuring the SSA level in the metabolite extracts would be a break through. In addition, over-expression of catalase in mitochondria would help to understand the effect of the H₂O₂ accumulation in *ssadh* phenotype.

The use of forward genetics provides an opportunity to unravel new genes which play a role in a specific pathway. In an effort to discover new genes and new pathways which operate in concert with the GABA shunt, EMS rescued *ssadh* lines were investigated. The phenotypic and chemotypic data confirmed that the EMS lines grow much better than the *ssadh* itself and that GHB was not the actual cause of the abnormal phenotype. Using the deep sequencing (next generation sequencing), it was possible to pin down the mutation to just 8 genes. Sequence analysis of SNP's from line 17J and 21H pointed towards similar mutations in both lines which are basically unusual. The probability of having the same mutation over 50 times in two independent lines is very unlikely. But, lines 17J and 21H shared such a similarity perhaps indicating seed contamination. The phenotypic and chemotypic data, indeed, showed similarity between these two lines. Further analysis on lines 7D and 13J should be made as the two lines look dissimilar to 17J and 21H.

References

- Akaboshi S, Hogema BM, Novelletto A, Malaspina P, Salomons GS, et al. (2003)** Mutational spectrum of the succinate semialdehyde dehydrogenase (ALDH5A1) gene and functional analysis of 27 novel disease-causing mutations in patients with SSADH deficiency. *Human Mutation* 22:442-450.
- Alberts (2008)** *Molecular Biology of the Cell*. Garland. pp. 264
- Allan WL, Clark SM, Hoover GJ, Shelp BJ (2009)** Role of plant glyoxylate reductases during stress: a hypothesis. *Biochem. J.* 423:15–22.
- Bouché N, Fait A, Bouchez D, Moller SG, Fromm H (2003)** Mitochondrial succinic-semialdehyde dehydrogenase of the γ -aminobutyrate shunt is required to restrict levels of reactive oxygen intermediates in plants. *Proc. Natl. Acad. Sci. U.S.A.* 100:6843–6848.
- Bino RJ, Hall RD, Fiehn O, Kopka J, et al. (2004)** Potential of metabolomics as a functional genomics tool. *Trends in plant sciences* 9(9):1360-1385.
- Fait A, Yellin A, Fromm H (2004)** GABA shunt deficiencies and accumulation of reactive oxygen intermediates: insight from *Arabidopsis* mutants. *FEBS Letters* 579:415–420.
- Gross CT, McGinnis W (1996)** DEAF-1, a novel protein that binds an essential region in a deformed response element. *EMBO J.* 15(8): 1961-1970.
- Hall R, Beale M, Fiehn O, et al. (2002)** Plant metabolomics: the missing link in functional genomics strategies. *Plant Cell* 14:1437–1440.
- Harholt J, Suttangkakul A, Scheller HV (2010)** Biosynthesis of pectin. *Plant physiology* 153:384-395.
- Hogema BM, Gupta M, Senephansiri H, Burlingame TG, Taylor M, Jakobs C, et al. (2001)** Pharmacologic rescue of lethal seizures in mice deficient in succinate semialdehyde dehydrogenase. *Nat Genet* 29:212-216.
- Jacobs C, Bojasch M, Monch E, Rating D, Siemens H, Henefeld F (1981)** Urinary excretion of gamma-hydroxybutyric acid in a patient with neurological abnormalities. The probability of the new inborn error of metabolism. *Clinica Chimica ACTA* 111:169-178
- Lind T, Tufaro F, McCormick C, Lindahl U, Lidholt K (1998)** The putative tumor suppressors EXT1 and EXT2 are glycosyltransferases required for the biosynthesis of heparan sulfate. *J. Biol. Chem.* 273:26265–26268.
- Ludewig F, Hueser A, Fromm H, Beauclair L, Bouche N (2008)** Mutants of GABA transaminase (POP2) suppress the severe phenotype of succinic semialdehyde dehydrogenase (*ssadh*) mutants in *Arabidopsis*. *PLoS ONE* 3(10):e3383.
- Kim YS, Schumaker KS, and Zhu JK (2006)** EMS Mutagenesis of *Arabidopsis*. *Methods in Molecular Biology* 323: Humana Press Inc., Totowa, NJ.

Knerr I, Pearl PL, Bottiglieri T, Snead OC, Jakobs C, Gibson KM (2007) Therapeutic concepts in succinate semialdehyde dehydrogenase (SSADH; ALDH5a1) deficiency (gamma-hydroxybutyric aciduria). Hypotheses evolved from 25 years of patient evaluation, studies in *Aldh5a1*^{-/-} mice and characterization of gamma-hydroxybutyric acid pharmacology. *J Inherit. Metab. Dis.* 30(3):279–294.

Kyte J and Doolittle R (1982) A simple method for displaying the hydropathic character of a protein. *J. Mol. Biol.* 157: 105-132.

Liu C, Zhao L, Yu G (2011) The dominant glutamic acid metabolic flux to produce γ -amino butyric acid over proline in *Nicotiana tabacum* leaves under water stress relates to its significant role in antioxidant activity. *J. Integr. Plant Biol.* 53(8):608–618.

Marchler-Bauer A, Lu S, Anderson JB, et al. (2011) CDD: a Conserved Domain Database for the functional annotation of proteins. *Nucleic Acids Res.* 39(D):225-229.

Michaeli S, Fait A, Lagor K, et al. (2011) A mitochondrial GABA permease connects the GABAshunt and the TCA cycle, and is essential for normal carbon metabolism. *The Plant Journal* 67(3):485-98.

Rouached H, Wirtz M, Alary R, Hell R, Bulak Arpat A, Davidian J-C, et al (2008) Differential regulation of the expression of two high-affinity sulfate transporters, SULTR1.1 and SULTR1.2, in Arabidopsis. *Plant Physiol* 8;147:897–911.

Winter D, Vinegar B, Nahal H, Ammar R, Wilson GV, et al. (2007) An Electronic Fluorescent Pictograph browser for exploring and analyzing large-scale biological data sets. *PLoS ONE* 2(8):e718.

Appendix 1: Abbreviations

ATP	Adenosine Triphosphate
AKT	Arabidopsis K ⁺ transporter
Ala	Alanin
Arg	Arginine
Asn	Asparagine
Asp	Aspartate
CaM	Calmoduline
cDNA	Complementary DNA
CO ₂	Carbon dioxide
Col-0	Colombia-0
°C	Degree celcius
DNA	Deoxyribonucleic acid
ddH ₂ O	Double distilled water
DMSO	Dimethyl sulfoxide
DW	Dry weight
dNTP	Deoxyribonucleotide triphosphate
DCF	2',7'-dichlorodihydrofluorescein diacetate
EDTA	Ethylenediaminetetraacetic acid
EMS	Ethyl methanesulfonate
FW	Fresh weight
F+R	Forward and Reverse primers
Fig	Figure
GAD	Glutamate decarboxylase
GABA	gamma-Aminobutyric acid
GABP	GABA permease
GABA-T	GABA transaminase
GHB	gamma-hydroxybutyric acid
GHBDH	GHB dehydrogenase
GAT1	GABA transporter
GABA _A	GABA receptor A
GABA _B	GABA receptor B
GABA _C	GABA receptor C
Glu	Glutamate

Gln	Glutamine
Gly	Glycine
GLR	Glutamate receptor
GC/MS	Gas chromatography mass spectroscopy
GORK	Guard cell outward rectifying K ⁺ channel
GR1/2	Glyoxylate reductase ½
GND1/2	6-phosphogluconate dehydrogenase
gs	<i>gaba-t x ssadh</i>
HCl	Hydrochloric acid
HPLC	High-performance liquid chromatography
H ₂ O	Water
HNO ₃	Nitric acid
HAK	High affinity K ⁺ transporter
H ⁺	Hydrogen ion
H ₂ O ₂	Hydrogen peroxide
Ileu	Isoleucine
ICP-MS	Inductively coupled plasma mass spectrometry
K ⁺	Potassium ion
KCl	Potassium chloride
KAT1	K ⁺ channel in <i>Arabidopsis thaliana</i> 1
K ₂ HPO ₄	Potassium phosphate
LiCl	Lithium chloride
Lys	Lysine
LB	Left border primer
LB	Luria-Bertani
<i>Ler</i>	<i>Landsberg erecta</i>
Leu	Leucine
Lys	Lysine
MS	Murashige and Skoog medium
mM	Milli molar
mg	Milli gram
M	Molar
MSTFA	N-methy-N-(trimethylsilyl) trifluoroacetamide
ml	Milli liter

mmol	Milli mol
mm ²	Milli meter square
m ² .s	Meter square second
mRNA	Messenger RNA
mA	Milli ampere
miRNA	Micro RNA
NAD ⁺	Nicotinamide adenine dinucleotide
NADH	Reduced NAD ⁺
NaCl	Sodium chloride
Na ⁺	Sodium
Na ⁺ /K ⁺	Sodium to potassium ratio
NADP ⁺	Nicotinamide adenine dinucleotide phosphate
NBT	Nitro blue tetrazolium chloride
nmol/g	nano mol per gram
OC8-HSL	3-oxo-octanoylhomoserine lactone
OsGAD	<i>Oryza sativum</i> GAD
OPA	o-phthaldialdehyde
ORF	Open reading frame
OD ₆₀₀	Optical density at 600nm
POP2	Pollen pistil incompatibility 2
Poly (A)	Poly adenine
PHB	Polyhydroxybutyrate
Phe	Phenylalanine
PMSF	Phenylmethanesulfonylfluoride
PBS	Phosphate buffered saline
PCR	Polymerase chain reaction
PCI	phenolchloroform-isoamylalchol
PXA1	Peroxisomal ABC transporter 1
qRT-PCR	Quantitative reverse transcription PCR
RH	Relative humidity
rpm	revolution per minute
RNA	Ribonucleic acid
RT-PCR	Reverse transcription PCR
ROS	Reactive oxygen species

SSA	Succinic semi aldehyde
SSADH	SSA dehydrogenase
SA	Succinic acid
SDS	Sodium dodecyle sulphate
TCA	Tricarboxylic acid
T-DNA	Transfer DNA
Thr	Threonine
Trp	Tryptophan
Tyr	Tyrosine
3'UTR	3' Untranslated region
5'UTR	5' Untranslated region
μ l	Micro liter
μ M	Micro molar
μ g	Micro gram
V	Volume
V/V	Volume per Volume
VMM	Vincent minimal medium
WC	Water content
Wt	Wild type
YP	Yeast peptone
YPD	Yeast peptone dextrose
YNB	Yeast nitrogen base
YEP	Yeast extract peptone

Appendix 2: List of primers

Primer name	Primer sequence	Purpose
35S-F	GGTCTCAGAAGACCAGAGGGCTATTG	Cloning (pAMPAT)
pD-TOPO-F	GTTGTAAAACGACGGCCAGTCTTAAG	Cloning
Actin-F	TGAGCTTCGTATTGCTCCTGAAGAG	RT-PCR
Actin-R	TGGAACAAGACTTCTGGGCATCTG	RT-PCR
GHBDH1-F	ATGGAAGTAGGGTTTCTGGGTT	RT-PCR
GHBDH1-R	TTCGCGGGAGAATTCACAGC	RT-PCR
GHBDH2-F	CTGCAATCTACTACTCCCTCTACC	RT-PCR
GHBDH2-R	CTCGTTCGCAGCGGCTGCAATCGG	RT-PCR
At4g20930-F	GGACTTGGAAATATGGGATTCAGAATG	RT-PCR
At4g20930-R	TGAACCACCACAGTAGATGGAGGTTC	RT-PCR
At5g14800-F	GTCTTCTCCACTAGCGAAGAAGTTG	RT-PCR
At5g14800-R	AGTTCATGAACTCCGGCTATTGTAGTG	RT-PCR
At1g64190-F	CTGAGCAAAAAGGATTGCTCTATTTAG	RT-PCR
At1g64190-R	ACTCAAATACCTACAATCCAACGAAGC	RT-PCR
At5g41670-F	TTGTATCATCGACGGTGGAAATGAG	RT-PCR
At5g41670-R	CTACAATCCAACGACGCAGCAATC	RT-PCR
At1g71180-F	AATAGCCCCAAAGAGTTAGCGGAG	RT-PCR
At1g71180-R	TTCACAATCATCTCCCCAAACAGC	RT-PCR
At1g71170-F	AACGATGTTAGATCGTTGCTTCTTGG	RT-PCR
At1g71170-R	AACAACGCTTGTTCAAAGCAGTTC	RT-PCR
At4g29120-F	TACACAGTCACCGTCTTCAATCGAAC	RT-PCR
At4g29120-R	TGAGCATAAATCAAACCTTCCACAAG	RT-PCR
GAD1-F	CTTGAACGATCTCTTGGTCG	RT-PCR
GAD1-R	CGCTGTTAGATTCACCTTCTC	RT-PCR

GAD2-F	CTGTCTGCACCATGTTCCGG	RT-PCR
GAD2-R	CACACCATTTCATCTTCTTCC	RT-PCR
GAD3-F	GCACATTTTTCCCTTACTTTTTCTTTAGC	RT-PCR
GAD3-R	GCTACTAACGGAACGCCG	RT-PCR
GAD4-F	CATTTCAAACCCAAAAATCAAAGTTCG	RT-PCR
GAD4-R	GCAAATTGTGTTCTTGTTGG	RT-PCR
GAD5-F	GCAAGGTACTTTGAGGTAGAGC	RT-PCR
GAD5-R	CCAATACTTAGTGATATCCTCC	RT-PCR
GAD1-F	GGCAAGTGGAGGATTCATTG	qRT-PCR
GAD1-R	TTTCTCCAGATCACCCAACC	qRT-PCR
GAD2-F	GAGATGCTACGTCGTTTTGG	qRT-PCR
GAD2-R	TGATGACAACACGCAGAACC	qRT-PCR
GAD3-F	CTTTAGGTGACGGTGAAGCCG	qRT-PCR
GAD3-R	TGGCTCCGGTTACAATATTAGGT	qRT-PCR
GAD4-F	GCTGATTTCGTCTTGGATTCG	qRT-PCR
GAD4-R	AAACGCCACTAACGGAACAC	qRT-PCR
GAD5-F	CAGGATTGCACATCTTGCTG	qRT-PCR
GAD5-R	CCACAAGGCGTTTCCAATAC	qRT-PCR
AKT1-F	CATGGATAAAGTCTACCTGTTTCGAGG	q/RT-PCR
AKT1-R	GCGCTTCGTTCTGCAAGATAAC	qRT-PCR
AKT1-R	CTGCGTGGTACTCCAACAGAAGAAG	RT-PCR
AKT2/3-F	GTTATTCAATCTTGGCCTCACTGC	qRT-PCR
AKT2/3-F	CACCAAAGAGAAACCTTTGTATCGC	RT-PCR
AKT2/3-R	CAAAGTTTGACGCTGCTTCAATGC	q/RT-PCR
AKT5-F	GCAGAAGAGAGGGCCTTCATTCTC	q/RT-PCR
AKT5-R	GGTCACGTGAACCACCAAGTTTG	qRT-PCR

AKT5-R	CAAAAACATGGCCGGTCTGTG	RT-PCR
KAT1-F	CTTGAACAATCTGCCAAAAGCAATC	qRT-PCR
KAT1-F	CTCAGCGTCTATATCTGAAACCAATTG	RT-PCR
KAT1-R	GATGTTTGTTCACAGCACCATTTC	q/RT-PCR
KAT2-F	GAGTTTCTCGCAACTTCCTATTCAG	qRT-PCR
KAT2-F	GATATCCGCTTCAACTATTTCTGGACAC	RT-PCR
KAT2-R	CTAGGATGTAGAGGTCAGTAGGAGCTTC	q/RT-PCR
KAT3-F	GGCCATAAGATCAAGCATTAAACCAAC	qRT-PCR
KAT3-F	CTTAATTTACTCCGCCTCTGGCG	RT-PCR
KAT3-R	CTTGTATTTGCGAAACCAGCTGG	q/RT-PCR
GORK-F	CAAGATTGCGCAATTATTGTATCTGC	q/RT-PCR
GORK-R	CCTGGAAGAAAATACTCTTCATGGAGC	qRT-PCR
GORK-R	CTTTCACAGCCTCAAACAATGGTG	RT-PCR
SKOR-F	CACTGAAGCAGCTGTTCTTCAAGAC	qRT-PCR
SKOR-F	TGCATGCCATGGGATATCATCTAC	RT-PCR
SKOR-R	TTCAGATGAGCATCCGCGAAAG	q/RT-PCR
HAK-F	CTGATCTAGGTCACTTCAGTGTTTCGAG	q/RT-PCR
HAK-R	GTATGTTTAGTTAGGTACGCAGCCTG	qRT-PCR
HAK-R	CCTCAGCTCGTACCGGTATTTGAG	RT-PCR
KUP1-F	GTATACCCGTGTTTGATACTTGCATAC	q/RT-PCR
KUP1-R	CCACAGCTGCAAATGTAGCCAC	qRT-PCR
KUP1-R	CGAATAGACCAGTCCTATTCTGGAAC	RT-PCR
GAD1-F	GCAAAGCTGAAGGCAAACC	genotyping
GAD1-R	ACAAATTTGACCTCCCATCC	genotyping
GAD2-F	TTCGTTTGTACGTTTATGACTCTGG	genotyping
GAD2-R	ACACACCATTCATCTTCTTCTCTC	genotyping

SSADH-F	CCATTCCAATTTACCTTCTTCTTCTTTCTG	genotyping
SSADH-R	CTCACCTGAGTAGCACGAGAAACAAAAG	genotyping
LB_SALK	GTCCGCAATGTGTTATTAAGTTGTC	genotyping
LB_GK	ATATTGACCATCATACTCATTGC	genotyping
GHBDH1-F	CTTGTGCTGCTCTTTCGGTATTTG	genotyping
GHBDH1-R	CCAACACCATTATTTTCAGAGCTTGC	genotyping
GHBDH2-F	CATCAATACTAATCAGCAAGC	genotyping
GHBDH2-R	GCGCATTGATAGCTCCCTGTG	genotyping
At4g20930-F	TTCCAAGTGACTGACCAAGAGCTAAG	genotyping
At4g20930-R	GCATTGATACAACTGCACGTTCTGTAG	genotyping
GABA-T-F	CTTCCCTTTTGGTGTCAATTTTA	genotyping
GABA-T-R	GGCTAATCTGGTTGAGAACTCC	genotyping
1.1-F	AACATCCAACGGTCTGAACC	mapping
1.1-R	CGTGTCCGGTGAAAAAGAGT	mapping
1.7-F	AAAACCCTGTTGTTTCTGAGC	mapping
1.7-R	GGTTGAGACTGGTAACAAGG	mapping
2.1-F	CCCATGCTTCCTCCTATTGC	mapping
2.1-R	GGAGGCTCTTGAACCTCACAC	mapping
2.6-F	TGTCACTGAAGAACCCTAGC	mapping
2.6-R	GCAGCTTCGAGTGGATTCTA	mapping
2.7-F	CTTCTTTCAAGGATCTCTTGC	mapping
2.7-R	CCATGAATTCACCTCTCTATTC	mapping
3.1-F	CACATTTTCAGTTATCTTAATGC	mapping
3.1-R	GGAATGAGACATTGACTTC	mapping
3.7-F	TGGGAACAAAGGTGTCATCC	mapping
3.7-R	GCAAGTTAAAACCTGAAACTAAG	mapping

4.2-F	GCTTTTAACCAGCTAACTTAGG	mapping
4.2-R	GGTCTCTCACCTAAGGAGAT	mapping
4.7-F	CCAATGATTGGTCACTACTGC	mapping
4.7-R	GGTCATCAATTCATTTCTTAAGC	mapping
5.3-F	CAGCTGCCTTCAAGTATTCC	mapping
5.3-R	GCTGTGTTTTTGTAGAGAGCG	mapping
5.6-F	CGTCAAAGACGACACATGG	mapping
5.6-R	GCTCATGCTTCCTCCCATTG	mapping
5.7-F	ATAAGATAGGTTTGGCAAATGG	mapping
5.7-R	CCTACTATTCAAATTGTTTAAGAA	mapping
5.8-F	CAAAAATTGATCGATCGATAGG	mapping
5.8-R	CGTTATTGAGTCCGGTTGAG	mapping
5.9-F	CTCTCGCTAACGCTCTTTGG	mapping
5.9-R	GCACGAGTTAACGTTATTGAG	mapping
VC-F	TCGGAAAAAGTATGTTGGGAGT	mapping
VC-R	TGTTCAACAATAGCTGCCAAA	mapping
VE-F	CCGATATAACTAAAGGTGCAGAGA	mapping
VE-R	AAAATTCCTACCAAACGAAGCA	mapping
VG-F	GATTCGCTCTCTGCCAAA	mapping
VG-R	AAAAATGACGGGACGAAAGT	mapping
VH-F	TCACCTTACTTAATTCAACTGCAAA	mapping
VH-R	CCAGATTCGATGTACTTCACTTTC	mapping

* **Note q/RT-PCR: these primers can be used for both qualitative and quantitative PCR**

Ich versichere, dass ich die von mir vorgelegte Dissertation selbständig angefertigt, die benutzten Quellen und Hilfsmittel vollständig angegeben und die Stellen der–Arbeit einschließlich Tabellen, Karten und Abbildungen, die anderen Werken im Wortlaut oder dem Sinn nach entnommen sind, in jedem Einzelfall als Entlehnung kenntlich gemacht habe; dass diese Dissertation nochkeiner anderen Fakultät oder Universität zur Prüfung vorgelegen hat; dass sie– abgesehen von unten angegebenen Teilpublikationen – noch nicht veröffentlicht worden ist sowie, dass ich eine solche Veröffentlichung vor Abschluss des Promotionsverfahrens nicht vornehmen werde. Die Bestimmungen der Promotionsordnung sind mir bekannt. Die von mir vorgelegte Dissertation ist von Prof. Dr. Ulf-Ingo Fluegge betreut worden.

Dereje Worku Mekonnen

Köln, 25/10/2012

Publication

“*Arabidopsis gad1/2* mutant reveals the importance of GABA in stomata closure and drought response” Paper submitted.

Conference Abstracts

“Succinic semialdehyde (SSA), a GABA shunt intermediate, causes cell toxicity via induction of reactive oxygen species accumulation” Botanical Science Society (Botanikertagung), Berlin, Germany. Sept. 18-23, 2011

“Characterization of *ghbdh1/2* line suggests the presence of a third homologue in *Arabidopsis*” Botanical Science Society (Botanikertagung), Leipzig, Germany, Sept. 6-10, 2009

Dereje Worku Mekonnen

Nationality: Ethiopian, **Address:** Deutzer Ring 5, 50679 Cologne, Germany
Cell Phone: +4917670278300, e-mail: dmekonne@smail.uni-koeln.de

Educational History

- 06/09-12/12 | **PhD study, Plant Molecular Biology**
Prof. Ulf-Ingo Fluegge,
Department of Botany, University of Cologne, Germany
- 09/06-08/08 | **MSc study, Biomolecular Sciences**
Dr. Bert de Boer
Department of Structural Biology, University of Amsterdam,
Netherlands
- Prof. Hans J. Bohnert
Department of Plant Biology/Crop Science, University of Illinois,
Urbana-Champaign, USA
- 09/98-06/02 | **BSc study, Plant Sciences**
Alemaya University, Ethiopia, with "Great Distinction"
- 09/94-06/98 | **High school**
Merti comprehensive secondary high school, Metahara, Ethiopia
- 09/86-06/94 | **Elementary and Junior secondary school**
Wonji No.1 elementary school, Wonji, Ethiopia

Work Experience

- 01/03-06/06 | **Junior Researcher**
Department of Plant Biotechnology
Ethiopian Agricultural Research Institute (EIAR), Ethiopia
- 10/02-12/02 | **Lecturer**
Technical, Vocational and Educational Training (TVET) College,
Bako, Ethiopia

Research Related Trainings

- 04/03 | **Advanced Tissue Culture Techniques**
Jommo Kenyatta University of Agriculture and Technology
(JKUAT), Kenya

05/05 | **Basic Molecular Biology Techniques**
Armahuer Hansen Research Institute (AHRI), Addis Ababa,
Ethiopia

July 4-15, 2010 | **Optical Imaging Intensive Program, Summer School**
University of Crete, Heraklion, Crete, Greece

Scientific Soft Skills

April 21-22, 2010 | Advanced scientific writing
Dr. Ruth Willmott, Bioscript Vienna

Aug. 9-10, 2012 | Career management for research scientist
Dr. Ruth Willmott, Bioscript Vienna

Computer Skill

Microsoft Offices (Excel, Word, Powerpoint)
Vector NTI, ImageJ, Sigma Plot
Adobe Photoshop